



Sustainable Inhibitors for Corrosion Mitigation in Aggressive Corrosive Media: A Comprehensive Study

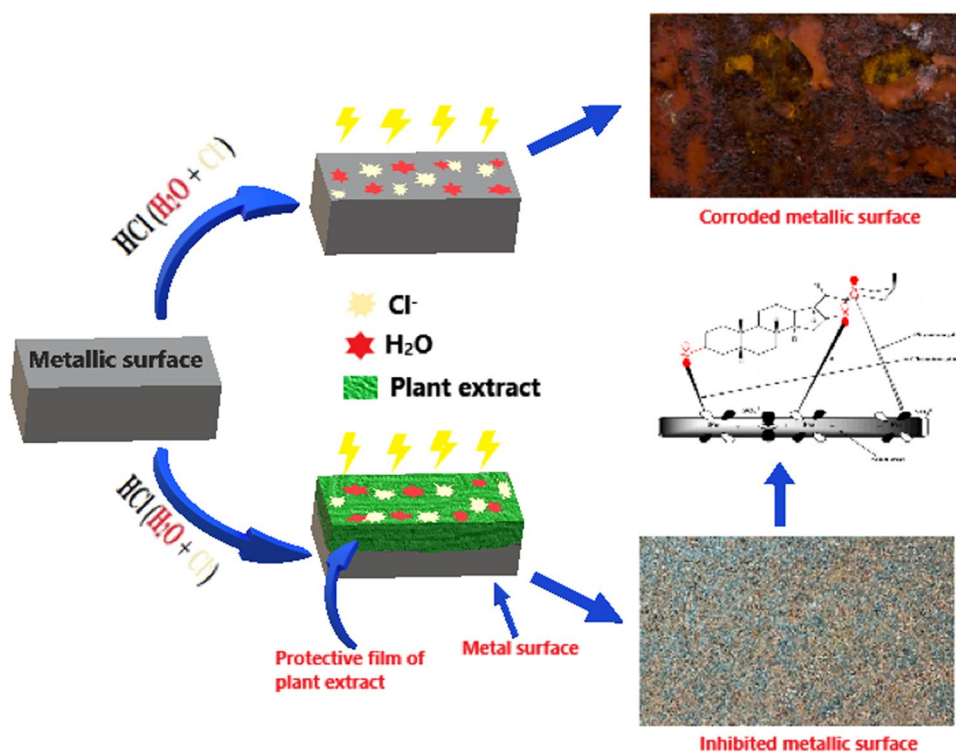
Abhinay Thakur¹ · Ashish Kumar¹

Received: 19 December 2020 / Revised: 26 February 2021 / Accepted: 7 March 2021 / Published online: 22 March 2021
© The Author(s), under exclusive licence to Springer Nature Switzerland AG 2021

Abstract

Green corrosion inhibitors are of immense interest because there has been an increase in environmental awareness and a change in regulations that restrict the use of hazardous and toxic synthetic corrosion inhibitors. These contain heteroatoms and/or pi electrons that make them a good candidate for metals corrosion inhibitor. This review gives a vivid account of the contributions made in recent years (2005 to 2020) based on the literature on the application of natural plant extracts as corrosion inhibitors for various metals such as mild steel, stainless steel, aluminium, copper along with their alloys in an aggressive corrosive environment (such as H_2SO_4 , HCl , HNO_3) at elevated temperatures. Additionally, the inhibition efficiency of these corrosion inhibitors, including the techniques used to evaluate them and the respective inhibition mechanisms, are discussed. Moreover, the emphasis has been given to the prominent metrics for the extract preparation, which covers all the essential steps for pre-extraction of plant samples and various methods involved in it. The challenges and outlooks in this area of research have been pointed out with future directions proposed.

Graphic Abstract



Extended author information available on the last page of the article

Keywords Corrosion inhibition · Plant extract · Acidic/basic solutions · Metals · Eco-friendly inhibitors · EIS

1 Introduction

1.1 General Introduction of Corrosion

Corrosion is a detrimental phenomenon of metals exposed to the environment. It is a natural latent hazard, that affects various manufacturing industries such as textiles, mechanical industries, oil and gas [1]. The corrosion of metals leads to various adverse effects, such as reducing the chemical reactivity of cathode active components, degrading the electrolytes, decreasing the electrical conductivity and intensifying the self-discharge rate [2–4]. Corrosion leads to chemical rupture and leakage of the corroded oil pipeline in oil and gas industries, causing an approximate overall annual cost of \$1.372 billion [5]. Corrosion is the degradation of metals due to cathodic and anodic electrochemical reactions. In an acidic environment, cathodic reactions occur due to the decrease of oxygen or an increase of hydrogen in their environment. Thus, oxidation gives rise to anodic reaction [6–8]. Oxidation is the loss of electrons during a reaction by a molecule, atom or ion. Oxidation occurs when the oxidation state of a molecule, atom or ion is increased. It means the substance that gives away electrons is oxidized. The iron reacts with water and oxygen to form hydrated iron(III) oxide, which results in rust formation. This reaction is responsible for the actual degradation of the mass of any corroding material or metal.

There are two forms of corrosion: dry and wet corrosion. Dry corrosion occurs when there is no moisture or water to aid corrosion. This type of corrosion occurs due to the direct chemical attack on metal surfaces by atmospheric gases such as oxygen, halogen, hydrogen sulphide, sulphur dioxide, nitrogen or anhydrous inorganic liquids present in the environment. This process is very sensitive to temperature and occurs at high temperature regimes, as can be demonstrated by holding a piece of metal to a flame and observing the layer of oxide that forms [9, 10]. Whereas, wet corrosion occurs in the presence of a liquid containing ions, an electrolyte. Seawater, chloride solutions and acids are some typical electrolytic environments in which wet corrosion occurs. This type of corrosion of metals occurs through electron transfer, involving two processes, oxidation and reduction. In oxidation, the metal atoms lose electrons. The surrounding environment then gains the electrons in reduction. The metal, where electrons are lost, is called the anode. The other metal, liquid or gas which gains the electrons is called the cathode. In short, a redox (Reduction–Oxidation) reaction in the presence of an electrolyte. It can be prevented by eliminating the moisture. The rate of corrosion is much faster in wet corrosion as compared to dry corrosion because in wet



Fig. 1 Schematic representation of the mechanism of reinforcement corrosion

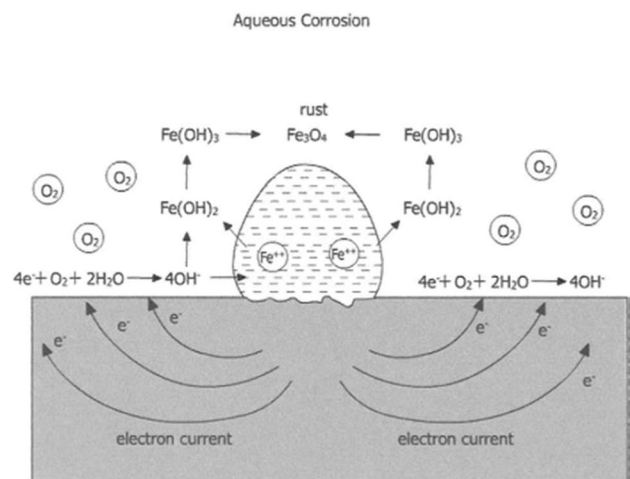


Fig. 2 Aqueous corrosion of iron (Source adapted from [12])

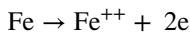
corrosion water acts as the electrolyte and thus facilitates the movement of electrons from anode to cathode. Zheng et al. in their recent study have effectively discussed the corrosion behavior of carbon steels used as pipeline material under wet H_2S environments. They have also enlightened the H_2S corrosion mechanisms with phase transitions of corrosion products and other iron sulphides [11]. In Fig. 1, deterioration of the iron rod in the aqueous electrolyte is being displayed.

1.2 Mechanism of Corrosion

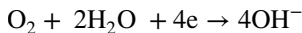
The mechanism of corrosion can be better understood with the help of Fig. 2 where a simplified mechanism of aqueous corrosion of iron is being displayed. In this figure, a metal surface is exposed to the atmosphere, there is only a limited quantity of water and dissolved ions are present, whereas the access to oxygen present in the air is unlimited. Corrosion products are formed close to the metal surface, unlike the case in aqueous corrosion, and they may prevent further corrosion by acting as a physical barrier

between the metal surface and environment, particularly if they are insoluble as in the case of copper or lead.

At the anodic areas, the anodic reaction takes place:



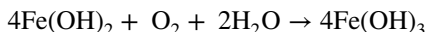
At the cathodic areas, reduction of oxygen takes place:



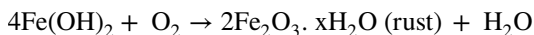
The OH⁻ ions react with the Fe⁺⁺ ions produced at the anode:



With more access to oxygen in the air, Fe(OH)₂ oxidizes to Fe(OH)₃ and later it loses its water:



Ferrous hydroxide is converted to hydrated ferric oxide or rust by oxygen:



The presence of soluble sulphate ions in the solution adversely affects the corrosion of iron. The sulphate ion continues to deteriorate iron and forms several pits on its surface. Layers of porous rust are formed in this case. The effect of SO₂ ions is illustrated in Fig. 3.

2 Corrosion Mitigation

Corrosion cannot be practically eliminated but may be controlled or inhibited up to some extent. The primary method for corrosion prevention is the use of green corrosion inhibitors as these are easily available, eco-friendly, non-hazardous as compared to commercially available toxic and hazardous chromatic inhibitors. Corrosion inhibitors can be defined as the chemical compounds that when added in small amounts to the environment, in which metal would corrode, corrosion inhibitors reduce, slow down, and prevent the corrosion rate of the metal.

Inhibitors work by adsorbing ions or molecules on metallic surfaces. They reduce the corrosion rate by;

- By blocking the anodic and/or cathodic reactions
- Reducing diffusion rate of reactants to the metal surface
- Reducing electrical resistance of the metal surface

There are also some specific categories of corrosion inhibitors such as organic and inorganic corrosion inhibitors. Organic compounds that consist of nitrogen, oxygen, and/or sulfur are considered as competent industrial corrosion inhibitors. These inhibitors inherit the ability to form a protective layer between the metal surface and corrosive environment through the adsorption process to delay the metal disintegration. Next, inorganic corrosion inhibitors contain the salts of zinc, copper, nickel, arsenic, and additional metals, with the arsenic compounds being the ones that are most commonly used. When these arsenic compounds are mixed with the corrosive solution, they scrape at the cathode cell of the unprotected metal surfaces. The plating reduces the percentage of hydrogen ion interchange due to the formation of iron sulfide amid the steel and acids that act as an obstacle. The reaction of an acid with iron sulfide is known as a dynamic process.

Throughout the work into the use of corrosion inhibitors, many researchers attributed the potential of corrosion inhibition to the donation of lone electron pairs to metal atoms. As a potent factor for showing corrosion inhibition, several organic heterocyclic compounds with heteroatoms such as O, S, N, and P were reported, respectively [13–17].

Among corrosion inhibitors “Green corrosion inhibitors” ideally plant extracts are of considerable importance, as there has been a rise in environmental concern and reforms in guidelines which due to their toxicity limit standard corrosion inhibitors [18]. Besides these all facts these also possess various advantages such as extracts of natural plants are environmentally friendly, non-toxic, readily available and relatively less expensive. They are also bio-sustainable and do not contain heavy metals or

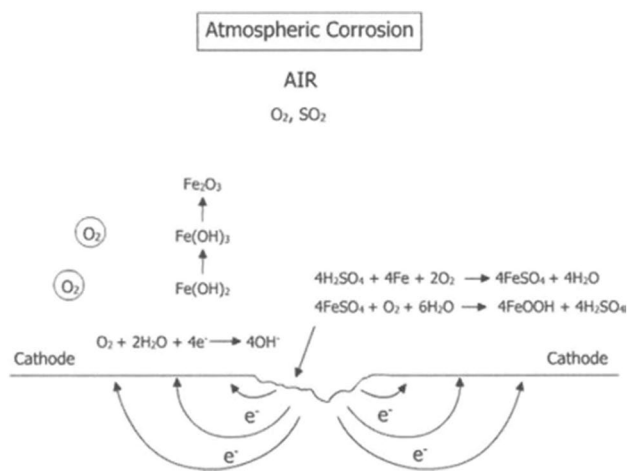


Fig. 3 Impact of SO₂ and humidity on metallic corrosion. The reaction occurs in a very thin (invisible) aqueous layer. (Source adapted from [12])

other toxic compounds. Additionally, plant extracts contain several simple to complex phytochemicals that have heteroatoms such as O, N, P, and S, which effectively get adsorbed on the surface of metals or alloys and thereby develop a layer of defensive film that protects the metallic surface against the corrosive ions and inhibit the corrosion rate [19]. Figure 4 showing the use of *Origanum vulgare* extract as a corrosion inhibitor for the metal which forms a defensive film on the metallic surface by the adsorption of its phytoconstituents on the surface.

Besides, this area is widely summarized in several review papers, book chapters in recent ones (published between 2017 and 2020): Some of them are;

- (a) Omnia S. Shehata, Lobna A. Korshed, and Adel Attia published a book chapter “Green Corrosion Inhibitors, Past, Present, and Future” in which they discussed the numerous natural products and their application in different processes, especially in steel reinforcement embedded in concrete [21]. Also, the green inhibitors behavior in different media and their protective role for different metals and alloys is discussed. Finally, industrial applications of vapor-phase inhibitors and their mechanisms are presented.
- (b) Marzorati et al. Trasatti published a review article “Green Corrosion Inhibitors from Natural Sources and Biomass Wastes” where they emphasize green chemistry based on the importance of protecting the environment and human health in an economically beneficial manner aiming at avoiding toxins and reducing wastes [21]. All the considerations listed are the focus of the

present review and are intended as a constructive critique to highlight the shortcomings of the green inhibitors in re-evaluating the literature and addressing future research that still needs rationalization in the field.

- (c) Lipiar K. M. O. Goni and Mohammad A. J. Mazumder explored their ideas about green corrosion inhibitor by writing a book chapter “Green Corrosion Inhibitors”. This chapter briefly discusses several types of corrosion inhibitors and their importance with a particular emphasis given on the several characteristic features of the green corrosion inhibitors reported in the literature as a comparison with organic inhibitors.

Here, in this article, we are exploring the recent advancements and work done in the field of green corrosion inhibitors from a period of 2005–2020. Additionally, we are discussing all corrosion monitoring techniques that includes destructive and non-destructive methods, and also the journey of using plant extracts as corrosion inhibitors will be briefly discussed from beginning to end which includes brief deliberation on several methods of extraction and various monitoring techniques.

2.1 Green Corrosion Inhibitors

The costs and adverse effects associated with industrial organic and inorganic inhibitors have raised significant concern in the field of corrosion prevention [22–30]. In this regard, there has been growing interest in the usage of green corrosion inhibitors. The title “green corrosion inhibitors” or “eco-friendly corrosion inhibitors” attests to those

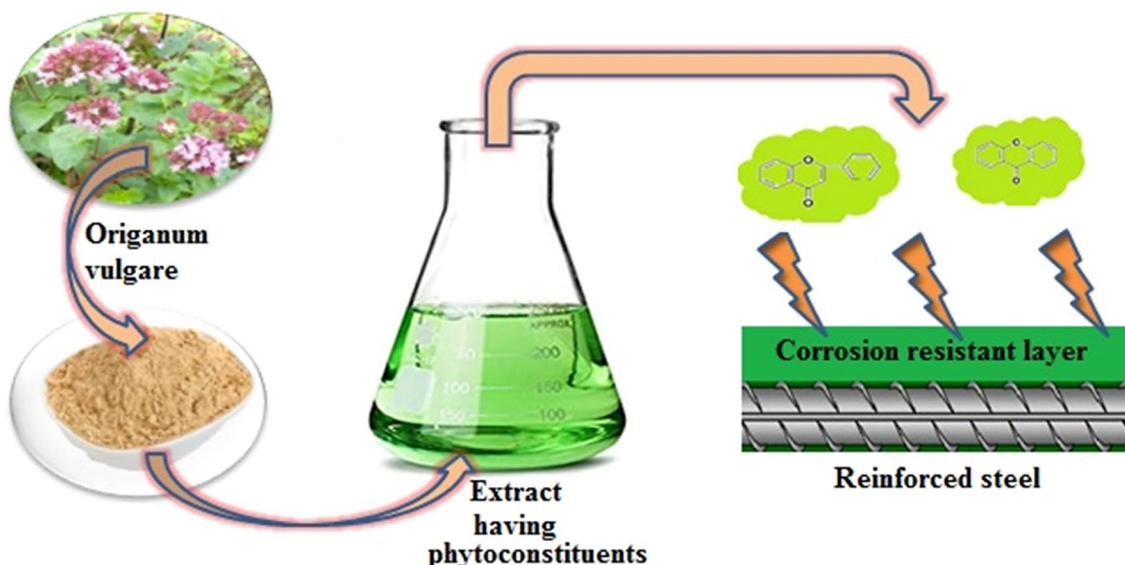


Fig. 4 The plant (*Origanum vulgare*) extract used as a corrosion inhibitor for reinforced steel which develops a layer resistant to corrosion (Source adapted from [20])

substances which have biocompatibility in nature [22]. In 1930, Celandine (*Chelidonium majus*) plant extracts (dried leaves, flower, root, and seeds) were used in the H_2SO_4 pickling bath. As an additive, ZH-1 consists of a finely divided oil cake that was developed to control corrosion through the use of a by-product formed in the phytin manufacture.

The green corrosion inhibitors such as plant extracts presumably possess biocompatibility due to their biological origin. In addition to the environmentally friendly and ecologically acceptable characteristics of plant extracts, these extracts have other advantages too such as low-cost, found abundantly, simple production procedures, readily available and renewable sources. These characteristics are justified by the abundant phytochemical constituents of the extracts, sharing many similarities with the molecular and electronic structures of conventional organic corrosion inhibitors, providing them the ability to adsorb onto metal surfaces. Plant extracts to be used as corrosion inhibitors can be readily produced by a common procedure: first, the plants are dried in sunlight or shade, then powdered. The powder derived from the plants is soaked in a solvent (distilled water, alcohol, or acidic solution, etc.) then refluxed for a few hours; after refluxing, the solution is cooled, filtered, and concentrated. Finally, the residue is diluted to the desired concentration for further use as a corrosion inhibitor [31]. Extracts from their leaves, barks, seeds, fruits and roots comprise mixtures of compounds having several phytochemical constituents like alkaloids, anthraquinones, polyphenols, flavonoids, saponin, proteins, amino acids, glycosides containing heteroatoms such as sulfur, nitrogen, oxygen atoms and have triple/conjugated double bonds of aromatic rings in their molecular structures that often reported to function as effective inhibitors of metal corrosion in different aggressive environments [32–36]. Due to the presence of lone pair electrons of heteroatoms and their interaction with the vacant d-orbital of the metal to be protected, these heteroatoms latterly get adsorbed on the metal surface and create a dense protective coating which effectively mitigates corrosion [37–39]. In Fig. 5. various forms of green corrosion inhibitor are displayed.

The number of published papers (patents included) on the topic “green corrosion inhibitors”, as obtained through a SciFinder® literature review, is represented in Fig. 6. The increase in the publication from 1940 to 2018 shows an exponential trend.

2.1.1 Mechanism of Corrosion Inhibition

The mechanism of corrosion inhibition involves the adsorption of inhibitors on the metallic surface. Various factors, such as the nature and charge of the metal, the chemical composition of the inhibitor such as the availability of functional groups, aromaticity, potential steric effects, and the form of aggressive electrolyte, affect the adsorption process.



Fig. 5 Different sources of green corrosion inhibitor

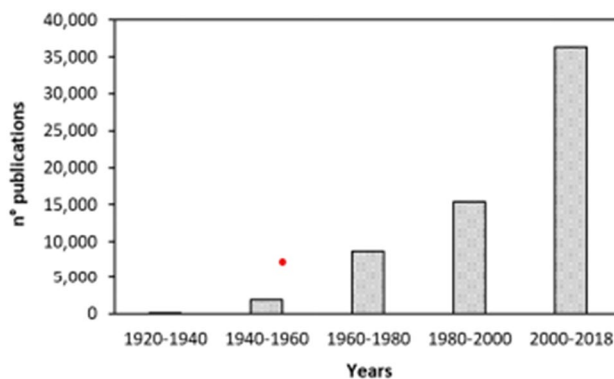


Fig. 6 The number of publications per 20-year-range from 1920 to 2018. (Source adapted from [21])

Some decisive factors contributing to the effectiveness of corrosion inhibition are the presence of heteroatoms, size of the organic molecule, the aromaticity and/or conjugated bonding, carbon-chain length, bonding strength to a metal substrate, the type and number of bonding atoms or groups in the molecule, the ability for a layer to become compact or cross-linked, the ability to form a complex with the atom as a solid within the metal lattice, and adequate solubility in the environment. Organic compounds containing N, S, or O atoms in their structures, functional electronegative groups, and π electrons in triple or conjugated double bonds are the essence of effective inhibitors. The inhibition potential of these organic compounds via an adsorption mechanism can be due to their interactions with the metal surface. Faiz et al.

[40] in their study of natural products extracted three alkaloids and explained the adsorption behavior of inhibitors on mild steel surface as shown in Fig. 7 in which the inhibition effects studied alkaloids were determined by the interaction between p electrons of phenyl rings and p-electrons from the electron donor groups (N and O) with the vacant d-orbitals of metal by which they form an insoluble, stable and uniform thin defensive film on a mild steel surface.

Corrosion inhibitors can form either a strong coordination bond with the metal atom or a passive film on the surface. The values of inhibition efficiency depend essentially on the electron density at the active center of the inhibitor molecule. The corrosion inhibition of metal may involve either physisorption or chemisorption of the inhibitor on the metal surface. The physisorption process of inhibition results from the electrostatic interactions usually van der Waals forces between electric charges of inhibitor molecules and the steel surface. This process is determined from the values of standard free energy (ΔG°) values that are over -20 kJ/mol with

an application of different adsorption models with coefficients of determination near to 1. Donor–acceptor interactions between free electron pairs of heteroatoms and π electrons of multiple bonds and vacant d-orbitals of metal result in the chemisorption of inhibitors. Strong changes have been observed in the electronic structure/electron density of the adsorbate molecule (>0.5 eV/surface site). Chemisorption has an irreversible aspect and high pressure is therefore desired. Chemisorption adsorption enthalpy is elevated to approximately 80 to 240 kJ/mol due to chemical bonding.

Bui et al. [41] studied the inhibition efficiency of Limonene, extracted from orange peel for steel corrosion in 1 N HCl solutions. The structure of Limonene can be seen in Fig. 8. In Limonene's structure, C–C, C=C, and C–H bonds are shown. The adsorbed film, however, contains other adsorbed groups, such as C=O, O–H, and C–O–C, suggesting that other active organic compounds are also present in the extract. It is therefore can be concluded that the presence of limonene and other compounds results in

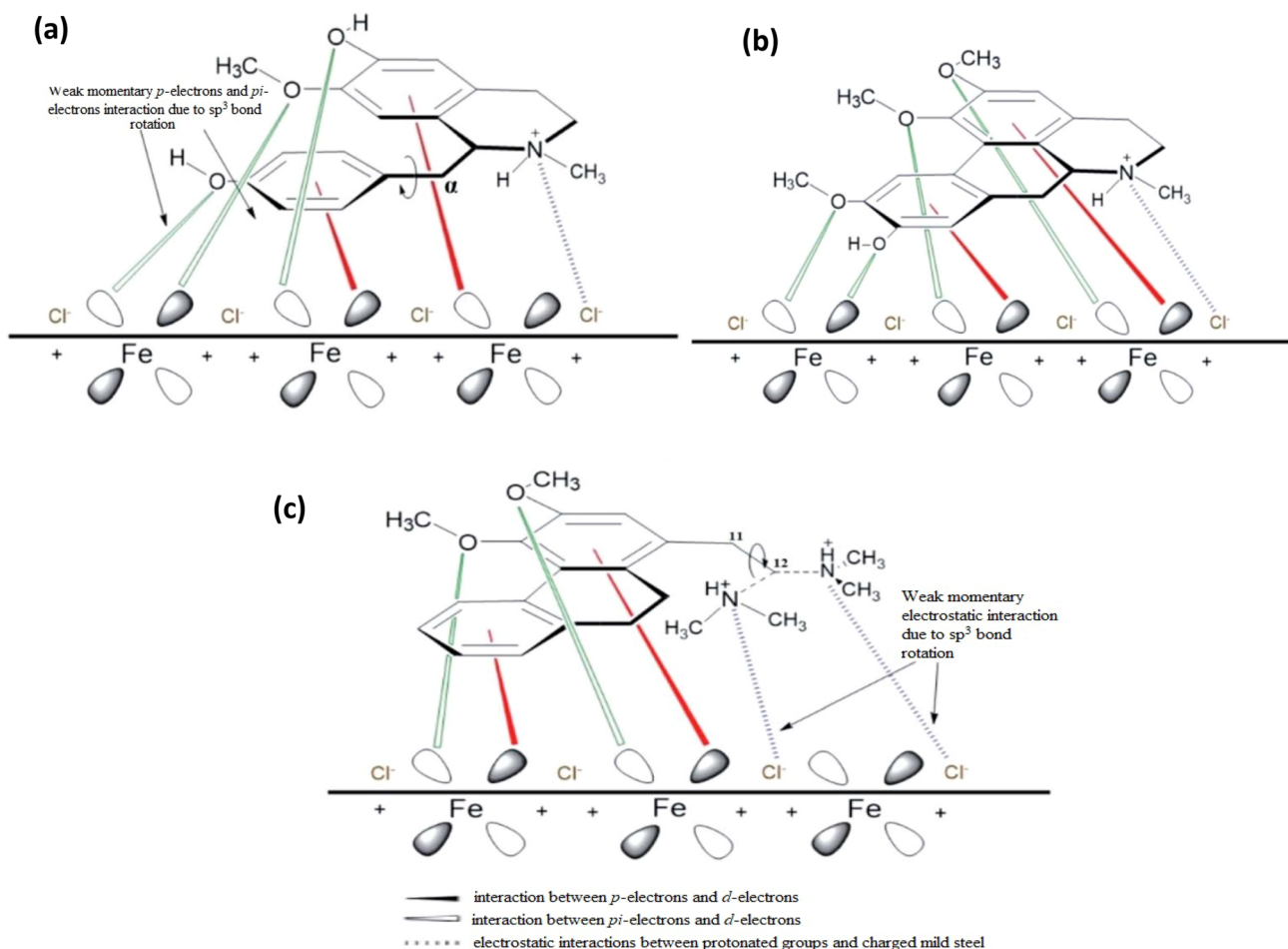


Fig. 7 Corrosion inhibition impact of crude extracts (hexane, dichloromethane, methanol) from the bark of *Cryptocarya nigra* and three alkaloids identified **a** N-methylisococlaurine, **b** N-methylaurotetanine and **c** atherosperminine extracted from the extract of *Cryptocarya nigra* dichloromethane (CNDE) tested for mild steel corrosion in 1 M HCl solution. (Source adapted from [40])

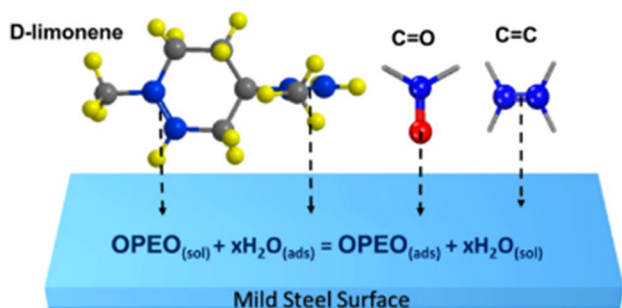


Fig. 8 The adsorption of OPEO extract (and constituent structures present in its extract) on the mild steel surface (Source adapted from [41])

the corrosion inhibition of mild steel in HCl acidic media. Besides, organic compounds in acid media can be acidified or participate in the formation of by-products or intermediates in physiochemical reactions that may function as secondary steel corrosion inhibitors in acid solutions. The adsorption of the extract on the steel surfaces can be visualized by D-Limonene adsorption and several other attribute bonds in extract constituents containing three elements, viz., C, H and O and functional groups such as C=C, C=O, O-H, -O- and aromatic rings as shown in Fig. 8. This figure explains the limonene adsorption model using two C=C bonds at carbon positions 3–4 and 8–9, as well as the adsorption model of the C=C and C=O bonds in the mild steel surface OPEO constituents. The corrosion inhibition was investigated with Potentiodynamic polarization where both cathode and anode branches of the Tafel curves shift towards the direction of lower current density. This demonstrates that OPEO alleviated anodic dissolution reactions and arrested cathodic hydrogen evolution reactions. This may result from the adsorption of OPEO on the whole corroding surface. Accordingly, OPEO worked as mixed inhibitors and restricted corrosion of the mild steel in the 1 N HCl acid.

Deyab [42] explained the inhibition of aluminum in biodiesel by Rosemary extract based on the adsorption of the organic compounds carnosol ($C_{20}H_{26}O_4$) and carnosic acid ($C_{20}H_{28}O_4$); flavonoids such as genkwanin ($C_{16}H_{12}O_5$), cirsimaritin ($C_{17}H_{14}O_6$) or homoplantagin ($C_{22}H_{22}O_{11}$); and triterpenes such as ursolic acid ($C_{30}H_{48}O_3$). The mechanism of inhibition can be explained based on the adsorption of the organic compounds present in Rosemary extract on the aluminum surface. Many of the organic compounds have at least one polar unit with atoms of nitrogen, sulfur, oxygen and in some cases phosphorous. The polar unit is regarded as the reaction center for the adsorption process. In this case, the author has discussed four types of adsorption that may take place involving organic molecules at the metal solution interface: (i) electrostatic attraction between charged molecules and the charged metal, (ii) interaction of π -electrons

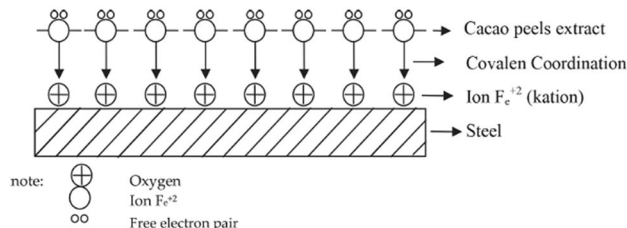


Fig. 9 Adsorption mechanism of cacao peel extracts on a mild steel surface. (Source adapted from [43])

with the metal, (iii) interaction of uncharged electron pairs in the molecule with the metal and (iv) a combination of the above.

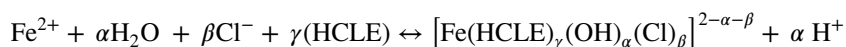
The extract inhibits corrosion by regulating both cathodic and anodic reactions. At cathodic sites on the metal surface, protonated species were frequently adsorbed and thus delayed the reaction of hydrogen evolution, which is possibly responsible for the pronounced cathodic inhibiting effect of rosemary extract. The adsorption of organic compounds present in extracts on anodic sites occurs by a lone pair of electrons on oxygen atoms. Therefore, the addition of Rosemary extract to biodiesel retards the biodiesel oxidation and hence decreases the corrosive action of biodiesel on the aluminum metal.

Yetri et al. [43] used the theobroma cacao peel extract as the eco-friendly corrosion inhibitor for mild steel. The corrosion inhibition takes place by the adsorption of inhibitor molecules and constituent structures that are present in the extract such as catechin, kaempferol, gallic acid, procyanidin, and tannin on the mild steel surface. This adsorption is due to the force of adhesion between the inhibitor and the surface of mild steel that occurred through functional group adhesion on the metallic surface. The inhibition process might appear due to the presence of phytochemical constituent adsorption through an oxygen atom and/or nitrogen atom on the metal surface. Possibly, this complex is absorbed into the steel surface through Van der Waals forces to form the protection layer to prevent the steel from corrosion. The bond existed on the mild steel surface during the inhibitor adsorption process as a coordination covalent bond involving chemical adsorption. The basic adsorption mechanism of cacao peel extracts on a mild steel surface can be seen in Fig. 9.

Nazari et al. [44] in his study of corrosion protection of steel in chloride solution by an apple-based green inhibitor revealed the effect of major constituent 1-Linoleoyl-sn-glycero-3-phosphocholine ($C_{26}H_{50}NO_7P$) in the inhibition properties of apple-based green inhibitor. The $C_{26}H_{50}NO_7P$ containing N, P, and O elements have polar functions, so get adsorbed onto the metallic surface forming a barrier organic layer and also responsible for transforming Fe_3O_4

into a more corrosion-resistant iron oxide layer (Fe_2O_3). The adsorption of the polar atoms on the surface of metal may occur through coordination between the lone pair or π -electrons cloud and the metallic surface. APE molecules, via their high electron density locations, are bound to the surface of the steel. The interaction of nonbonding electrons on nitrogen and oxygen with the steel surface entails the adsorption of APE. Higher charge transfer resistance (R_{ct}) and coatings resistance (R_f) values were correlated with more APE, demonstrating the creation of a more protective surface layer. (Note: The R_{ct} is a function for the electrochemical corrosion reaction intensity at the coating/metal interface. The higher value of R_{ct} reflects the higher integrity of the coating system and then the slower rate of corrosion reactions under the coatings. Therefore, the greater is the R_{ct} value, the greater will be corrosion inhibition effect of the inhibitors. Whereas, in the case of higher values of R_f , the rate of the solution permeation into coatings will be reduced, due to the existence of a defensive layer of coating on the metallic surface by inhibitor molecules by adsorption).

Le Thanh Vu [45] studied the corrosion inhibition of *Houttuynia cordata* leaf extract for steel in an HCl medium in which it was found that *H. cordata* leaf extract has diverse organic compounds containing multiple bonds and functional groups. The quantum chemical calculation showed that when the inhibitor interacts with the steel substrate and acidic solution, key positions are formed by the effects of highly electronegative C, O, N, P, and π -conjugated bonds, as well as heterocycles on the organic frameworks play different roles in donating or consuming electrons. HCLE's corrosion resistance on the steel surface is shown in two ways. First, nitrogen and oxygen from heterocyclic compounds and functional groups as well as hydrocarbon branch binding sites with functional groups tend to bind to positive H_3O^+ ions to minimize their impacts on the steel surface and also serve as a bridge to Fe^+ ions for the formation of the protective film from the solution/steel substrate interface. Secondly, functional groups comprising strongly electronegative N and O atoms and sigma bonds near them were electron-consuming places to trap negative Cl^- ions, helping to avoid localized corrosion acceleration on the steel surface. The reduction of the interaction of the active ions H_3O^+ and Cl^- on the steel substrate and the existence of protective film formation also limit the process of charge transfer at the solution/steel substratum interface. The reactions for adsorption of HCLE inhibitor on the steel surface are thus suggested:



It is inferred that the film formation of precipitated $[\text{Fe}(\text{HCLE})_\gamma(\text{OH})_\alpha(\text{Cl})_\beta]^{2-\alpha-\beta}$ species on the surface of

steel is responsible for the achieved effective corrosion inhibition.

After the brief review and understanding the corrosion inhibition mechanism, there are some crucial points every researcher should think before selecting the suitable "green corrosion inhibitors" for their study.

- (a) The first step is to choose the part of the plant with the major concentration of active compounds of interest.
- (b) Then the screening of the particular obtained extract should be done to get details about the several phytoconstituents and heterocyclic organic compounds present in the extract.
- (c) The heterocyclic organic compounds should contain N, S, or O atoms with lone pair of electrons in their structures, functional electronegative groups, and π electrons in triple or conjugated double bonds to exhibit effective inhibition. (The mechanism of corrosion mechanism based on these terms has been discussed above in several cases).

2.2 Prominent Metrics for Extract Preparation

2.2.1 Extraction

Extraction plays an important role and is regarded as the first step toward the separation of the essential active phytoconstituents such as saponin, tannin, quercetin, flavonoid from the plant raw material. The most frequently used process is the extraction with solvents. Generally, a natural product extraction comprises the following steps: solvent perforates into the solid substrate > solute get dissolves in the solvent > solute to get diffused from solid substrate > finally extracted solutes are obtained. The variations in various extraction techniques that directly impact an extract's quantity, quality, and composition depend on various factors such as extraction type, extraction period, temperature, solvent nature, solvent concentration, and polarity of the solvent.

Plant Material Bioactive phytoconstituents can be attained from any part of the plant such as barks, leaves, flowers, fruits, seeds, roots as shown in Fig. 10 [46]. The characteristics of a formidable solvent in extraction procedure usually involve qualities such as non-hazardous nature, low heat requirement for evaporation, rapid physiological absorption of the extract, conservative action, and ineffective to cause complexity or dissociation of the extract. The solvent selection also impacts the extraction of aimed active

phytoconstituents whereas the alteration in the method of extraction normally depends on the time required for the

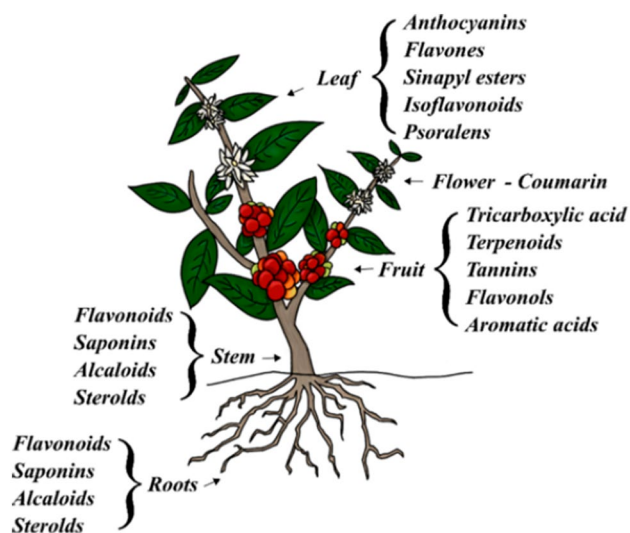


Fig. 10 Basic parts of a plant and its common active compounds. (Source adapted from [47])

extraction period, selected solvent, solvent pH, solvent-to-sample ratio, and temperature maintained during the extraction procedure.

The core part is the refined grinding of the plant material (dry or wet) that increases surface area for extraction and therefore results in increasing the extraction rate [48–50]. Various researches indicated that the solvent-to-sample ratio of 10:1 (v/w) should be ideally preferred.

Various solvents used for the extraction of active components are: Water, Methanol, Acetone, Ethanol, Chloroform and Ethyl acetate.

2.2.2 Pre-extraction of Plant Sample

The plant parts such as barks, leaves, roots, flowers, fruits can be obtained from fresh and dried plants. Some preparation techniques such as grinding and drying also have a significant effect on preserving phytochemicals in the extracts.

Fresh vs. Dried Samples Both the fresh and dried samples can be used in the procedure. Instead of fresh samples, several researchers prefer the dried sample because fresh samples are frail and likely deteriorate more rapidly than dried samples. Whereas, a comparative study of various samples of plants for both fresh and dried leaves found no notable effect in total phenolic content but found higher flavonoid content in the case of dried samples.

Grinded vs. Powdered Samples The reduction in the particle size increases the surface contact among solvent and sample used for extraction. Grinding has culminated in coarser, finer samples; whereas, powdered samples provide a generally homogenized and finer material, resulting in better surface contacts with the solvent. This preparation method is

essential for the efficient extraction where solvent contact the targeted analytes (also particle size < 0.5 mm is advisable).

Air-Drying Air-drying generally takes 3–7 days and sometimes up to months depending upon the type of dried samples (e.g., leaves, roots, seeds). This process does not include the use of high temperature to dry plant materials; due to which heat-sensitive compounds are conserved.

Microwave-Drying Microwave-drying involves electromagnetic radiation that has electrical as well as magnetic fields. The electrical field induces concurrently heating by dipolar rotation; synchronization of molecules with a dipole moment (e.g. solvent) on the electrical field, and ionic induction that creates molecular oscillation [51]. This method may have less drying duration but frequently cause phytochemicals to degrade.

Oven-Drying This is a simple and fast method to get dry plant material. Nevertheless, the drying effect on the sample shows no significant effect on the antioxidant activity but the content of bioactive phytochemicals such as tannins and saponin was affected by oven drying, proposing the temperature sensitivity of the compounds.

Freeze-Drying This process is based on the sublimation principle that converts a solid into a gas without reaching the liquid state. Before lyophilization, the sample containing any fluid (e.g. solvent, moisture) is frozen at -80 °C to -20 °C to make the sample solidify. Following a freezing overnight (12–14 h), the sample is instantly lyophilized to prevent the melting of frozen liquid [32, 48–50, 52–54]. To stop sample loss during the process, the mouth of the equipment containing the sample is covered with a parafilm. This method is confined to fragile, heat-sensitive materials.

2.2.3 Methods of Plants Extraction

Hot Continuous Extraction (Soxhlet) In this procedure, the coarsely ground raw product is inserted in a permeable container or "thimble" formed of formidable filter paper embedded into the chamber of the Soxhlet apparatus. In a flask, the solvent being used for extraction is heated, and its vapors condense in the condenser. The condensed solvent drips into the thimble containing the crude plant raw material [55]. When the liquid level in the chamber rises to the top of the siphon tube, the liquid content of the chamber siphon falls back into the flask. This method is continuous and is conducted until a drop of siphon tube solvent leaves no trace when evaporated. The soxhlet apparatus is being displayed in Fig. 11.

Ultrasound-Assisted Extraction (UAE) or Sonication Extraction The mechanical effect of ultrasonic acoustic cavitation improves surface contact between solvents and materials, and cell wall permeability; the apparatus can be seen in Fig. 12 [56]. The physical and chemical properties of the products subjected to ultrasound are altered and disturbed to

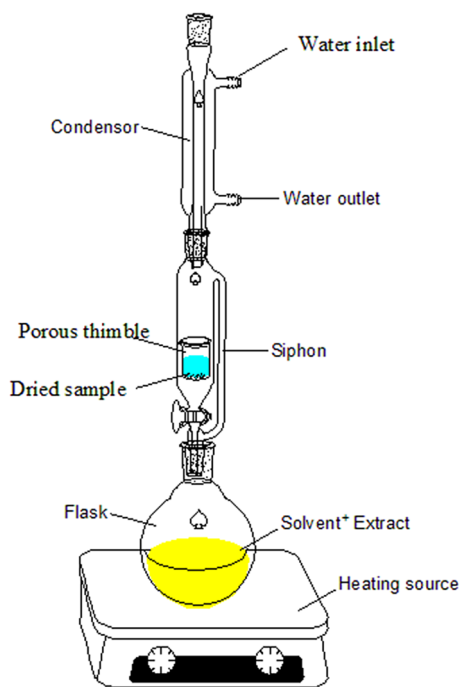


Fig. 11 Extraction of active phytochemicals from plant dried sample by Soxhlet apparatus

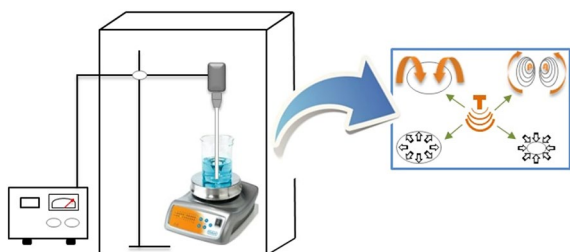


Fig. 12 Schematic representation of the ultrasound-assisted extraction (UAE) process used in the extraction technique. (Source adapted from [57])

the plant cell wall; enabling the release of compounds and improving the mass transfer of the solvents into the plant cells.

Supercritical Fluid Extraction (SFE) Supercritical fluid are also labeled as dense-gas is a process that contains both gas and liquid physical characteristics at its critical stage as shown in Fig. 13; the instrument used for supercritical fluid extraction (SFE). Interest in Supercritical CO₂ (SC-CO₂) extraction is widely accessible and affordable and has low toxicity due to the excellent solvent for non-polar analytes.

Maceration In this method, plant material or specific part is soaked in a halted jar filled with a solvent and permitted to stand at room temperature for 2–3 days. The process is aimed at softening and breaking down the cell wall of the plant to unleash the soluble phytochemicals. The mixture

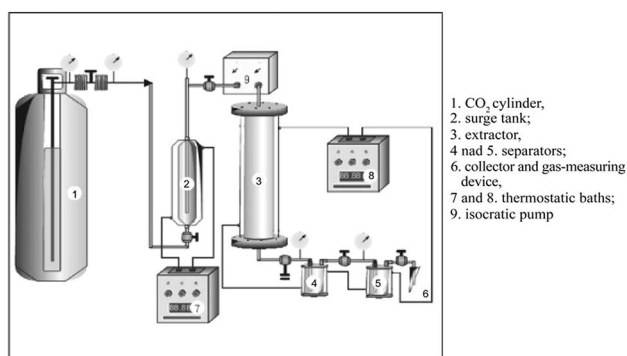


Fig. 13 Representation of supercritical fluid extraction (SFE) instrument (Source adapted from [58])

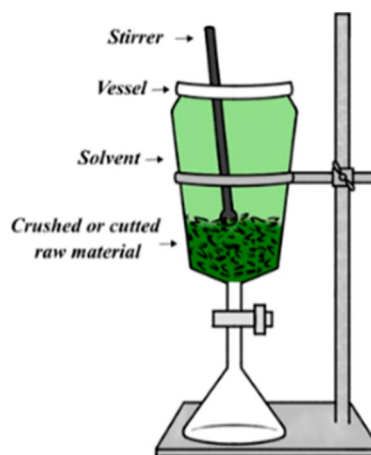


Fig. 14 Maceration procedure for extraction (Source adapted from [47])

is then pressed or strained by filtration after 3 days. Then the heat is transferred via the convection and conduction method. The quality of extracted compounds is generally influenced by the selection of relevant solvents. The diagrammatic representation can be seen in Fig. 14.

Decoction This method is only effective in extracting heat-stable compounds, raw plant parts (e.g., barks and roots), as shown in Fig. 15 where the aqueous decoction of plant raw material is done with oil-soluble compounds compared to infusion and maceration.

Counter-Current Extraction: In this process, the material to be extracted is shifted in one direction inside a cylindrical extractor where it comes into contact with the extraction solvent as seen in Fig. 16. The more the substance begins to flow, the more concentrated the extract becomes. Thus complete extraction is possible if the solvent and material quantities and their flow rates are configured [56, 59–61].

Pressurized Liquid Extraction (PLE) Various researchers have identified PLE as rapid solvent extraction and high pressure solvent extraction. The PLE instrument and process

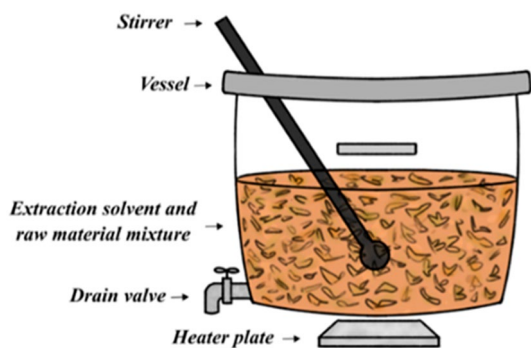


Fig. 15 The aqueous decoction of plant raw material (Source adapted from [47])

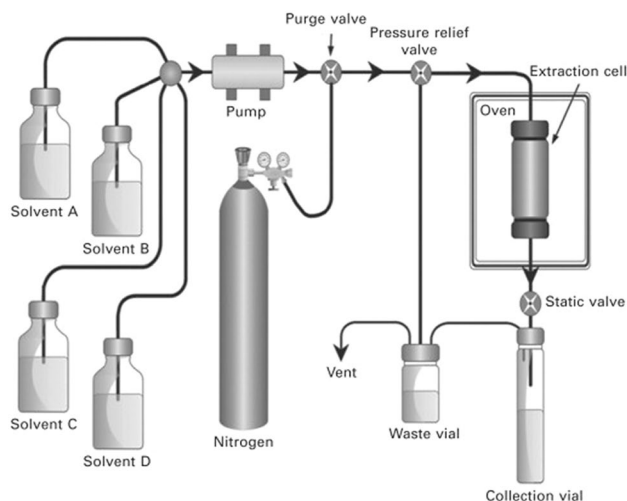


Fig. 17 Pressurized liquid extraction (PLE) process. (Source adapted from [62])

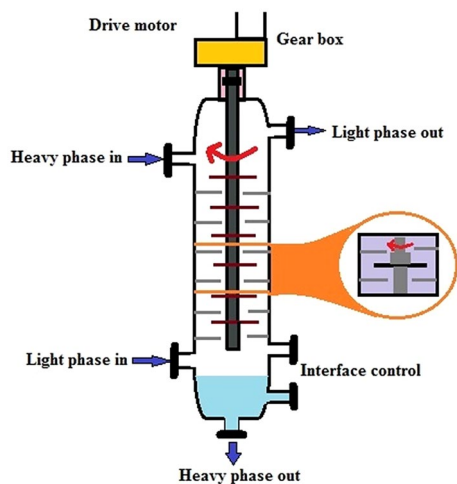


Fig. 16 Counter-current extraction apparatus

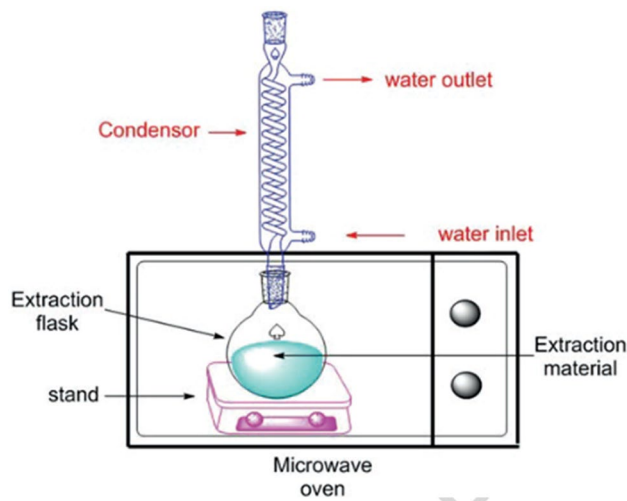


Fig. 18 Microwave-assisted extraction (MAE) extraction procedure (Source adapted from [63])

have been displayed in Fig. 17. In extraction, PLE imposes high pressure. High pressure holds solvents beyond their boiling point in a liquid state, leading to high solubility and higher incidence of lipid solvent diffusion in solvent and higher penetration of solvent into the matrix.

Microwave-Assisted Extraction (MAE) In MAE, heat and mass transfer relies on the same axis, creating a synergistic impact that accelerates extraction and improves extraction yield. MAE has several advantages such as increased extract yield, reduced thermal decay, and targeted material heating. MAE is often revalued as the green mechanism, as it eliminates the use of organic solvent. An MAE extraction instrument can be easily understood in Fig. 18.

3 Plant Extracts as Corrosion Inhibitors for Metals and their Alloys

Corrosion inhibitors have been in use since the nineteenth century. Vegetables, fruits and their waste, extracts from plants and oils are being used as corrosion inhibitors. Numerous parts of the plant such as stem, flower, bark, root, leaves, whole plants often used as corrosion inhibitors. The specific part or whole plant is dried for approx. 2–3 weeks in shadow dry condition [64, 65]. Afterward, extraction of the essential phytochemicals by different methods discussed above is practiced. The adsorption of

natural corrosion inhibitors on the metal surface is influenced by several factors, which include metal composition, test solution, the chemical structure of inhibitor, inhibitor moieties, additives, mixture temperature, and concentration of the solution. Xhanari et al. [66] in their review article in RSC Advances represented a pie chart as shown in Fig. 19 where they show the distribution of the research work performed in the last two decades on natural products as corrosion inhibitors for aluminium and its alloys presented in their review article. Through the pie chart, it is observed that plant extracts particularly in the case of aluminium alloys have been used at the rate of 68% as others lying far away in usage level. It indicates how often plant extracts are being immensely used in the field of corrosion inhibitors.

3.1 Plants Extracts as Corrosion Inhibitors for Mild Steel: HCl and H₂SO₄ System

Due to its superior mechanical properties and thermal conductivity, mild steel is globally used for the manufacturing of reactors, storage vessels, gathering pipelines, drilling equipment, and other apparatuses. Mild steel corrosion occurs commonly in acidic solutions during pickling, scale-removal, and rust-cleaning procedures, resulting in metal deterioration and massive economic losses [67–70]. The application of corrosion inhibitors is a frequently implied convenient technique for the corrosion protection of mild steel. Natural products such as plant extract, amino acids,

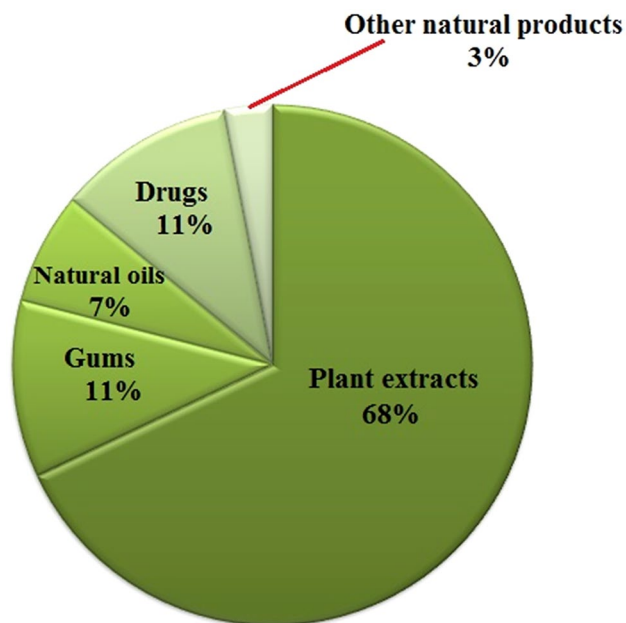


Fig. 19 A pie chart showing percentage-wise usage of various green corrosion inhibitors at the global level (Source adapted from the [66])

proteins, and natural polymers have been claimed to be effective corrosion inhibitors. Among these, plant extracts are regarded as a significant source of naturally modulated chemical compounds that can be extracted at a reasonable cost through simple procedures. These natural extracts are similar to the organic synthetic inhibitors and are known to serve almost as well as their synthetic equivalents. In the acid concentration range (0.1–2 M) studied, plant parts extracts are effective corrosion inhibitors behaving mostly as a mixed type corrosion inhibitor and following Langmuir adsorption isotherm exhibiting maximum inhibition efficiency up to >95% (Tables 1 and 2). Down below Fig. 20 illustrates the adsorption of phytochemicals derived from plant extract forming a protective layer on the mild steel surface.

3.2 Plant Extracts as Corrosion Inhibitor for Stainless Steel in Acidic Media: HCl and H₂SO₄ System

Stainless steels is iron-based alloy containing at least 10.5% chromium and the highest of 1.2% carbon. Due to its resistant properties to corrosion in both manufacturing and coastal realms, this metal is used in several industrial and domestic applications such as piping systems, steam turbines, containers and food processing vessels, chemical, pharmaceutical, paper, and pulp, as well as other industrial purposes. Stainless steel is coated with a highly protective chromium oxyhydroxide film, which is resistant to corrosion in many aggressive environments. Hydrochloric acid is widely used in industries for removing harmful oxide films and components of corrosion on the steel surface. Corrosion inhibitors are used to prevent the excessive dissolution of metals and the impact of acid during the cleaning process. This intends for several researchers worldwide at finding inexpensive, environmentally friendly, non-toxic natural compounds that could be used in an acidic solution for corrosion protection during acidization and stainless steel acid pickling [120]. Figure 21 and Table 3 show the efficiency and adsorption of active phytochemicals/constituents present in the plant extract; which develop a protective layer on the metallic surface and inhibits the corrosion in corrosive media.

3.3 Plant Extract as Corrosion Inhibitor for Aluminium and Alloys: HCl, H₂SO₄, NaOH System

Aluminium is used for several different purposes such as spanning from wrapping foils, to high-tech applications in aerospace engineering, space programs, energy sources, and electronics in every engineering field. Most aluminium alloys have a strong resistance to corrosion against natural atmospheric conditions and other constraints because

Table 1 Plant extracts as corrosion inhibitors in hydrochloric acid solution involving various plants, techniques, nature of metal and electrolyte and nature of the adsorption of active phytoconstituents

Plant name	Part used	Techniques	Metal and electrolyte	Nature of adsorption	Remark	Refs.
<i>Pongamia pinnata</i>	Seeds	Weight loss method (WL), electrochemical impedance spectroscopy (EIS), Fourier transform infrared spectroscopy (FTIR)	Mild steel/1 M HCl	Langmuir adsorption isotherm	6-methoxy-2-phenyl-4H-furo[2,3-h]chromen-4-one and 2-(benzo[d][1,3]dioxol-5-yl)-4H-furo[2,3-h]chromen-4-one are the main active constituents	[71]
<i>Urtica dioica</i> L	Leaves and stems	EIS, potentiodynamic polarization measurement (PDP), energy dispersive X-ray spectroscopy (EDS), atomic force microscopy (AFM), scanning electron microscopy (SEM)	Mild steel/1 M HCl	Langmuir adsorption isotherm	Maximum efficiency of 92.24% was achieved at 0.3 g/L inhibitor conc. at 40 °C	[72]
<i>Nyssa fruticans</i> wurrmb	Leaves	WL, FTIR	Mild steel/0.1 M HCl	NA	The highest inhibition efficiency of 75.11% was observed using <i>N. fruticans</i> extract	[72]
<i>Oxandra asbeckii</i>	Leaves	EIS, PDP	Mild steel/1 M HCl	Langmuir adsorption isotherm/ mixed type inhibitor	Oxoaporphinoid alkaloids as liriiodenine, azafluorenones alkaloids are the main active constituent of <i>O.A</i>	[73]
<i>Origanum Vulgare</i>	Whole plant	WL, EIS, PDP, SEM, density functional theory (DFT)	Mild steel/1 M HCl	Langmuir adsorption isotherm	Maximum efficiency of 91.2% at 1000 mg/L inhibitor conc. at 30 °C was achieved	[64]
<i>Telfaria occidentalis</i>	Leaves	WL, electrochemical frequency modulation trend (EFMT), Hydrogen evolution	Mild steel/2 M HCl	NA	Synergistic effects increased the efficiency of the extract in the presence of halide additives in the order $KCl > KBr > KI$	[74]
<i>Murraya koenigii</i>	Leaves	WL, EIS, PDP, X-ray photoelectron spectroscopy (XPS)	Mild steel/1 M HCl	Langmuir adsorption isotherm	Main constituents of <i>Murraya koenigii</i> leaves are murrayaline-I, pyrayafoline-D and mahabamine-A	[75]
<i>Euphorbia falcata</i>	Leaves	PDP, EIS, SEM	Mild steel/1 M HCl	Langmuir adsorption isotherm	Maximum I.E. (%) of 93% is achieved at 3.0 g/L	[76]
<i>Capsicum annuum</i>	Fruit	WL, EIS, SEM	Mild steel/1 M HCl	Langmuir adsorption isotherm	Maximum efficiency of 85% found at 1400 mg/L inhibitor concentration	[77]
<i>Glycine max</i> leaves	Leaves	WL, SEM, EDS, X-ray powder diffraction (XRD), FTIR	Mild steel/0.5 M HCl	Langmuir adsorption isotherm	Optimum inhibition efficiency reached up to 91.07% at 2 g/L (308 K). Genistein and daidzein are the two major phytochemical components present in the extract	[78]
<i>Mollugo cerviana</i>	Fruits	WL, EIS, SEM	Mild steel/1 M HCl	Langmuir adsorption isotherm	<i>Mollugo cerviana</i> extract acts as a good inhibitor for the corrosion of mild steel in 1M HCl solution	[79]

Table 1 (continued)

Plant name	Part used	Techniques	Metal and electrolyte	Nature of adsorption	Remark	Refs.
Nutmeg	Oil	EIS, DFT, Monte Carlo simulations (MC)	Carbon steel/1.0 M HCl	Langmuir adsorption isotherm	Peak efficiency of 94.73% at 500 ppm nutmeg oil was achieved	[80]
Musa paradisiaca	leaves	WL, AFM, EIS, FTIR, high performance liquid chromatography (HPLC)	Mild steel/1 M HCl	Langmuir adsorption isotherm	The maximum corrosion inhibition efficiency (about 88%) and surface coverage (about 72%) were obtained in the presence of 800 ppm Glycyrrhiza glabra leaves extract after 24 h immersion	[81]
Aloe vera	Whole plant	WL, PDP, EIS	Mild steel/0.2 M HCl	Mixed type inhibitor /Langmuir adsorption isotherm	The inhibition efficiency value increases with increased concentration of the extract, although its efficiency decreases with higher temperature	[82]
Euphorbia falcata	Leaves	WL, EIS, SEM	Mild steel/1 M HCl	Langmuir adsorption isotherm	The corrosion inhibition efficiency increases with increasing EFE concentration, and the maximum efficiency of 93% was achieved at 3.0 g/L	[76]
Ananas sativum	Leaves	WL, EIS	Mild steel/0.1 M HCl	Langmuir adsorption isotherm	Plant extracts disrupts metallic corrosion by getting adsorbed on the metallic surface	[83]
Andrographis paniculata	Leaves	FTIR, EIS	Mild steel/1 M HCl	Langmuir adsorption isotherm	Mahabinine and Brucine are the two major phytochemical constituents present in the extract	[84]
Justicia gendarussa	Leaves	WL, EIS, FTIR	Mild steel/1 M HCl	Langmuir adsorption isotherm	Inhibition efficiency of 93% was achieved with 150 ppm JGPE conc. at 25 °C	[85]
Tiliacora acumminata	Leaves	WL, SEM, XRD, EIS	Mild steel/ 1 M HCl	Langmuir adsorption isotherm	Maximum efficiency of 93.02% at the highest concentration of 320 ppm at 333 K was achieved	[86]
Moringa oleifera	Fruits	WL, EIS, PDP	Mild steel/1 M HCl	Langmuir/ Temkin adsorption isotherm	Arginine is the major phytochemical found in the Moringa ol. extract	[87]
Piper nigrum fem. Piperaceae	Whole plant	WL, PDP, EIS	Mild steel/1 M HCl	Langmuir adsorption isotherm	Maximum inhibition efficiency 98% attained at 120 ppm at 35 °C. Piperine is the major active component	[88]
Adathoda vasica	Stems, roots	WL, EIS	Mild steel/1 N HCl	Langmuir adsorption isotherm	Plant extract showed 99.6% inhibition efficiency at 8.0% v/v concentration	[89]

Table 1 (continued)

Plant name	Part used	Techniques	Metal and electrolyte	Nature of adsorption	Remark	Refs.
<i>Palicourea guianensis</i>	Leaves	EIS, PDP	C38 steel/1 M HCl	Langmuir, Temkin and Frumkin adsorption isotherms	Inhibition efficiency of 89% attained with 100 mg/L of AEPG conc. at 25 °C	[90]
Gramine	Barks, stems	WL, EIS	Mild steel/1 M HCl	Langmuir adsorption isotherm	3-(dimethylaminomethyl)-indole is the active constituent and revealed good inhibition efficiencies in the concentration range (0.75–7.5 mM) particularly at higher concentrations	[91]
<i>Glycyrrhiza glabra</i>	Leaves	WL, EIS, AFM	C38 steel/1 M HCl	Langmuir adsorption isotherm	The maximum corrosion inhibition efficiency (about 88%) and surface coverage (about 72%) were obtained in the presence of 800 ppm conc. of Glycyrrhiza glabra leaves extract	[81]
<i>Acalypha torta</i>	Aerial part	WL, EIS, PDP, SEM	Mild steel/1 M HCl	Langmuir adsorption isotherm	<i>Acalypha torta</i> corrosion efficiency increases with increasing concentration and decreases with increasing temperature	[92]
<i>Thevetia peruviana</i>	Whole plant	WL, EIS, EFMT	Mild steel/1 M HCl	Temkin adsorption isotherm	Peruvoside, Cannogenin, Thevetin are the three major active constituents present in the extract	[35]
<i>Cucurbitamaxima</i>	Peel	WL, FTIR	Mild steel/1 N HCl	Langmuir adsorption isotherm	Maximum efficiency of 93% is achieved at the inhibitor concentration of 2% v/v	[93]
<i>Strychnos Nuxvomica</i>	Seeds	WL, EIS, PDP, FTIR	Mild steel/1 M HCl	Langmuir adsorption isotherm/mixed type inhibitor	Main constituent of extract of Kuchla (<i>Strychnos Nuxvomica</i>) seed is Brucine	[94]
<i>Isertia coccinea</i>	Whole plant	HPLC, EIS, PDP	C38 steel/1 M HCl	Langmuir adsorption isotherm	Inhibitor revealed a maximum efficiency of 91% at 100 mg/L	[95]
Fig leaves	Leaves	WL, EIS	Mild steel/2 M HCl	Langmuir adsorption isotherm	Inhibition efficiency of 87% attained at above 200 ppm	[96]
<i>Antiba rosaeodora</i>	Barks, stem	XPS, WL, EIS	C38 steel/1 M HCl	Langmuir adsorption isotherm	Anibine found to be major phytochemical component showing good inhibition efficiency	[75]
<i>Zenthoxylum alatum</i>	Fruits	WL, EIS, SEM, Gas chromatography mass spectroscopy (GC-MS), FTIR	Mild steel/5% HCl	Langmuir adsorption isotherm	Plant extract reduced steel corrosion more effectively in 5% HCl than in 15% HCl	[97]

Table 1 (continued)

Plant name	Part used	Techniques	Metal and electrolyte	Nature of adsorption	Remark	Refs.
Pimenta dioica	Leaves	WL, EIS, DFT	Mild steel/0.5 -1 M HCl	Langmuir adsorption isotherm	Eugenol, Methylugenol, caryophyllene, Myrcene, Limonene and 1,8-Cineole are the major phytochemicals present in Pimenta di. extract	[98]
Plectranthus amboinicus	Leaves	WL, EIS	Mild steel/1 M HCl	Langmuir adsorption isotherm	Two main constituents of the leaf thymol and 1, 8-cineole were monitored for their inhibition behavior with upto 93% of maximum inhibition efficiency	[99]

aluminium alloy surfaces are coated with a natural oxide film about 4–6 nm thick. Aluminium forms a stable oxide film that can induce corrosion protection in a variety of environments such as in low and high pH environments, still it becomes susceptible to corrosion. In recent times, economic and environmental concerns have driven the study of plant extracts and natural corrosion-preventing products for viability [137]. The use of natural products has several tangible benefits because they are biodegradable, sustainable, and affordable, consisting of a large number of organic compounds (such as alkaloids, tannins, carbohydrates, vitamins, saponins, amino acids, proteins, pigments, resins) analogous to conventional organic corrosion inhibitors in the electronic structure and function. Figure 22 and Table 4 show the corrosion inhibition efficiency of various plant extracts as corrosion inhibitors for aluminium in various corrosive media and deliberates various techniques involved, nature of metal and electrolytes, and nature of adsorption of active constituents.

3.4 Plant Extracts as Corrosion Inhibitor for Copper: HCl, H₂SO₄, HNO₃ System

Copper has a broad range of applications due to its beneficial properties. It is used in the manufacture of electronic appliances, cables, boards, tubes, and also in the formation of some alloys. Copper is blended with zinc to form brass which has higher corrosion resistance and is simple to manufacture. When the brass containing more than 15% of zinc is exposed to a corrosive phase, they are significantly impacted by both general corrosion damage and dezincification (preferable zinc dissolution) phenomenon, forming a deteriorate mass of copper on the surface of the material [156]. Figure 23 and Table 5 show the efficiency of various plant extracts as corrosion inhibitors for copper in various corrosive media and deliberates various techniques involved, nature of metal and electrolytes, and nature of adsorption of active constituents.

4 Corrosion Testing and Monitoring Techniques

Corrosion Monitoring is a process that evaluates and monitors equipment components, structures, process units, and facilities for signs of corrosion. Monitoring programs aim to identify certain conditions to extend the life and serviceability of assets while increasing safety and reducing replacement costs. Corrosion monitoring covers all types of corrosion and materials.

The key advantage to implementing corrosion monitoring is to detect early warning signs of corrosion and to determine trends and processing parameters that may induce a corrosive environment. Processing parameters that may

Table 2 Plant extracts as corrosion inhibitors in sulphuric acid solution involving various plants, techniques, nature of metal and electrolyte and nature of the adsorption of active phytoconstituents

Plant name	Part used	Techniques	Metal and electrolyte	Nature of adsorption	Remark	Refs.
<i>Chenopodium ambrosioides</i>	Leaves	WL, EIS, SEM	Mild steel/0.5 M H ₂ SO ₄	Langmuir adsorption isotherm	94% Inhibition efficiency attained at 4 g/L	[33]
<i>Chamaerops humilis</i>	Leaves and fruits	WL, PDP, EIS	Mild steel/0.5 M H ₂ SO ₄	Langmuir adsorption isotherm	Inhibition efficiency reached a maximum value of 78.55% at 100 mg/L	[100]
<i>Anacyclus pyrethrum L.</i> extracts	Leaves	WL, EIS, PDP	Mild steel/0.5 M H ₂ SO ₄	Langmuir adsorption isotherm	Saponins, alkaloids, flavonoids are some active constituents	[101]
<i>Nicotiana tabacum</i>	Leaves	WL, EIS, DFT	Mild steel/2 M H ₂ SO ₄	Langmuir adsorption isotherm	The active constituent is nicotine	[13]
<i>Pongamia Pinnata</i>	Leaves	WL, EIS, FTIR, GC-MS, SEM	Mild steel/1 N H ₂ SO ₄	Temkin adsorption isotherm/mixed-type inhibitor	<i>P. pinnata</i> leaf extract retards both anodic metal dissolution	[102]
<i>Strychnos nux-vomica</i>	Seeds	WL, EIS, FTIR	Mild steel/1 M H ₂ SO ₄	Temkin adsorption isotherm	Brucine is the major phytochemical component present in the extract	[103]
Black pepper	Seeds	WL, EIS, SEM	Mild steel/1 M H ₂ SO ₄	Temkin adsorption isotherm	Corrosion inhibition efficiency attained due to the presence of alkaloidal constituents such as piperine	[104]
<i>Corchorus olitorius</i>	Stems	WL, EIS, GC-MS	Mild steel/0.5 M H ₂ SO ₄	Langmuir adsorption isotherm	Inhibition efficiency of 93% attained	[105]
<i>Citrus aurantium</i>	Leaves	WL, FTIR, SEM	Mild steel/1 M H ₂ SO ₄	Langmuir adsorption isotherm	Higher inhibition efficiency was 89% at 40 °C and 10 ml/L inhibitor concentration	[54]
<i>Argemone mexicana</i>	Flower	WL, EIS, SEM, UV	Mild steel/1 M H ₂ SO ₄	Langmuir adsorption isotherm	Nearly 80% corrosion inhibition observed at 200 mg/L inhibitor concentration and maximum 92.5% for 500 mg/L extract concentration in 1 M HCL	[106]
<i>Argemone mexicana</i>	Flowers and leaves	WL, EIS, FTIR	Mild steel/0.5 M H ₂ SO ₄	Langmuir adsorption isotherm	Maximum inhibition efficiency of 87% attained using 600 mg/L of the inhibitor	[107]
<i>Tagetes erecta</i>	Flower	WL, EIS, DFT	Mild steel/0.5 M H ₂ SO ₄	Langmuir adsorption isotherm	Lutein found as major component of TEE	[108]

Table 2 (continued)

Plant name	Part used	Techniques	Metal and electrolyte	Nature of adsorption	Remark	Refs.
<i>Lannea coromandelica</i>	Leaves	WL, EIS, FTIR, XRD, AFM, SEM	Mild steel/1 M H ₂ SO ₄	Langmuir adsorption isotherm	Alkaloids, flavonoids, glucosides, Carbohydrates, phenols, amino acids, steroids are the main chemical constituents	[109]
<i>Telfaria occidentalis</i>	Leaves	WL, SEM	Mild steel/1 M H ₂ SO ₄	Langmuir adsorption isotherm	Protonated species in the extract play a predominant role in the observed inhibitive behavior, with a possible contribution by molecular constituents	[74]
<i>Garcinia kola</i>	Seeds	WL, XPS	Mild steel/5 M H ₂ SO ₄	Langmuir adsorption isotherm	Alkaloids, flavonoids and polyphenols marked responsible for the corrosion inhibition property of extract	[110]
<i>Wrightia tinctoria</i>	Leaves	WL, EIS, PDP, SEM	Mild steel/0.5 M H ₂ SO ₄	Langmuir adsorption isotherm	It is concluded that the range of ER % (97–98%) is achieved	[111]
<i>Kleinia grandiflora</i>	Leaves	WL, EIS, FTIR, SEM, Ultra violet visible spectroscopy (UV)	Mild steel/1 M H ₂ SO ₄	Langmuir adsorption isotherm	Tetradecamethylcycloheptasiloxane, 6-deoxy D-galactose, 2-ethoxycarbonyl-5-oxopyrrolidine are the major active constituents	[112]
<i>Aster koraiensis</i>	Leaves	WL, EIS, SEM, Energy dispersive X-ray spectroscopy (EDX)	Mild steel/1 M H ₂ SO ₄	Langmuir adsorption isotherm	90.53% maximum efficiency achieved at 2000 ppm of the extract	[113]
<i>Murraya koenigii</i>	Leaves	WL, EIS, PDP	Mild steel/0.5 M H ₂ SO ₄	Langmuir adsorption isotherm	Main constituents of <i>Murraya koenigii</i> leaves are murrayafoline-I, pyrayafoline-D, mahabamine-A	[114]
<i>Datura metel</i>	Leaves	WL, EIS	Mild steel/1 M H ₂ SO ₄	Langmuir adsorption isotherm	The presence of alkaloids such as scopolamine and atropine in <i>D. metel</i> may be the reason for the anticorrosive activity	[115]
<i>Syzygium cumini</i>	Seeds	WL, EIS, PDP	Mild steel/1 M H ₂ SO ₄	Langmuir adsorption isotherm	Constituents of <i>S. cumini</i> seed extracts are ellagic acid, gallic acid, quercetin and caffeic acid	[116]

Table 2 (continued)

Plant name	Part used	Techniques	Metal and electrolyte	Nature of adsorption	Remark	Refs.
Raphia hookeri	Gum	WL, PDP, FTIR	Mild steel/1 M H ₂ SO ₄	Langmuir adsorption isotherm	Activation energies were higher in the presence of the exudates gum revealing the physisorption mechanism	[117]
Rosemary	Oil	WL, PDP, EIS	Carbon steel/0.5 M H ₂ SO ₄	Langmuir adsorption isotherm	A maximum of 84.15% of inhibition efficiency was obtained through 600 ppm of inhibitor examined by EIS procedure	[118]
Curcumin, Parsley, Cassia	Whole plant and cassia bark	WL, PDP, Galvanostatic	Carbon steel/0.5 M H ₂ SO ₄	Temkin adsorption isotherm	A maximum of inhibition efficiency shown is Cassia 88.02% > Parsley 84.76% > Curcumin 82.72% in 500 ppm inhibitor conc	[119]

need to be altered include temperature, pressure, pH, etc. Additionally, corrosion monitoring serves to measure the effectiveness of corrosion prevention methods to determine if different inspection and/or monitoring techniques should be utilized. Destructive and non-destructive are methods are used to measure corrosion levels. Additionally, a brief technical approach is addressed, which appears to simply provide some key conclusions about the methods used for different experimental procedures.

Corrosion monitoring includes a wide variety of techniques that include corrosion measurement, control, and prevention. These techniques can be broadly classified into two types: Inspection and monitoring.

4.1 Inspection Techniques

Before applying inspection techniques, it is necessary to log the operational parameters of equipment that may increase the risk of corrosion. These parameters include the pH of the system, flow rate (velocity), pressure, and temperature, but are not limited to these.

First, non-destructive testing (NDT) and inspection techniques are conducted to locate and classify the type of corrosion damage. Ultrasonic testing, radiographic testing, and magnetic flux leakage are the common NDT methods used to detect corrosion.

Additional methodologies that can enhance a screening program are risk-based inspection and fitness-for-service tests. These strategies include qualitative and quantitative methods which provide information on the current condition of the equipment and its durability.

4.2 Monitoring Techniques

Corrosion measuring methods can be used to collect information about the corrosive environment until corrosion is detected. During the operation, the use of probes is considered to track changes in the mechanical, electrical, or electrochemical devices. Besides this, several techniques can be used to provide direct and indirect knowledge about a process during an operation. By using analytical chemistry techniques, some crucial data such as pH, the amount of dissolved gas (e.g., O₂, CO₂, and H₂S) and the oxidation of metal ions (e.g., Fe²⁺, Fe³⁺) can be attained. The use of corrosion coupons, electrical resistance, linear polarisation resistance, and galvanic monitoring are some of the typical monitoring techniques.

4.3 The Need for Corrosion Monitoring

The corrosion rate determines the durability and operational span of any equipment. Corrosion monitoring techniques can be useful in several ways as discussed below:

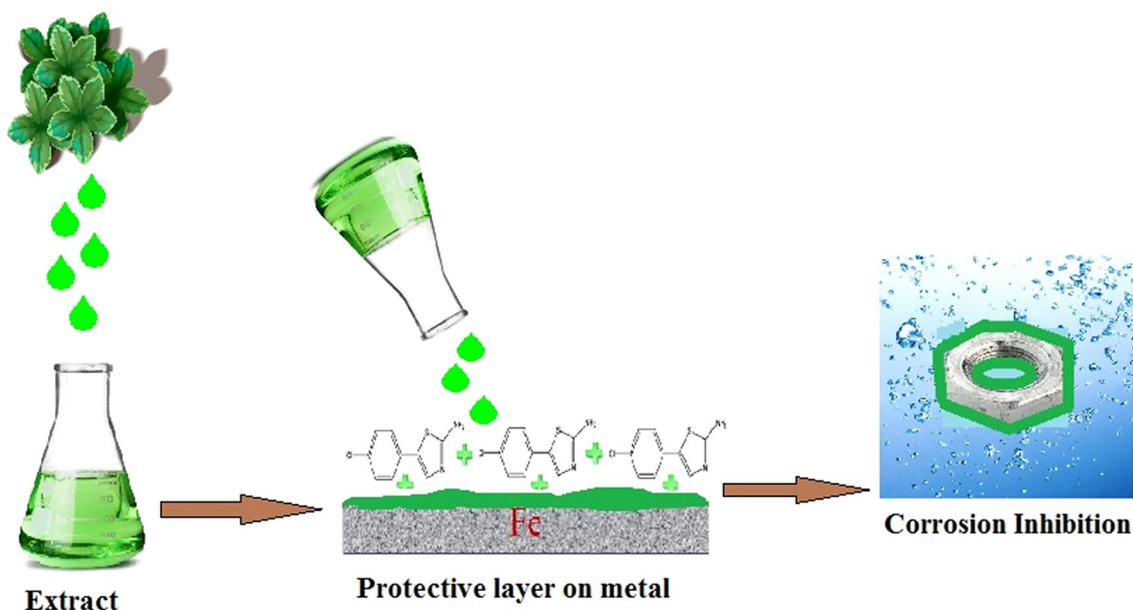


Fig. 20 Diagrammatic illustration of the adsorption of phytochemicals derived from plant extract forming a protective layer on the mild steel surface

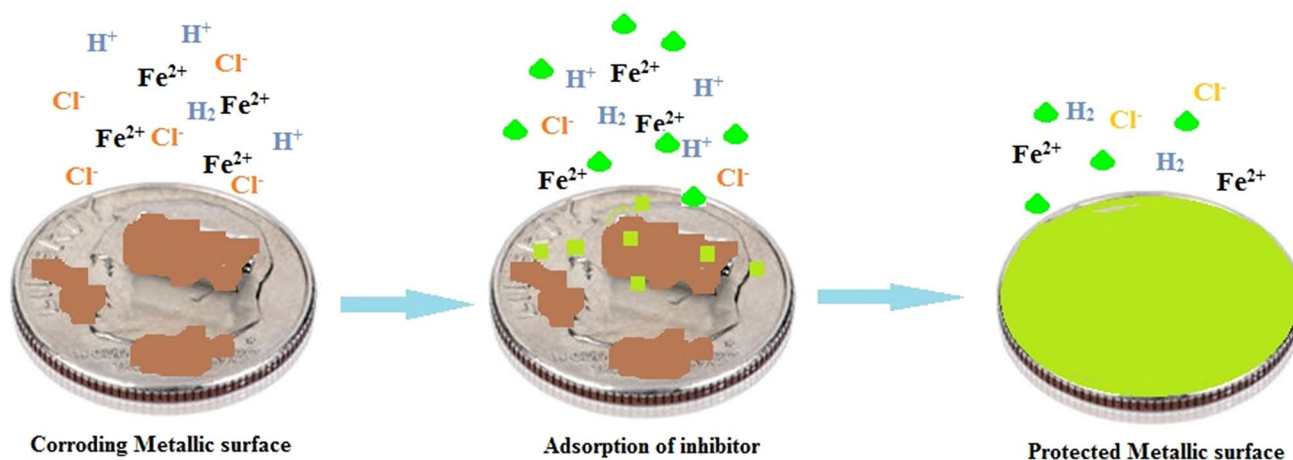


Fig. 21 Diagrammatic illustration of the adsorption of phytochemicals present in the plant extract developing a thick defensive layer on the stainless steel surface

- (1) By giving an early warning about the existence of an unsafe process condition which may result in a failure caused by corrosion.
- (2) By analyzing the correlation of changes in process parameters and their effect on the corrosive system.
- (3) Identifying and diagnosing the cause of corrosion and its rate controlling parameters, such as strain, temperature, pH, flow rate.
- (4) By assessing the efficacy of a technique for corrosion control/prevention such as chemical inhibition and determining optimum applications.

4.4 Methods for Corrosion Detection and Monitoring

4.4.1 Non-destructive Method

Non-destructive testing (NDT) is a broad set of research techniques used without causing any harm to the physical and mechanical properties of a material, part, or device. Types of the non-destructive method are as:

Ultrasonic Technique The ultrasonic technique can be used to measure the material thickness and the size of a

Table 3 Plant extracts as corrosion inhibitors for stainless steel in different electrolytic media involving various plants, techniques, nature of metal and electrolyte, and nature of the adsorption of active phytoconstituents

Plant name	Part used	Techniques	Metal and electrolyte	Nature of adsorption	Remark	Refs.
<i>Juglans regia</i>	Leaves	WL, EIS, PDP, FTIR	Stainless steel/1 M HCL	Langmuir adsorption isotherm	Maximum inhibition efficiency was found upto 88.8%	[121]
<i>Chenopodium Ambrosioides</i>	Whole plant	WL, EIS, PDP	Stainless steel/0.5 M H ₂ SO ₄	Langmuir adsorption isotherm	Maximum inhibition efficiency of 94% was attained at 4 g/L	[33]
<i>Ferula gummosa Boiss</i>	oleo-gum-resin exudate	WL, EIS	304 Stainless steel/2 M HCL	Temkin adsorption isotherm	Main constituents, b-pinene and a-pinene are responsible for corrosion inhibition	[122]
Gum Arabic	Whole plant	WL, EIS, PDP	API 5L X42 pipeline steel/1 M H ₂ SO ₄	Langmuir adsorption isotherm	Maximum inhibition efficiency found to be 92% at 2 g/L with arabinogalactan as an active constituent	[123]
<i>Lanvandula Stoekas</i>	Leaves	EIS, PDP	Stainless steel/ 5.5 M H ₃ PO ₄	Langmuir adsorption isotherm	Inhibition efficiency increases with increased organic oil concentration attaining a maximum value of 87.3% at 1.2 g/L	[124]
<i>Thymus vulgaris</i>	Leaves	WL, EIS, PDP, DFT	304 Stainless steel/1 M HCL	Langmuir adsorption isotherm	Thymus extract act as a green inhibitor	[70]
Fennel	Seeds	WL, EIS, PDP	304 Stainless steel/1 M HCL	Langmuir adsorption isotherm	Anethol and Fenchone are the main active constituents in the extract of fennel seed	[69]
Coriander Seeds	Seeds	WL, EIS, EFMT	304 Stainless steel/1 M HCL	Langmuir adsorption isotherm	Physical adsorption mechanism was proposed for the inhibition with Linalool and Geraniol as main active constituents	[125]
<i>Calotropis procera</i>	Roots	WL, Electrochemical frequency modulation (EFM), PDP, FTIR, AFM, SEM	304 Stainless steel/2 M HCL	Langmuir adsorption isotherm	Tannins, Flavonoid acid, Saponin, glycosides are the main phytochemicals present in the extract	[68]
Bee Wax Propolis	Honeycomb waste	WL, EIS, FTIR, HPLC	304SS /1 M H ₂ SO ₄	Langmuir adsorption isotherm	Quercetin (2-(3,4-dihydroxyphenyl)-3,5,7-trihydroxy-4H-chromen-4-one) observed as the active phytoconstituent revealing 97.29% inhibition efficiency at 2000 ppm	[67]
<i>Cassia fistula</i>	Leaves	WL, EIS, Linear sweep voltammetry (LSV)	Stainless steel/0.5 M HCL	Langmuir adsorption isotherm	10 g/L conc. of Cassia fistula leaf extract exhibited optimal inhibition efficiency of 88.46%	[126]

Table 3 (continued)

Plant name	Part used	Techniques	Metal and electrolyte	Nature of adsorption	Remark	Refs.
<i>Morus alba pendula</i>	Leaves	WL, EIS, SEM, AFM, FTIR, UV	Stainless steel/1 M HCl	Langmuir adsorption isotherm/ mixed type inhibitor	Maximum inhibition efficiency of 93% was achieved in presence of 0.4 g/L at room temperature 25 °C	[127]
<i>Tectona grandis</i>	Roots, stem, leaves	WL, EIS, FTIR	SS304 stainless steel/2 M HCl	Langmuir adsorption isotherm/ mixed type inhibitor	Anthraquinone, tannin-theaflavin, saponin were the main phytoconstituents	[128]
<i>Dendrocalmus sinicus</i>	Aerial part	WL, EIS, PDP, AFM, FTIR	Stainless steel/1.0–5.0 M HCl	Langmuir adsorption isotherm	Active constituents are orientiuxyloside, Isoorient, vitexin-4-O-CH ₃ , luteolin-7-O-glucoside, d-hydroxy lysine with inhibition efficiency of 89%	[129]
<i>Nicotiana</i>	Leaves	WL, SEM	304 austenitic stainless steel/0.5 M H ₂ SO ₄ + 5% NaCl	Langmuir adsorption isotherm	Inhibition efficiency value of 67.2% was attained	[130]
<i>Aloe Vera</i>	Whole plant	WL, EIS, GC-MS, SEM	Stainless steel/1 M H ₂ SO ₄	Langmuir adsorption isotherm	Active compounds found in Aloe Vera extract are Aloins, Aloesin, Aloeresin, Aloeresin	[131]
<i>Vernonia amygdalina</i>	Leaves	WL	Stainless steel/1 M H ₂ SO ₄	Langmuir adsorption isotherm	An inhibition efficiency of 69% was observed	[132]
<i>Gnetum Africanum</i>	Leaves	WL	Stainless steel/1 M H ₂ SO ₄	Langmuir adsorption isotherm	Optimum inhibition efficiency of 90.95% in 1 M HCl for 20 mL concentration was showed	[133]
<i>Ginkgo</i>	Leaves	WL, EIS, AFM, SEM	X70 Stainless steel/1 M HCl	Langmuir adsorption isotherm	Inhibition efficiency exceeded 90% in the presence of 200 mg/L GE	[134]
<i>Santolina chamaecyparissus</i>	Aerial part	WL, EIS, SEM	Stainless steel/6 M HCl	Langmuir adsorption isotherm	Inhibition efficiency of 95.5 pct was achieved with the addition of 1.0 g/L extract	[135]
<i>Salvia officinalis</i>	Leaves	WL, EIS, PDP, DFT	304 stainless steel/1 M HCl	Langmuir adsorption isotherm	Some of the active compounds reported are salvigenin, lupeol, b-sitosterol, stigmasterol, physcion, carnosol, rosmadial, rosmanol, epirosmanol, isorosmanol	[136]

defect. The ultrasonic wave passes from the transducer through the material to the back end of the material, and then reflects the transducer. The thickness of the material is determined by the material being measured based on the speed of sound. This method is commonly used to determine the condition of pipelines, vessels, and structures during inspection and NDT surveys. Ultrasonics have the advantage of being able to take measurements from the outside wall while the plant is in operation. Since they do not need access to both sides of the sample, they are very useful for pipeline thickness measurements where it is very difficult to access the internal wall [168]. It is also possible to build them to cope with coatings, linings, etc. Unfortunately, corrosion under pipe supports (CUPS) is problematic for guided wave inspection as at the low frequencies required to detect gradual wall thinning, the support itself gives a significant reflection, and the locations of concern are inaccessible for conventional ultrasonic thickness gauging. Similar issues arise when testing the floor of storage tanks from the small region of the floor protruding outside the tank wall. This suggests that it would be desirable to test at higher frequencies where the reflection from the support is negligible and sensitivity to smaller defects would be improved. Another disadvantage is that each material usually needs calibration before getting tested [169].

Electromagnetic Method The main principle of this method is inducing electric currents or magnetic fields or both into the test object and observe the electromagnetic behavior of the material. There are many types of electromagnetic methods like i. Magnetometer and di-electrometers: Meandering Winding Magnetometers (MWM) and Interdigital Electrometers (IDED) which detects concealed corrosion under the paint and calculate the depth of moisture inside barrier paint coatings due to the reduction in conductivity near a metal surface where there might be a risk of oxygen diffusion layer on the metal surface, which is also considered as an early stage of the corrosion. For calculating different properties of the material, MWM uses magnetic fields and inductive coupling. To measure the properties of multi-layered insulating media, such as paint on metal oxides formed during corrosion, the IDED utilizes electric fields and capacitive coupling. ii. Magnetic flux leakage (MFL): The basic concept of MFL technology is to apply a magnetic field to the test material using a large magnet and detect local changes in the field. MFL is used over a long distance in larger diameter pipes. MFL instruments consist of a total of two parts: (1) magnet and sensor magnetizer, (2) electronics and batteries. To produce the magnetic circuit along with the pipe wall, the magnets are placed between the brushes and the instrument shell. The sensors detect interruptions in the magnetic circuit as the tool moves along the pipe. Interruptions are normally caused by metal loss, which in most cases is corrosion, and the measurements of the possible

metal loss are previously referred to as "feature." These technologies are generally being developed to detect and size cracks rather than metal loss anomalies. The reliability of using such method as it potentially able to find anomalies as a function of the depth, length, and width of the metal loss [170]. Although in the case of MFL tool design, magnetization direction is a dominant parameter, with trade-offs being between sensitivity to long narrow anomalies, velocity effects, and tool complexity. Magnet pole spacing is also important. The tight spacing provides the ability to traverse tight bends, but with less accurate detection and sizing of some anomalies. Magnet strength affects detection and sizing accuracy. Stronger magnets are often used, which makes signal interpretation easier for metal loss anomalies, but with reduced sensitivity to some anomaly types [171, 172].

Eddy current testing (ECT) By giving an Alternating Current (AC) to a wire coil, the wire coil produces an alternating magnetic field around itself. As the coil enters a conductive material, the eddy current is caused in the material by currents as opposed to those in the coil. It is the fundamental concept of testing the eddy current. Surface inspection is used in two primary applications: in the aerospace and petrochemical industries. Both ferromagnetic and non-ferromagnetic materials may be subject to surface inspection. Tubing inspection is only applicable to non-ferromagnetic materials. Laminar defects and wall thickness types of flaws can be found using ECT testing cracks. It is a very useful non-destructive testing used for the detection of defects, the measurement of conductivity, and the estimation of the thickness of coatings. There is also no need for any couplant—unlike ultrasonic inspection, it can be used on wet surfaces—and there is no need for consumables as with dye penetrant and magnetic particle inspection techniques [173]. Eddy current testing is suitable for a wide range of applications. It is universally applied in crack detection. By measuring material conductivity, it is used in quality control in nonferrous metal sorting and in sorting ferrous metals according to required material properties. It is used to assess coating thickness and tube wall thickness, and it is also used to detect subsurface corrosion. It can detect defects through several layers, including non-conductive surface coatings, without interference from planar defects [174, 175].

However, conventional eddy current instruments suffer from limited corrosion monitoring functionality, both in terms of speed of inspection and in terms of inspecting for corrosion at different depths within a structure [176]. This is especially important in the aerospace sector, where structures are often assembled using riveted lap jointing of various layers or skins. Also, other disadvantages are that it can only be used on conductive materials, it is very susceptible to magnetic permeability changes—making testing of welds in ferromagnetic materials difficult—but with modern digital flaw detectors, the depth of penetration is variable and

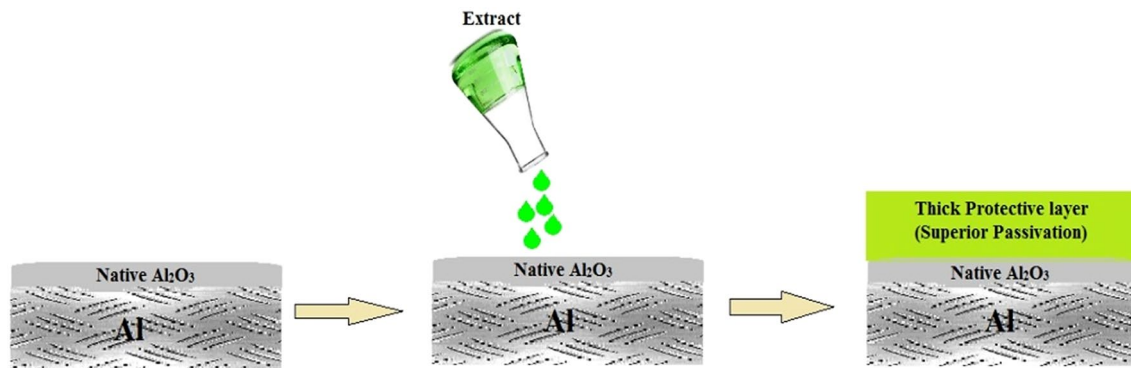


Fig. 22 Diagrammatic illustration of the adsorption of phytochemicals derived from plant extract forming a protective layer on the native Al₂O₃ layer of aluminium metal

unable to detect defects that are parallel to the test object's surface [177].

Radiographic Method The radiographic technique is used to generate images of physically inaccessible metallic components obstructing the direction of radiation using high frequency gamma radiation and X-rays. This corrosion monitoring radiation system has low sensitivity and requires radiation protection. Radiography is used widely in determining pipe thickness in the chemical and petroleum industries. Radiography is very helpful in the identification of various forms of internal deposits. Tangential radiographic inspection (TRI) is a suitable method measuring accurately the wall thicknesses of pipe walls about comparators [178]. The accuracy of the wall thickness determination depends on the calibration of the software evaluation tool, the detector pixel size and the image unsharpness in asymmetric projection mode over 360°. This method provides some advantages over common methods for the determination of the thickness of the insulation, pipe and deposit as well as detecting internal and external corrosion. There are also some limitations in this method including the need for higher energy and intensity of the radiation due to long beam pass through the matter [11]. Measurement errors increase with this technique when pipes contain insulation, deposit or are filled with a substance. The radiography arrangement also affects the density and the results of measurements [179]. The other limitation of this technique is that density measurements refer to both sides of the beam path of the pipe and any indication of thickness loss would be the sum of the thickness reduction of the pipe wall (top and bottom wall) under the investigated area.

4.4.2 Destructive Method

To understand the behavior and output of material under several stress and environment, various methods and measurements are used known as the Destructive Physical Analysis

(DPA) test. In general, these experiments are much easier to run, provide more evidence and are easier to interpret than non-destructive testing. Types of Destructive Method are as:

Electrochemical Measurement Corrosion is an electrochemical reaction, in which an anode (positive electrode) is oxidized (losses electrons) and a cathode (negative electrode) is chemically reduced (gained electrons). Therefore it is possible to determine corrosion properties and corrosion behavior by conducting an electrochemical test and calculating the characteristic values. Electrochemical measurements is one of the effective analytical technique for corrosion investigation. Electrochemical methods have the advantages of being quite fast in terms of measurement time and they can provide not only information about the corrosion resistance but also other mechanistic data that might help in the design of corrosion inhibitors and strategies.

Electrochemical Impedance Spectroscopy (EIS) EIS is a viable and quantitative method for the accelerated evaluation of the anti-corrosion performance of protective coatings in the aqueous corrosion of metals and alloys. EIS measurements provide accurate data within a short time allowing for the prediction of the long-term performance of the coatings. A Metrohm Autolab EIS apparatus with a corrosion cell has been displayed in Fig. 24. In electrochemical experiments, an electrochemical reaction is initiated on a sample in a solution in a cell, and the electrical outcome is measured. For example, if a specimen of iron, steel, or some other metal material is immersed in an aqueous solution, an oxidation–reduction reaction will occur at the specimen surface due to dissolved oxygen and/or ions in the solution, and as a result, its electrical potential is determined. The electrode potential can then be measured by measuring this potential against that of a reference electrode as a standard. In general electrochemical measurements, three electrodes are immersed in a test solution (electrolyte). These three electrodes consist of a working electrode (WE), which is the sample material being tested, a counter electrochemical (CE)

Table 4 Plant extracts as corrosion inhibitors for aluminium in corrosive media discussing various plants, techniques, nature of metal and electrolyte and nature of the adsorption of active phytoconstituents

Plant name	Part used	Techniques	Metal and electrolyte	Nature of adsorption	Remark	Refs
<i>Maesobatrachya barteri</i>	Root	WL	Aluminium/0.5 M HCl	Langmuir adsorption isotherm	ΔH^0_{ads} for aluminium corrosion in 0.5 M HCl being positive indicate the endothermic nature of the adsorption process	[138]
<i>Delonix regia</i>	Seeds and leaves	WL	Aluminium/2 M HCl	Langmuir adsorption isotherm	93% of maximum inhibition efficiency observed	[139]
<i>Phyllanthus amarus</i>	Leaves	WL, EIS	Aluminium/2 M NaOH	Langmuir adsorption isotherm	76% inhibition efficiency at the highest concentration in the alkaline environment was confirmed with phyllanthin and hypophyllanthin as active constituents	[140]
<i>Gossipium hirsutum</i>	Leaves	WL, EIS	Aluminium/2 M NaOH	Langmuir adsorption isotherm	GE extract gave 97% inhibition efficiency with gossypol as major constituent	[141]
<i>Asparagus Racemosus</i>	Stem, roots and leaves	WL, AFM, DFT	Aluminium/1 M HCl	Langmuir adsorption isotherm	At 4000 ppm concentration of inhibitor, 72.28% corrosion inhibition efficiency is observed	[7]
<i>Origanum Vulgare</i>	Stem and leaves	WL, SEM, DFT	Aluminium/1 M HCl	Langmuir adsorption isotherm/ mixed type inhibitor	At 4000 ppm, maximum inhibition efficiency revealed to be 97.7% with Carvacrol and Thymol as main components	[8]
<i>Sapindus</i>	Leaves and roots	WL, EIS, PDP, SEM, DFT	Aluminium/1 M HCl	Langmuir adsorption isotherm	Sapindus revealed 98% of inhibition efficiency at 2000 ppm	[65]
<i>Trachyspermum copticum</i>	Seed	WL, EIS	Aluminium/0.5 M NaOH	Langmuir adsorption isotherm/ mixed type inhibitor	Maximum inhibition efficiency of 94% at 500 ppm inhibitor concentration revealed	[142]
<i>Capparis decidua</i>	Fruit, stem bark and root bark	WL, PDP	Aluminium/0.5 N H ₂ SO ₄ , 1 N H ₂ SO ₄ , 2 N H ₂ SO ₄	NA	94.79% of inhibition efficiency was observed in 3 N HCl	[143]
<i>Ananas sativum</i>	Leaves	WL, AFM, EIS	Aluminium/0.1 M HCl	Langmuir adsorption isotherm	The obtained values of ΔG^0_{ads} were low and negative, revealing spontaneity nature of the adsorption process	[83]

Table 4 (continued)

Plant name	Part used	Techniques	Metal and electrolyte	Nature of adsorption	Remark	Refs
<i>Sida acuta</i>	Roots, stem and leaves	WL, PDP	Al-Cu-Mg alloy/HCl	NA	Inhibition efficiency improves from 37.42% to 93.63% over a ten-day period with an rise in the extract percentage volume	[144]
<i>Citrullus colocynthis</i>	Whole plant	WL, DFT	Aluminium/0.5 N HCl	Langmuir adsorption isotherm	87.29% inhibition efficiency observed	[145]
<i>Jasminum nudiflorum</i> Lindl	Leaves	WL, EIS, SEM	Aluminium/0.1 M HCl	Langmuir adsorption isotherm	Jasmoside, jasmisnyrioxide, jasmnin, verbascoside, syringing are the some actice constituents	[146]
<i>Opuntia</i>	Stem, roots, leaves, fruit	WL, PDP	Aluminium/2.0 M HCl	Langmuir adsorption isotherm	IE % increases as increasing extract conc	[147]
<i>Dendrocalamus brandisii</i>	Leaves	WL, EIS, PDP, SEM	Aluminium/1 M HCl, 1.0 M H ₃ PO ₄	Langmuir adsorption isotherm	Maximum efficiency observed at 1.0 g/L at 20 °C was 91.3% in 1.0 M HCl and 47.1% in 1.0 M H ₃ PO ₄	[148]
<i>Aspilia africana</i>	Leaves	WL, EIS, DFT	AA3003 Al alloy/0.5 M HCl	Langmuir, Temkin, Freundlich and the Flory-Huggins adsorption isotherm	Main active compounds were Thiamine and Niacin	[149]
<i>Dryopteris cochleata</i>	Leaves	WL, EIS, XRD, SEM	Aluminium/1 M H ₂ SO ₄	Freundlich adsorption isotherm	Extract increases the charge transfer resistance (R_{ct}) and decreases the double-layer capacitance (Cdl)	[150]
<i>Newbouldia leavis</i>	Leaves	WL	Aluminium/1.0 M HCl and 0.5 M H ₂ SO ₄	Langmuir adsorption isotherm	Presence of active components such as flavonoids, tannins, terpenes, steroidal and cardiac glycosides	[151]
<i>Newbouldia leavis</i>	Leaves	WL	AA8011 aluminium alloy/0.5 M H ₂ SO ₄	Langmuir adsorption isotherm	Spontaneous physical adsorption by the plant extract molecules	[152]
<i>Azadirachta indica</i>	Bark, stem, leaves	WL, SEM	Aluminium/1.85 M HCl	Langmuir, Temkin adsorption isotherm	Optimum inhibition concentration observed was 50% v/v of the Azadirachta indica extract	[153]
<i>Spondias mombin</i> L	Leaves	WL, DFT	Aluminium/0.5 M H ₂ SO ₄	Langmuir adsorption isotherm	Ascorbic acid, riboflavin, thiamine are the some active compounds present in extract	[154]

Table 4 (continued)

Plant name	Part used	Techniques	Metal and electrolyte	Nature of adsorption	Remark	Refs
<i>Sansevieria trifasciata</i>	Leaves	WL, PDP	Aluminium/2 M KOH, 2 M HCl	Freundlich adsorption isotherm	Addition of halide salts synergistically increased the inhibition efficiency of the extract in the order $KCl < KBr < KI$	[155]



Fig. 23 Diagrammatic illustration of the adsorption of phytochemical derived from plant extract forming a thick defensive layer on the copper surface

for passing a current, and a reference electrode (RE), which serves as a standard. The result of EIS is the impedance of the electrochemical system as a function of frequency [180]. This approach has gained prominence because it can be performed in situ and because the corrosion process typically does not require any artificial acceleration. The primary advantage of this method is the low strength of the excitation signal used that causes minimal disturbance in the state of the electrochemical system, which consists of a non-destructive technique and reduces the error associated with the measuring process. Impedance spectra generated by this process is calibrated to a combination of resistors and capacitors (equivalent circuits) electrical circuit to comprehend the corrosion mechanism. In this method, measurement of polarization resistance (R_p) is a direct measure of corrosion rate. To run an EIS measurement, a small amplitude signal, usually a voltage between 5 and 50 mV is applied to a specimen over a range of frequencies of 0.001 Hz to 100,000 Hz. The EIS instrument records the real (resistance) and imaginary (capacitance) components of the impedance of the system. Depending upon the nature of the EIS data, a circuit model or equivalent circuit diagram and initial circuit parameters are assumed and input by the operator. The main difficulties are related to data interpretation because it includes the building of an equivalent circuit model in a metal solution interface.

Ashish et al. performed the electrochemical measurements on mild steel using venlafaxine. The results obtained are being shown in Fig. 25a as Nyquist plot and Fig. 25b as Bodes plot. The semi-circular impedance spectra obtained reveal the process is driven by charge transfer. The charge transfer resistance was used to calculate the inhibition efficiency.

Following equations were used to obtain the electrochemical parameters such as C_{dl} and $IE\%$:

Table 5 Plant extracts as corrosion inhibitors for copper in different electrolytic media involving techniques, nature of metal and electrolytes, and nature of adsorption of active constituents

Plant name	Part used	Technique(s)	Metal and electrolyte	Nature of adsorption	Remark	Refs.
Cannabis	Whole plant	WL, EIS, PDP, SEM	Copper/0.5 M H ₂ SO ₄	Langmuir adsorption isotherm, Flory Huggins isotherm/cathodic type inhibitor	Analysis suggested that only one water molecule was displaced by each cannabis species	[157]
Zygodhllum coccineum L	Leaves	WL, EIS, EFMT, PDP, SEM	Copper/1 M HNO ₃	Langmuir adsorption isotherm	Double-layer capacitances decrease with respect to blank solution confirms the adsorption of plant extract molecules on the copper surface	[158]
Euphorbia Heterophylla	Whole plant	WL, EIS, EFMT, PDP, SEM	Copper/0.5 M HNO ₃	Frumkin adsorption isotherm	Main active component is Saponin	[159]
Ceratonia siliqua	Aerial part	WL, EIS, EFMT, XRD, SEM	Copper/1 M HNO ₃	Langmuir adsorption isotherm	Process was spontaneous and exothermic	[160]
Thymus Vulgarise	Whole plant	WL, EIS, EFMT, PDP, SEM	Copper/1 M HNO ₃	Langmuir adsorption isotherm	Double-layer capacitances decrease with respect to blank solution revealing adsorption of plant extract molecules on the copper surface	[36]
Aloe Vera Barbardensis	Roots, leaves	WL	Copper/2 M HCl	Langmuir adsorption isotherm	Folic acid, Aloe-emodin, aloetic-acid, anthranol, aloin A, Pure mannan, acetylated mannan, acetylated glucomannan, glucogalactomannan are some major active phytoconstituent	[161]
Citrullus colocynthis	Leaves	WL, EIS	Copper/1 M H ₂ SO ₄	Langmuir adsorption isotherm/mixed type inhibitor	Alkaloids, flavonoids and saponins content in Citrullus colocynthis extract was confirmed	[161]
Morinda tinctoria	Leaves	WL, EIS, EDXS, SEM, FTIR	Copper/0.5 M HCl	Freundlich adsorption isotherm	Inhibition efficiency increases by further addition of halide additives	[162]
Inula viscosa	Roots, stem	WL	Copper/1 M NaOH	Langmuir adsorption isotherm	2,5-dihydroxy-isocostic acid, 1,3-dicaffeoylquinic acid are some active components found in the extract	[163]
Dialium indium	Pod	WL, FTIR, EIS	Copper/0.5 M H ₂ SO ₄	NA	Velvet Tamarind concentration range of 0.05–0.25 g/500 mL exhibited a good corrosion inhibition of 71.76%	[164]
Arecanut Husk	Whole plant	WL, EIS, FTIR, SEM	Copper/0.5 M HCl, 0.5 M NaOH	Langmuir adsorption isotherm	Inhibition efficiency of 93.750% for copper in 0.5 M HCl medium and 90.000% for copper in 0.5 M NaOH medium was revealed	[165]
Azadirachta Indica	Aerial part	WL	Copper/1 N, 2 N and 3 N HNO ₃	NA	95% of maximum inhibition efficiency at 1% inhibitor concentration was found	[166]

Table 5 (continued)

Plant name	Part used	Technique(s)	Metal and electrolyte	Nature of adsorption	Remark	Refs.
Moringa oleifera	Leaves	WL, EIS, EFMT, SEM, AFM	Copper/1 M HNO ₃ + H ₃ PO ₄	Langmuir adsorption isotherm	The maximum inhibition efficiency was found to be 89% at concentration 0.300 mol/L of the extract at 298 K after 3 h immersion period	[167]

$$Cdl = 1/2 \cdot \pi f_{\max} R_{ct}$$

where Cdl is the double-layer capacitance, fmax is the frequency and R_{ct} is the charge transfer resistance.

$$IE(\%) = (R_{ct_{inhibitor}} - R_{ct_{acid}} / R_{ct_{inhibitor}}) \times 100$$

where IE(%) is the corrosion inhibition efficiency, and $R_{ct_{inhibitor}}$ and $R_{ct_{acid}}$ are the charge transfer resistances of inhibited and uninhibited solutions, respectively. It is evident from the findings that mild steel corrosion mitigation occurs upon inhibitor inclusion. Increasing the concentration of the inhibitor is seen as a noticeable improvement in inhibition effectiveness. R_{ct} values increase and Cdl values decrease with increased inhibitor concentration, which can be due to inhibitor adsorption on the surface of the metal.

Potentiodynamic Polarization (PP) Measurement Potentiodynamic polarization (PP) is also used to evaluate the corrosion rate and behavior in several metals or alloys as it rapidly generates data. The stable electrical potential obtained between the metallic surface and the electrolyte is the open-circuit potential (OCP). To activate the PP, the metal/electrolyte system is first polarized cathodically (negative over OCP positive), followed by a sweep in anodic polarization (positive over OCP potential). Then the polarization curves are used to determine the cathodic and anodic slopes of the Tafel (applied potential vs. measured current density) [182–186].

The intersection of the Tafel slopes provides the potential for corrosion potential (E_{corr}) and density of corrosion current, which is used to obtain the corrosion current (I_{corr}) separated by the area exposed. For sample/solution combinations, potentiodynamic experiments may provide a range of data relating to the pitting, crevice corrosion and passivation behavior. The pitting corrosion begins when the potential is increased, at a certain value known as the breakdown potential (BP, the lowest potential at which pitting occurs). As pitting corrosion refers to an increase in the oxidation rate, the corresponding increase in the calculated current is determined by the BP. Higher resistance to corrosion by pitting is associated with an increase in BP. On the reverse scan, when the potential is decreased, there is a reduction in the current. For the reverse scan, a hysteresis is observed and a hysteresis loop is traced. At the potential, where the reverse scan crosses the forward scan, the sample is repassivated. The potential for repassivation, or potential for protection (PP), exists at a lower potential than the BP. Susceptibility to crevice corrosion is linked to the disparity between BP and PP. The greater the hysteresis in the polarization curve, the greater the susceptibility to corrosion. Figure 26. Represents the potentiodynamic cyclic polarization curves.

In Fig. 27, the Tafel polarization curves of aluminium in 0.5 M HCl in 1000 to 4000 ppm conc. of inhibitor in the temperature range of 298 K to 328 K are being displayed

Fig. 24 Autolab EIS apparatus with corrosion cell

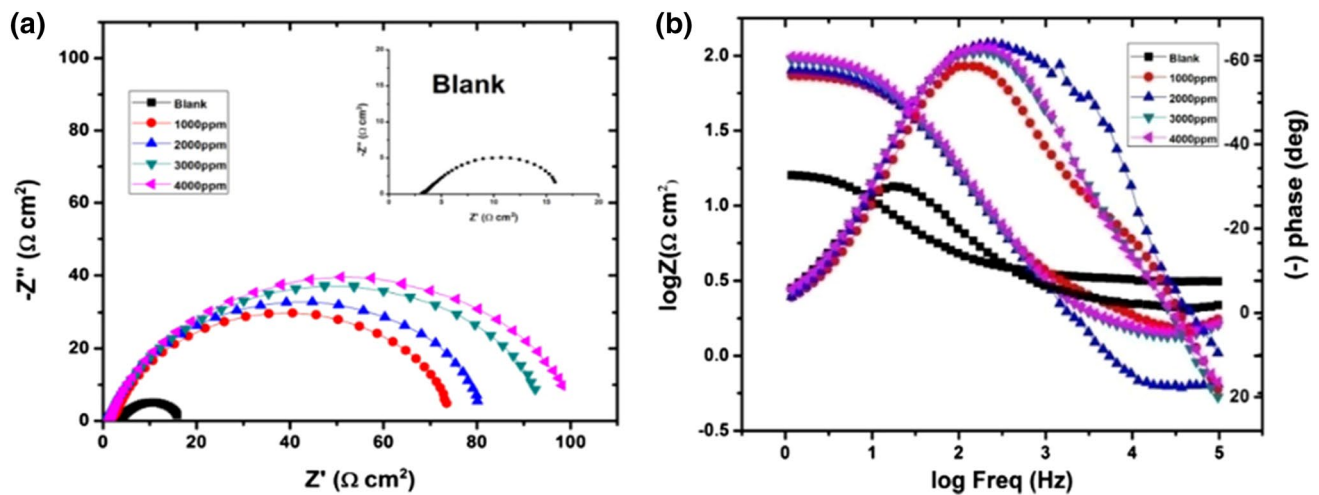


Fig. 25 **a** Nyquist plot and **b** Bode plot for corrosion inhibition of mild steel in acidic medium using Venlafaxine. (Source adapted from [181])

[188]. It is evident from the figure that the inclusion of the phenylephrine change E_{corr} to a more positive potential with minimum I_{corr} values causes the anticorrosive properties of the metal to increase. The shift in E_{corr} is a difference of ± 85 mV, suggesting phenylephrine as a mixed type of inhibitor. Corrosion potential (E_{corr}), corrosion current density (I_{corr}), anodic and cathodic slopes (ba, bc), and corrosion inhibition efficiency are the parameters that were deduced from this analysis.

Electrochemical Noise (EN) In recent years, the EN technique has been promoted as a research tool for both corrosion science and localized corrosion for monitoring engineering alloys. The basics behind the principle of localized corrosion is centered between two nominally equivalent electrodes in the galvanic current and by carefully monitoring the corrosion potential of a single electrode. So, a metastable pitting can be identified by applying a signal to the assembly of the electrode and obtaining a current response from it. The status of metal corrosion can be determined by the current noise signal response and the harmonic content of the current response.

Figure 28 shows a schematic illustration of the system for detecting electrochemical noise. The sample was put into an electrochemical cell that was installed in an electromagnetic shield enclosure. The deaerated test solution was

poured into the cell to start corroding the three coupons. A potentiostat (Toho Giken Co. Ltd., Model 2090LN) in electrometer mode, a differential amplifier (NF Circuit Block Co. Ltd., Model 5307), and a digital multimeter (Takeda Riken Co. Ltd., Model TR6841) measured the potential difference between two of the three coupons. A zero resistance ammeter (Keithley Co. Ltd., Model 6514) was used to test the short-circuit current between the two coupons, one of which was normal with one of those for possible calculation. As for polarity, the minus terminals of both systems were as usually linked with the center coupon together. The two electrochemical signals were simultaneously collected through the GPIB interface (Contec Co. Ltd., GP-IB(PM)) on a personal computer (IBM Co. Ltd., ThinkPad 230Cs). In 1024 s, the sampling rate was 0.5 s, and acquired signal data were 2048 points. Using the fast Fourier transformation (FFT) process, these time-series data of the potential difference and the short-circuit current were transformed into the frequency domain. Their power spectrum densities (PSDs) at a given frequency were obtained from the power spectra of the potential and current to be compared with the corrosion rate of the steel.

Typical signal patterns of the potential difference and the short-circuit current are shown in Fig. 29. The test was performed at pH 8.5 at $0.1 \text{ kmol/m}^3 \text{ NaHCO}_3$ and the patterns

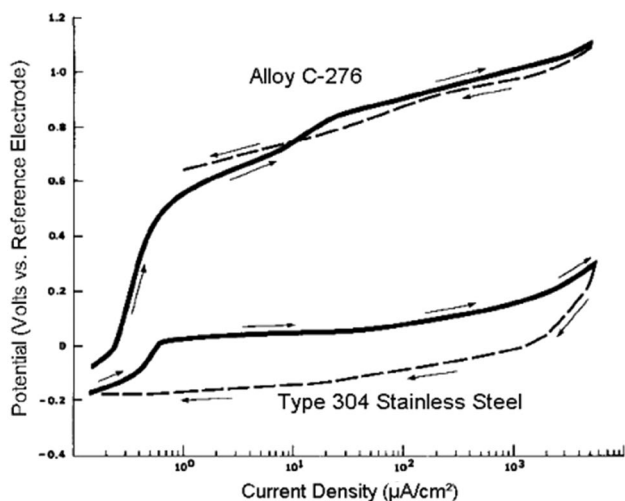


Fig. 26 Representation of potentiodynamic cyclic polarization curves (Source adapted from [187])

were assessed at 98.7 ks after immersion. In the statistics, it is noticed that both signals oscillate constantly and irregularly. A couple of peaks were synchronized with each other as both patterns were compared, but the others were not. The variations between the maximum and the minimum values for the potential difference and the short-circuit current were around 1.3 mV and 13.2 nA, respectively. In comparison, the potential signal between the 10 kX electrical resistance terminals and the actual signal under open-circuit conditions was determined to validate the internal electrical noise of the measuring device. As a result, the two oscillated signals, and the variations between the maximum and minimum values for the potential difference and current were approximately 0.03 mV and 0.05 nA, respectively. These values were quite smaller than those for the corrosion system, so it can be claimed that this method can be used to calculate the electrochemical noise signals of the potential difference and the short-circuit current for this corrosion system.

Linear Polarisation Resistance (LPR) Monitoring The LPR method aims to monitor the microscopic corrosion cells that exist inside the plant on a microscopic scale. The

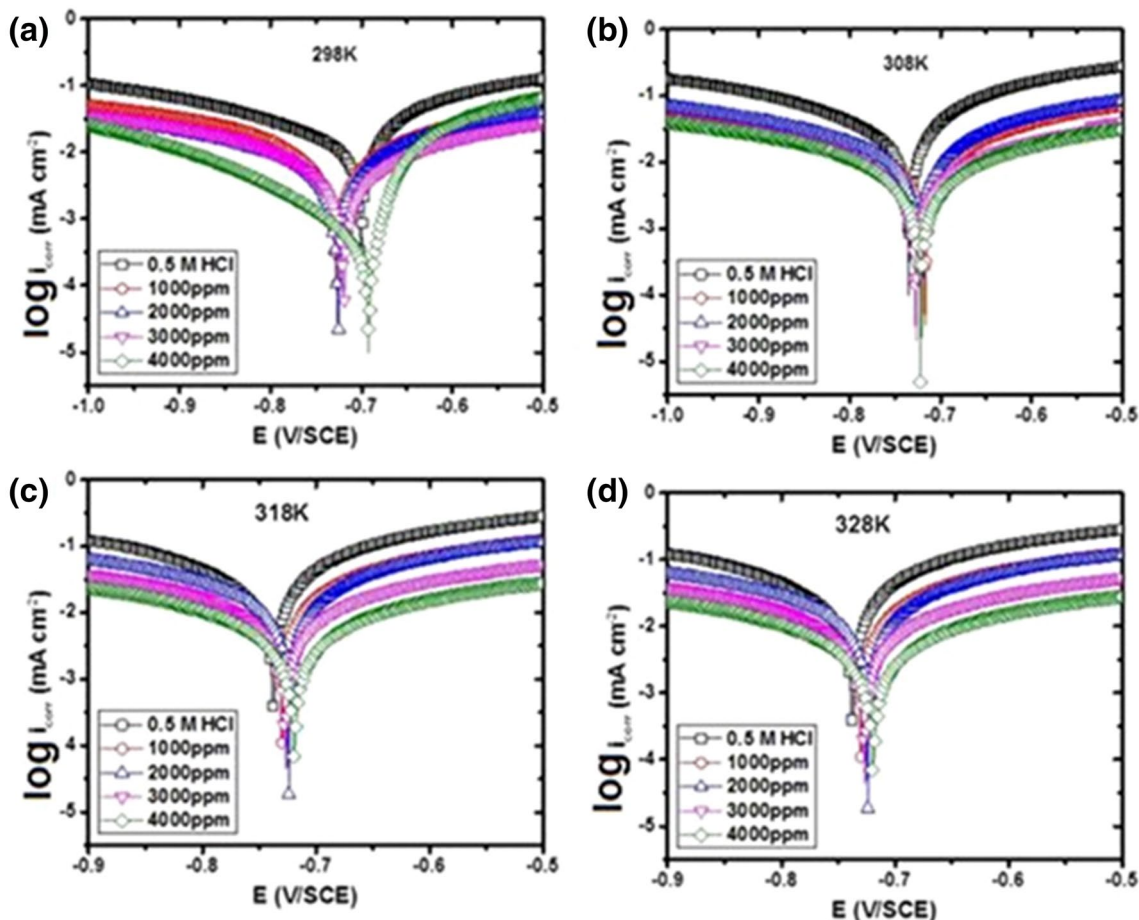


Fig. 27 Polarization plots for Al in 0.5 M HCl with and without different concentrations of phenylephrine at different temperatures. (Source adapted from [188])

LPR method is used to evaluate the internal corrosion monitoring of subsea production flow lines, the corrosion rate of concrete reinforcement, nuclear waste tanks, the effectiveness assessment of corrosion inhibitors in oil and gas pipelines, dig site outer pipe surfaces, and water cooling systems. The corrosion current flowing between anodic and cathodic half cells is calculated by LPR. Measurements are obtained by applying a small voltage to a corroding metal electrode (about 10–30 mV) and measuring the resulting flow of current. LPR measurements are obtained by disrupting the reinforcing steel’s equilibrium potential. It can be achieved either potentiostatically, i.e. by adjusting the steel reinforcement potential by a static quantity, ΔE and tracking the current decay, ΔI after a fixed time, or galvanostatically, i.e. by adding a small fixed current, ΔI to the steel reinforcement and observing the potential shift, ΔE after a fixed time. In both cases, the conditions are so chosen that the difference in potential falls within the linear Stern-Geary range of 10–30 mV. The calculation of polarization resistance (R_p) of the steel is done by,

$$R_p = \Delta E / \Delta I$$

From the above equation:

$$I_{\text{corr}} = B / R_p$$

where B is Stern-Geary constant.

Corrosion current density, I_{corr} , can be determined if the surface area of steel, A is polarised

$$I_{\text{corr}} = I_{\text{corr}} / A$$

The remaining durability can be obtained by concluding the present residual strength of the structure. The method is not used commonly because it requires mathematical calculation for calculating the corrosion rate.

Applications of Electrochemical Measurement Electrochemical measurements are not limited to the general state of an aqueous solution, but may also be carried out

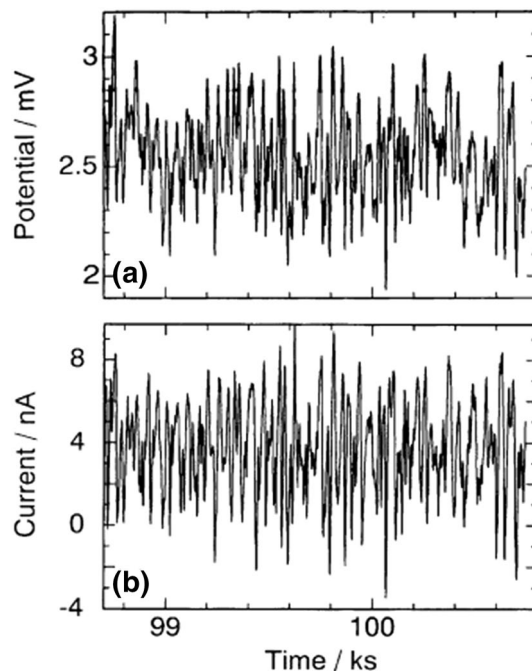
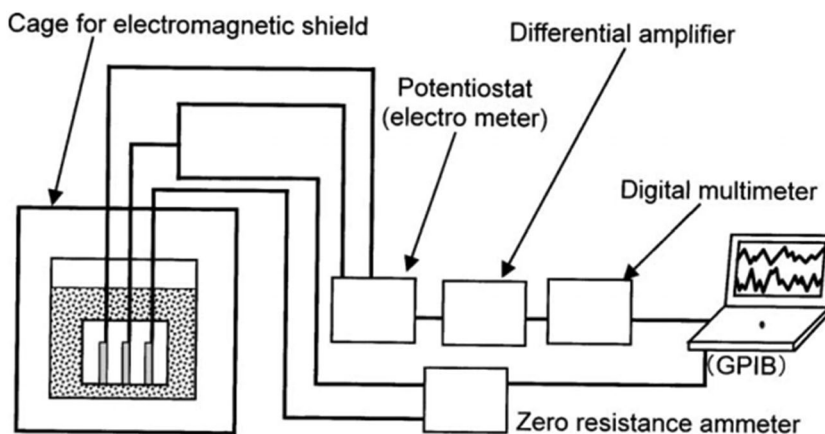


Fig. 29 Typical signal patterns of **a** potential difference and **b** short-circuit current of the carbon steel in $0.1 \text{ kmol m}^{-3} \text{ NaHCO}_3$ solution. The patterns were measured from 98.7 ks after immersion. (Source adapted from [189])

in simulating environments. As per demand, it can perform many electrochemical measurements, including corrosion crevice repassivation potential measurement (ER, CREV), pitting potential measurement, electrochemical potentiokinetic reactivation ratio (ERP) measurement, hydrogen diffusivity measurement (hydrogen diffusion coefficient). Figure 30. shows a schematic representation of the electrochemical instrumentation setup.

Harmonic Distortion Analysis (HDA), or Harmonic Analysis (HA) This approach is based on the measurement of basic, second, and third harmonic currents from the current corrosion potential response by disturbing a low amplitude

Fig. 28 Schematic illustration of the system for detecting electrochemical noise. (Source adapted from [189])



corrosion network with a non-distorted sinusoidal signal. HDA is a calculation of low frequency impedance and depends on a steady-state approximation, similar to LPR, but needs more mathematical treatment than the LPR technique. Because of the non-linearities of the charge transfer phase, the current response to a low frequency voltage sinusoidal wave is distorted. To provide values for corrosion current, the Tafel constants, and Stern-Geary constant B, this distortion is analyzed in terms of the higher harmonics. This technique relates to the EIS where the resulting current response, an alternating potential disturbance is applied to one sensor in a probe of three components. It is possible to directly measure all kinetic parameters (including the Tafel constants). No other technique provides such advantages. HDA is focused on the evolution and improvement of the LPR technique's efficiency. The resistance of the corrosive solution can be determined by harmonic analysis of the resulting signals by applying a low frequency sine wave to the measurement current. It is possible to establish a more reliable general corrosion rate for both the polarization resistance and the solution resistance. For calculating corrosion rates of metals in acids, neutral electrolyte solutions, and concrete, both EIS and HDA are used. The benefit of HDA is that the handling of mathematical data facilitates the direct calculation of the constants of the Tafel and the rate of corrosion. It also has certain limitations such as in the LPR technique, the assumption of uniform corrosion has to be made; if localized corrosion occurs, the data obtained is qualitative and not much quantitative.

Zero Resistance Ammetry (ZRA) Zero Resistance Ammetry is a current-to-voltage converter that gives the external circuit a voltage that is equal to the current flowing between the input terminals while introducing a 'zero' voltage drop. In the ZRA technique, a macrocell current is calculated in an electrolytic environment between two corroded sensor components. It is used between two dissimilar or similar electrodes to measure the galvanic coupling current. A corrosion rate value obtained by Faraday's Law is the resulting galvanic current. This method is often used to calculate the coupling current for controlling electrochemical current noise between two identical" electrodes. These electrodes are slightly different in practice and there is a minimal coupling current. Such measurements are important in the detection of early stages of corrosion. The drawback is that the measured macrocell current can not accurately represent the magnitude of the attack if significant corrosion occurs on both electrodes.

Acoustic Emission (AE) Technique Acoustic Emission is a natural momentary elastic wave phenomenon created by the rapid discharge of energy inside the material from a localized source when subjected to stress. It is a non-intrusive method that can be used for local damage. The primary cause of AE is crack progression. The technique is useful

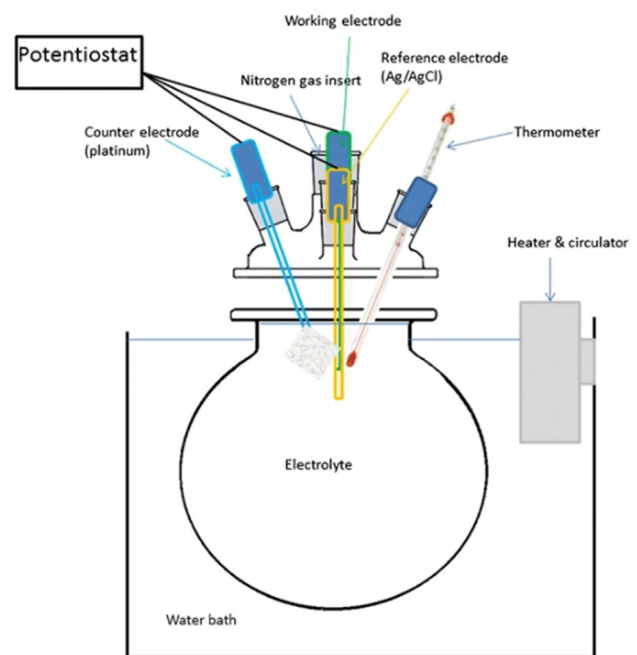


Fig. 30 Schematic representation of the electrochemical instrumentation setup. (Source adapted from [190])

for detecting real-time corrosion and is highly sensitive to mechanical, physical, or chemical damage. One or more AE sensors are used to record occurrences taking place in a bulk material. In this method, a piezoelectric transducer is used as an AE sensor, a device that transforms mechanical energy into an electrical signal. Here two different methods are used to acquire AE signals: HDD and TDD15. The edge-measured method is Hit Driven Data (HDD). When the AE signal voltage crosses a predefined edge, AE wave data are obtained. Amplitude, length, and signal intensity are the parameters that can be used for the analysis. On the other hand, Time-Driven Data (TDD) is an edge-free process. AE wave is implied at a constant rate for every 5 s. for a pre-set length interval. Due to fixed-rate acquisition, when a continuous AE phenomenon occurs, TDD becomes the better choice. The parameters such as Average Signal Level (ASL) and Absolute Energy (AbE) are obtained.

The AE technique can be obtained by focusing on the initiation and propagation of corrosion. The potentiodynamic method with 3 electrochemical cells and Tafel plot can be used to calculate current (I_{corr}) used for determining corrosion rate (in milli-inches/year)

$$\text{Corrosion rate (MPY)} = 0.13i_{\text{corr}} (\text{E.W.})/d.a.$$

where E.W. = equivalent weight (in g/eq.)

A = Surface Area of Steel (in cm^2).

d = Density (in g/cm^3).

0.13 = metric and time conversion factor

In the chemical and petrochemical industries, AE technology has applications to sense stress corrosion in stainless steel cracking, pitting, and crevice corrosion. Several efforts are being made to identify and locate the beginning and initial stage of the cracks that trigger the corrosion of concrete steel reinforcement.

Quantum Chemical Calculations Quantum chemical calculations are useful in the determination of the molecular structure and the elucidation of the electronic structure and reactivity. Some of the software used for quantum chemical calculations are ORCA, NWChem, GAMESS, Firefly, CP2K, and Gaussian. Using computational chemistry, the idea of determining the efficiency of a corrosion inhibitor is a quest for compounds with desired properties through chemical instinct into a mathematically quantified and computational form. Quantum chemical methods and molecular simulation models allow the description of a wide number of molecular quantities characterizing a complete molecule reactivity, form, and binding properties, as well as molecular fragments and moieties. The use of theoretical variables provides two major benefits: first, the compound and its numerous fragments and substituents can be described explicitly only based on their molecular structure; and second, the conceptual mechanism of action can be specifically compensated for in terms of the chemical reactivity of the compound being studied. Quantum chemically determined parameters fundamentally from experimentally calculated quantities. For quantum chemical equations, there is no statistical error, as compared to laboratory measurements. However, there is an intrinsic error correlated with the premises designed to improve the calculations [191–193]. The statistical error is known to be roughly constant in the sequence using quantum chemistry-based parameters for a set of related compounds. The prevalent parameters of the quantum chemical can be segmented into many aspects such as atomic charges, molecular orbital energy, dipole moment, total system energy. Quantum chemical computed parameters include the energy of the highest occupied molecular orbital (E_{HOMO}), the energy of the lowest unoccupied molecular orbital (E_{LUMO}), energy bandgap ($\Delta E = E_{\text{LUMO}} - E_{\text{HOMO}}$), global electronic chemical potential (μ), chemical softness (σ), chemical hardness (η) and electrophilicity index (ω). Down below Fig. 31 illustrates the most stable low energy configuration for the adsorption of inhibitor on metal in the H_2O interface.

Weight Loss Technique The weight loss technique is one of the most commonly known, simple, and cheapest technique for calculating corrosion rates. The metallic coupons of specific dimensions used in this method and the impact of corrosive media with and without inhibitor are being shown in Fig. 32. The method for mass loss experimentation is given in the standard ASTM G31. The standard method ASTM G31 provides the overall procedure for cleaning samples of the material. A technique for analyzing

certain material corrosion through a mass loss approach is as follows:

The metallic coupons (samples) grinded with emery paper (400–1600 grade) and washed with acetone solvent and dried for further use. The weight of polished samples should be measured for a fixed period before immersing in the solvent.

The materials have to be withdrawn from the solvent after a certain time of immersion. Then the use of sodium hydroxide should be done which eliminates the excess volume of corrosive solvent, followed by water cleaning.

Subsequently, the material washed with water is dried to evaporate the weight of the water. And the final weight should be measured and the difference between the initial and final weight should be noted down.

The equation shown down below is used to calculate the weight loss and rate of corrosion.

$$\text{CR} = 87.6W/\text{DAT}$$

Here CR = corrosion rate in mm/year.

W = weight loss (g).

D = coupon density (g/cm^3).

A = metallic coupon area (cm^2).

T = immersion time (h).

Besides the level of corrosion, the data from the study may be used to estimate the reduction in thickness. It is fundamental to provide error bars in these results because the presence of defects in the analyzed metal sample could greatly affect the analysis. The reproducibility of the measurement should be hence checked.

Electrical Resistance (ER) Monitoring ER is one of the most commonly used techniques for corrosion monitoring, which consists of measuring the change in resistance of metal as it corrodes in a process system. The corrosion action on the component helps to reduce the cross-sectional area, thereby increasing the electrical resistance. The element is typically in the form of a cable, strip, or tube, and a change in resistance is proportional to an increase in corrosion if the corrosion is approximately uniform.

The electrical resistance of a metal or alloy element is given by:

$$R = r \cdot L/A$$

where:

L = Element length.

A = Cross-sectional area.

r = Specific resistance.

Practical measurement is achieved using ER probes equipped with an element that is freely "exposed" to the corrosive fluid, and a "reference" element sealed within the probe body.

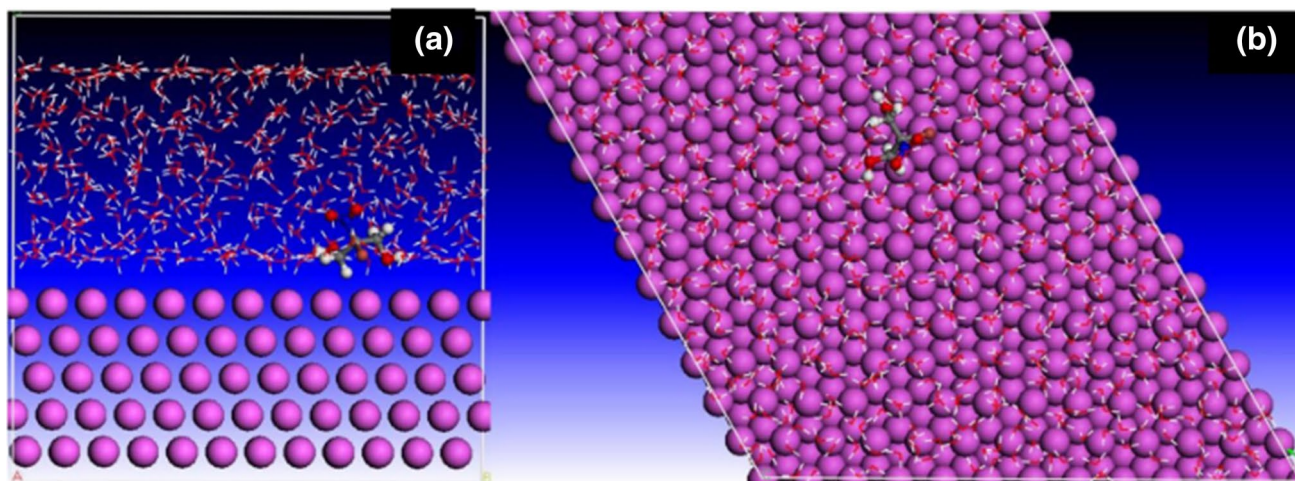


Fig. 31 The most stable low energy configuration **a** side view, **b** top view representing inhibitor adsorption on Al (111)/H₂O system. (Source adapted from [194])

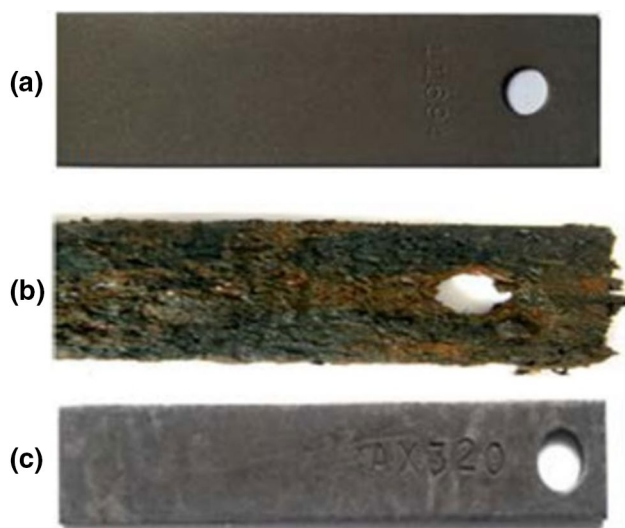


Fig. 32 Coupons strips showing: **a** Carbon steel unexposed to corrosive media, **b** carbon steel immersed in corrosive media, **c** carbon steel immersed in a mixed solution of corrosive media and inhibitor added. (Source adapted from [195])

The arrangement of ER probes for erosion-corrosion measurement at different pipe locations is shown in Fig. 33. A 1-inch FNPT packing body is supplied with retractable probes to allow probe insertion and removal through a customer-supplied ball valve, in systems with pressures not exceeding 2000 psi. To avoid backing out in systems with high vibration, a protective frame of rods and plates is connected to the probe. The Simple Tool for probe insertion or retraction in systems with pressure above 150 lb includes metal samples corrosion monitoring systems.

Electrical resistance Probes are robust and well equipped for any corrosive environment. In practice, the ER method is well known and is easy to use and interpret. ER monitoring enables the establishment of periodic or continuous monitoring for one or more probe numbers. Thus, corrosion can be linked to process variables. The major advantage is its ability to measure corrosion in any environment, liquid, gas, or particle streams.

Surface Morphology Analysis In the engineering of materials particularly for oxidized surfaces, surface topography plays a significant role. Parameters such as roughness, amplitude, order, or directionality provide useful information on the surface of a substance used in the corrosion test [197].

Scanning Electron Microscopy (SEM) SEM is commonly used for the study of surface topography and spectral observation. Researchers assessed the topography of the metallic surface using SEM. Scanning Electron Microscopy or SEM analysis offers high-resolution imaging that is useful for determining various surface defects, weaknesses, pollutants, or corrosion materials. A systematic and informative way to investigate surface structure is to analyze sample morphology based on the SEM technique and acquire structural functions and fractal dimensions in micro and nano scales [198].

Ashish et al. used the corrosion inhibitor phenylephrine for aluminium Fig. 34 to present the SEM photomicrographs of aluminum alloy in 0.5 M HCl in the absence and presence of 4000 ppm phenylephrine. The specimen shows a very rough surface in the absence of an inhibitor, which can be attributed to metal dissolution. Nonetheless, the surface damage seems to be diminished on the specimen in the presence of inhibitor, with lesser cavities in comparison to the blank material. This is a consequence of the protective layer formed on the surface of the metal in the presence of an inhibitor.

Atomic Force Microscopy (AFM) Atomic force microscopy is used for the surface topography analysis, including measurements of surface roughness. The Atomic Force Microscope was invented by scientists working at IBM in 1982, just after Gerd Binnig and Heinrich Rohrer of IBM Research in Zurich invented the Scanning Tunneling Microscope in 1980. This was first used in 1986 experimentally and placed on the market in 1989 for commercial sale.

The Atomic Force Microscope (AFM) uses a cantilever to perform surface sensing (an element made of a rigid block like a beam or plate that connects to the end of the support, from which it protrudes to create a vertical, perpendicularly flat link like a wall). The cantilever has a sharp tip that scans the surface of the sample by creating an enticing force between the surface and the tip as it draws closer to the surface of the sample. When it draws very close contact with the sample surface, a repulsive force progressively takes place on the surface by averting the cantilever. There is a shift in the direction of reflection of the beam during the deflection of the cantilever away from the sample surface,

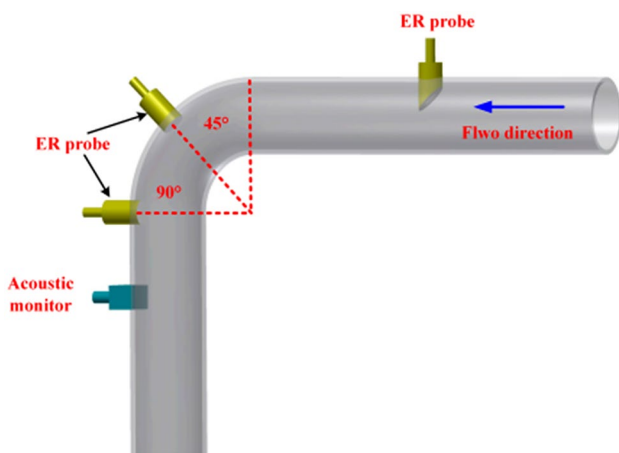


Fig. 33 The arrangement of ER probes for erosion-corrosion measurement at a different pipe locations (Source adapted from [196])

and a laser beam senses aversion by reflecting a beam from the flat surface of the cantilever. It monitors and records these changes of deflection and changes in the direction of the reflected beam using a positive-sensitive photo-diode (PSPD—a part based on silicon PIN diode technology and used to calculate the location of the integral focus of an incoming light signal). In AFM, the tip-sample interactions are detected to characterize the topography and biophysical properties of the sample.

The adherence of the inhibitor film or corrosive film to the substrate material (base metal or alloys) has always been difficult to report on by acquiring only the topographical images as being shown in Fig. 35 where AFM images of a metal immersed in the blank solution and another image of the same metal immersed in inhibitor solution for overnight which demonstrates the formation of a defensive layer on a metal surface by adsorption of inhibitor molecules on it which further protects it from the attack of corrosive ions [199]. As a result, AFM current images and force vs. distance curves are also used which provide detailed information on surface film properties, such as corrosion inhibitor adhesion and coating. AFM has the benefit of working under liquid conditions and enables real-time monitoring of surfaces in corrosive environments.

X-ray Diffraction Spectroscopy X-ray Diffraction (XRD) spectroscopy can be explained as an analytical method used to provide detailed information on crystalline compounds, including the identification and quantification of crystalline phase morphology. This is a valuable tool to identify a contaminant or corrosion product and foreign phases for crystalline powder purity analysis positively. X-ray diffraction is important for assessing mineral deposits, polymers, products for corrosion, and unidentified materials. For most cases, the samples analyzed at the elementary level are analyzed using samples prepared as finely ground powders using powder diffraction. This research method is achieved by focusing an X-ray beam at a sample and calculating the distributed intensity as a function of the path out. The scatter, also called

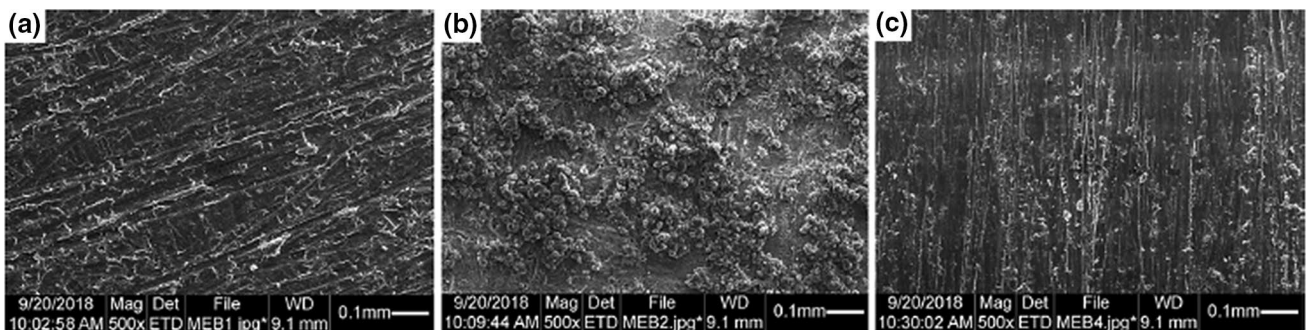


Fig. 34 SEM images of **a** polished metal, **b** metal immersed blank solution, **c** metal immersed in an inhibited solution of 4000 ppm of phenylephrine. (Source adapted from [188])

a diffraction pattern, shows the crystalline structure of the sample until the beam is dispersed. Then, the technique of Rietveld refinement is used to describe the crystal structure that most likely produced the pattern observed.

Synchrotron-sourced XRD overcomes the XRD problem with a traditional source, as it offers an adequate signal-to-noise ratio to analyze carbon steel film structures under corrosive environments. Synchrotron radiation XRD (SR-XRD) is widely known among crystallographers as it provides good resolution through a parallel beam that helps alleviate low-angle peak expansion as a result of geometry focusing. It includes several advantages such as high brightness quality, high frequency, high resolution, high polarization, and low transmittance. Hongwie Liu et al. in their study illustrated the energy dispersive X-ray spectrum analysis of corrosion product film and SRB biofilm on specimens after 14 days of incubation in the absence and presence of inhibitor SRB as results obtained shown in Fig. 36 [201].

Fourier Transform Infrared Spectroscopy (FTIR) By using FTIR, unique molecular patterns can be produced based on the absorption and transmission of infrared radiation. The quality and quantity of different components can be established in samples (mixtures) using this method. FTIR is widely used because it delivers several beneficial, such as accurate measurement, fast data collection, high sensitivity, non-destructive, no external calibration required. Traditional FTIR, which is usually studied in the mid-IR wavelength region, has been effectively implemented in surface film investigations on metal or alloy surfaces.

This facilitates insight into the mechanisms of adsorption of the corrosion inhibitors on metallic surfaces can be seen in Fig. 37 where the adsorption of various inhibitor molecules on the metallic surface can be observed.

Energy Dispersive X-ray Spectroscopy (EDS or EDX) Energy Dispersive X-ray Spectroscopy (EDS or EDX) is a chemical microanalysis technique used in conjunction with scanning electron microscopy (SEM). It is used for the characterization of the elemental composition of the examined volume. For this the EDS technique detects X-rays emitted from the sample during bombardment by an electron beam. By this technique phases as small as 1 μm or less can be analyzed.

In this technique, electrons are ejected from the atoms comprising the sample's surface when the sample is bombarded by the SEM's electron beam. Electrons from a higher state occupy the resulting electron vacancies, and an X-ray is released to offset the energy difference between the states of the two electrons. The energy of the X-ray is characteristic of the material it is emitted from.

The EDS X-ray detector measures the relative abundance of emitted X-rays versus their energy. The detector is usually a solid-state system with lithium-drifted silicon. It produces a charge pulse that is equal to the energy of the X-ray when an incident X-ray hits the detector. A charge-sensitive preamplifier converts the charge pulse to a voltage pulse (which remains proportional to the X-ray energy). Then the signal is sent to a multichannel analyzer where the voltage is sorted by the pulses. The energy, as calculated from the voltage measurement, is sent to a computer for display and further data evaluation for each X-ray event. To evaluate the elemental composition of the sampled volume, the spectrum of X-ray energy versus counts is assessed.

Contact angle (CA) Measurement Contact angle (CA) measurement is a simple method for the characterization of the surfaces. It provides a lot of useful data such as information between a hydrophobic and a hydrophilic surface. When an interface occurs between a liquid and a solid, the

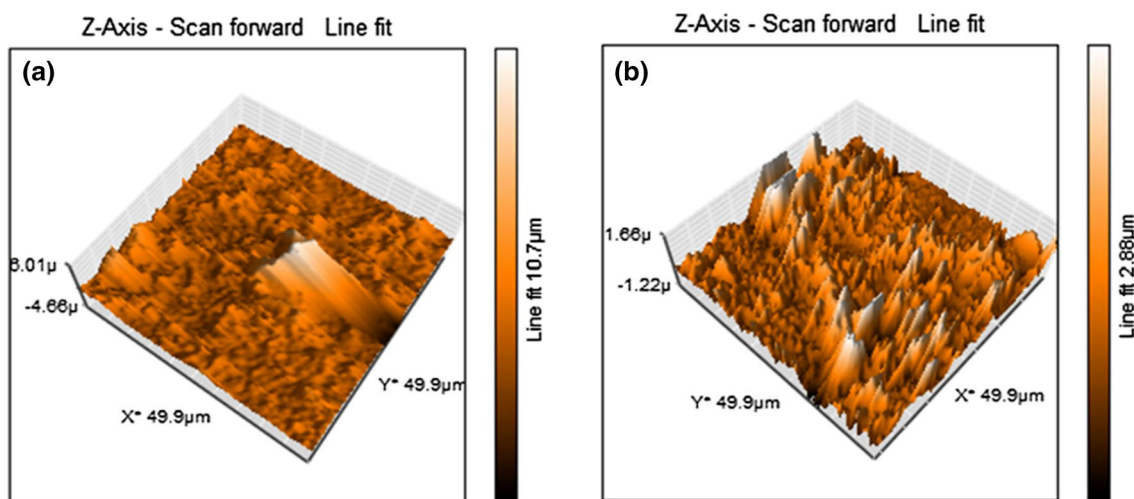


Fig. 35 AFM images for the metal in **a** blank, **b** inhibited solution of inhibitor (Source adapted from [200])

angle between the surface of the liquid and the outline of the contact surface is defined as the contact angle (lower case theta). The angle of contact (wetting angle) is an indicator of the liquid wettability of a solid. The touch angle is 0° in the case of full wetting (spreading). Around 0° and 90° , the solid is wettable and is not wettable above 90° . The contact angle approaches the theoretical limit of 180° in the case of ultra hydrophobic materials with the so-called lotus effect.

Thermodynamic/Adsorption Parameters The thermodynamic parameters can be utilized to comprehend the mode by which the inhibitor gets adsorbed on the surface of the metal in process of corrosion inhibition and adsorption isotherms can be utilized to gather details about the mechanism of adsorption. The phenomenon of adsorption involves the defensive layer formation potential of an adsorbent on the common interface of two phases. As a result of unbalanced and unsaturated forces present on the interface, a two-dimensional adsorption arrangement takes place. The forces of attraction and retention of solute balance the residual force on the surface on the contact of a solute onto the surface, leading to the higher concentration of molecules of solute in the nearby vicinity of the solid surface.

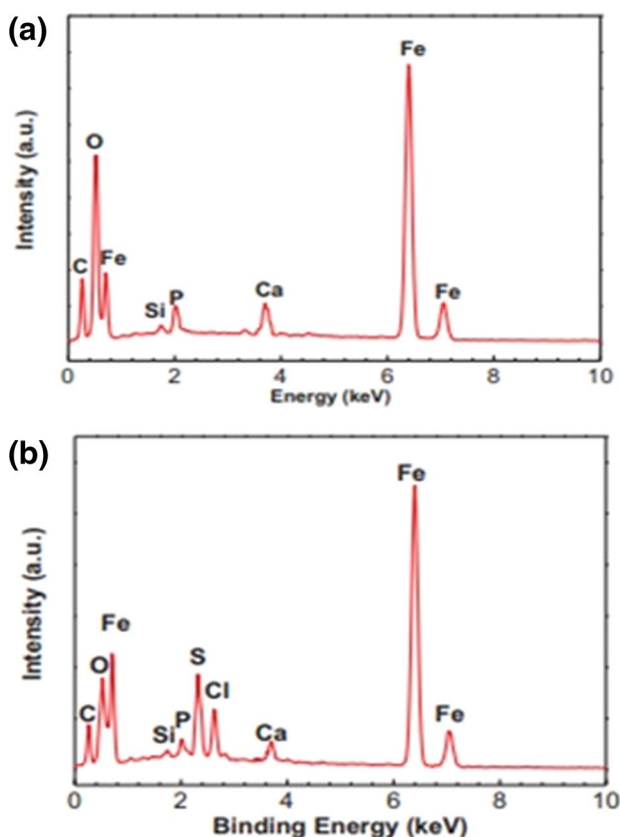


Fig. 36 Energy dispersive X-ray spectrum analysis of corrosion product film and SRB biofilm on specimens after 14 days of incubation in the absence (a) and presence (b) of SRB, respectively. (Source adapted from [201])

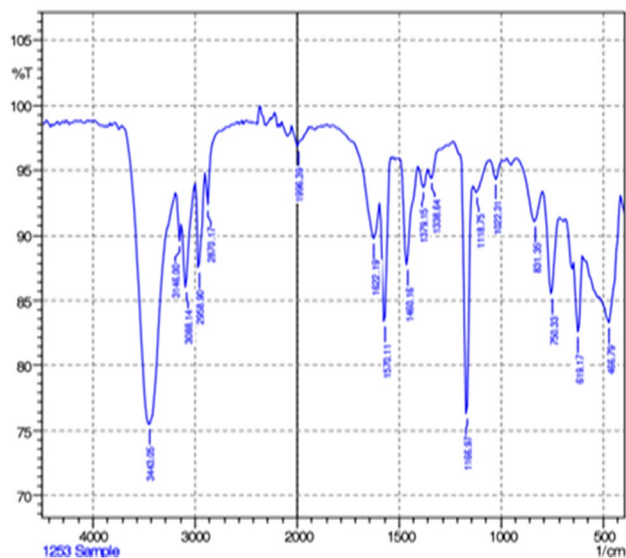


Fig. 37 IR of inhibitor with metal showing absorbance of inhibitor molecule on the metal surface (Source adapted from [202])

The adsorptive molecules present in the solute tend to get accumulated or adsorbed on the surface of an adsorbate [203].

The standard adsorption free energy measurement (ΔG_{ads}^0) provides a measure of the adsorption intensity of the molecule on the surface. ΔG_{ads}^0 high values suggest that the compound in the corrosive media is firmly adsorbed on the metal surface [204]. The ΔG_{ads}^0 value of 40 kJ/mol is generally considered as a threshold value between chemisorption and physisorption. Gibb's free energy is determined from adsorption equilibrium constant K_{ads} from the following equation:

$$\Delta G_{\text{ads}}^0 = RT \ln (55.5 K_{\text{ads}})$$

where R indicates gas constant, T is the temperature, 55.5 is the molar concentration of H_2O .

The entropy of the adsorption Process (ΔS_{ads}^0) and enthalpy of the adsorption process (ΔH_{ads}^0) can be calculated by Van't Hoff equation:

$$d \ln K_{\text{ads}} / dT = \Delta H_{\text{ads}}^0 / RT^2$$

By taking the logarithm of the above eqn and rearranging it, we get:

$$\log K_{\text{ads}} = -\Delta H_{\text{ads}}^0 / 2.303RT + D$$

Here D indicates the disintegration constant, T is the absolute temperature and R indicates gas constant with the value 8.314 J/K/mol. The plot of $\log K_{\text{ads}}$ vs $1/T$ gives a straight line with a slope $-\Delta H / 2.303R$, from which the value of enthalpy is calculated.

The entropy of adsorption is obtained from the values of enthalpy and Gibb's free energy using the following equation:

$$\Delta S_{\text{ads}}^0 = \Delta H_{\text{ads}}^0 - \Delta G_{\text{ads}}^0 / T$$

The energy of activation, E_a can be calculated using the Arrhenius equation:

$$\log C_R = -E_a / 2.303 RT + \log A \quad (4.2.15)$$

where C_R indicates corrosion rate, E_a indicates effective activation energy, R indicates gas constant, T indicates absolute temperature, and A indicates the Arrhenius constant.

If negative values are obtained for ΔH_{ads} , the adsorption of inhibitor molecules is an exothermic mechanism with a physical nature (physisorption). Afterward, the Arrhenius equation estimates the activation energy (E_a). E_a values coming below the threshold value required for chemical adsorption, simply indicate the physical adsorption nature of the inhibitor. These parameters are crucial in understanding the mechanisms involved.

Additionally, based on the forces included in the process of adsorption, adsorption can be categorized into two classes:

- (a) Physical adsorption (Physisorption)
- (b) Chemical adsorption (Chemisorption)

In physisorption, the adsorption is primarily due to the dipole–dipole or Van der Waal forces leading to relatively weaker binding forces between adsorbate and adsorbent. On the other hand, chemisorption occurs as a result of stronger interactions between the adsorbent and adsorbate forming a covalent bond.

Ashish et al. used the corrosion inhibitor venlafaxine on mild steel, where they plotted a graph between $\log C$ and $\log C/\theta$ represented in Fig. 38a which gives a straight line with the value of the regression coefficient close to 1 confirming the inhibitor adsorption on the metallic surface.

From the adsorption parameters, Gibb's free energy was determined from adsorption equilibrium constant K_{ads} from eqn.

$$\log C_R = -E_a / 2.303 RT + \log A$$

where CR indicates corrosion rate, E_a indicates effective activation energy, R indicates gas constant, T indicates absolute temperature, and A indicates the Arrhenius constant.

The activation energy was calculated from the graph of $\log I$ vs. $1/T$ given in Fig. 38b, the straight line is perceived. The slopes ($-E_a/2.303R$) have been utilized for the calculation of activation energy. The Arrhenius equation was used to calculate this kinetic parameter. The plot of $\log K_{\text{ads}}$ vs. $1/T$ represented in Figure b gives a straight line with

slope $-\Delta H/2.303R$, from which the value of enthalpy is calculated.

Hydrogen Monitoring Hydrogen monitoring is an important component of corrosion monitoring, as hydrogen detection gives an indicator that there is or has been corrosion. The formed hydrogen can penetrate the metal lattice, resulting in metal blisters, and indicates the current situation about the impact of corrosion and its failures on metal. Sulphur formed by the creation of hydrogen complexes, allows more hydrogen to penetrate the metal.

Several instruments have been created to track the amount of hydrogen entering a metal tube, such as the electrochemical probes. Until detection is possible, these methods enable hydrogen to permeate through and escape from the substrate metal. These devices contain liquid electrolytes. A solid-state electrochemical concentration cell using hydrogen uranyl phosphate tetrahydrate (HUP) is an additional tool that can be used to calculate the presence of hydrogen, both in the atmosphere and when dissolved in metals. The principle of such a method is based upon the Nernst expression:

$$-nFE = \frac{RT \ln P_{1H_2}}{P_{2H_2}}$$

where n is the charge carried, F the Faraday constant, E the potential measured across the electrolyte, R the gas constant, T the temperature, and P_{1H_2} and P_{2H_2} are the partial pressures of hydrogen on either side of the electrolyte membrane.

4.5 Applications of Corrosion Monitoring Techniques

Corrosion monitoring techniques are typically used in the following situations:

- Where the risks are extremely high such as high temperature, high pressure, explosive, flammable, toxic processes.
- Where high corrosion can be trigger using any method.
- Where variations in operating conditions can cause major changes in the rate of corrosion.
- Where there is a critical concern about product contamination due to corrosion.
- Where corrosion inhibitors are used.
- Where performance or operating parameters from design requirements are modified.
- In determining the corrosion nature of several alloys.
- In batch systems, where corrosive constituents are concentrated due to repetitive cycling.

The corrosion monitoring should be done in those industries where corrosion prevention is a primary requirement

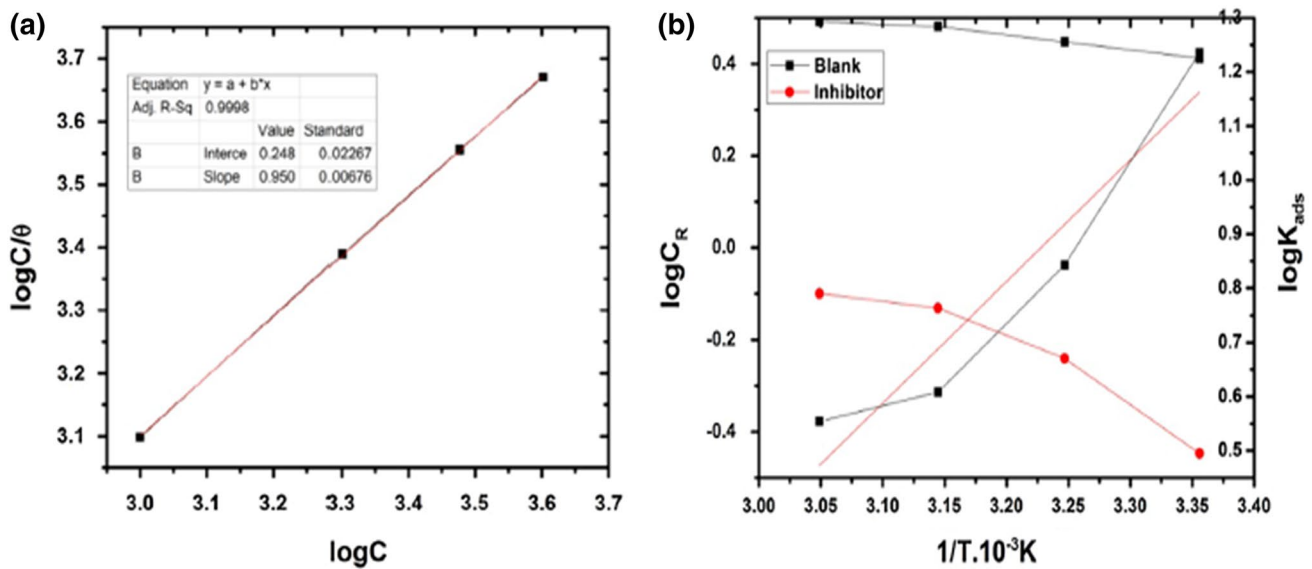


Fig. 38 a Langmuir adsorption plot, b Arrhenius plot and enthalpy plot for corrosion inhibition of mild steel using Venlafaxine in 1 M HCl (Source adapted from [181])

such as oil and gas manufacturing, mining, pulp, and paper industry, petrochemical/chemical/processing industries.

5 Challenges and Outlooks

Green compounds are perhaps the most appealing field of corrosion inhibitors. For forthcoming research concerning corrosion inhibition, it is advisable to utilize plant extracts as metallic corrosion inhibitors, since they have several advantages such as cheap, readily available, non—toxic, soluble, highly efficient and eco-sustainable nature. Even so, it is critical to understand many factors before such inhibitors can be used in practical commercial processes as the “green” facet of the natural products under analysis requires to be assessed properly. Toxicity, biodegradability and bioaccumulation experiments should be conducted to reiterate what is genuinely green and what is not.

Authors don't generally mention the specific components present in the extracts throughout which makes it an uncovered topic for prospective studies. It would be valuable if isolation and analysis of specific components should be unsightly carried out before evaluating the corrosion inhibition efficiency of an extract. A lot of lab technical instruments can seek help for the research in this regard as LC–MS, HPLC–MS or GC–MS could be of great help to uncover the compounds that are responsible for the overall effectiveness of the extract used for corrosion inhibition.

The preference of the extraction method is of vital importance. Bearing in mind the plethora of issues related to the high processing temperatures and long processing times in traditional extraction procedures, the creation, and implementation of alternate extraction techniques that do not involve extreme operating conditions like higher computational temperatures and harmful organic solvents are important. The temperature has a very marked effect on effective plant extract preparation. A very low temperature limits the effective solubility of the phytochemicals, while a very high temperature causes the decomposition of the active constituents (phytochemicals). Generally, extraction is being carried out in the temperature range of 60–80 °C to find optimal extraction yield [78, 205, 206]. Taking into account plant drying temperature, often the plant materials are allowed to dry at room temperature in shade. However, this type of drying requires several days, weeks and sometimes even months; therefore oven drying has also gained significant advancement. Moreover, the effect of solvents on the surrounding environment should also be considered as some extraction procedures require the use of highly harmful organic solvents. Theoretically, in comparison to organic extracts, the use of aqueous extracts is preferred as aqueous extracts contain relatively polar phytochemicals that offer a strong bond with the metallic surface compared to the non-polar phytochemicals of organic extracts. Although, because of their biological origin plant extracts irrespective of the aqueous and organic nature, are treated as environmental benign however generally they exhibit

low protection effectiveness at relatively higher concentrations. Their limited solubility in polar electrolytes, especially at their higher concentration, is one of the biggest challenges of using organic extracts as corrosion inhibitors. In most cases, practically it has been observed that organic extracts get precipitated in the polar electrolytes. Another disadvantage of the use of plant extracts as corrosion inhibitors is that extract preparation is extremely lengthy as several steps are involved. More so, the preparation of organic extracts generally employs toxic solvents that can adversely affect the surrounding environment along with soil and aquatic life after their discharge. Most of these solvents are extremely costly and can adversely affect the extract preparation economy. The probable technique for phytochemical extraction, i.e. Supercritical fluid extraction is an alternative to the extraction methods presented in the study so that natural compounds can be selectively extracted from natural materials at moderate temperatures. Whereas, microwave and oven drying procedures for getting dried samples are not well appreciated because it degrades the vital phytoconstituents in the extract and it will directly influence the corrosion inhibition performance. The main limitation of using plant materials as CIs is their frequently low stability; however, this limitation can be minimized or avoided by adding biocides such as N-cetyl-N,N,N-trimethyl ammonium bromide [31].

There is still quite much space for these green corrosion inhibitors to enhance their inhibition performance. Considering the enormous publications on plant extracts as corrosion inhibitors specifically for mild steel, stainless steel, copper, and aluminum, it is important to address the use of extracts for many other metals and alloys such as nickel, zinc, magnesium.

Taking into account corrosion testing techniques, most work has so far stated that not too much attention is being given to the analytical methods. Currently, computational techniques, especially quantum chemical calculations premised on density functional theory and simulations of molecular dynamics (MD) have evolved as the modern strategies which explain the potency of a specific group of compounds evaluated as corrosion inhibitors. Every plant extract retains numerous active bio-constituents (phytochemicals), so these comparatively simpler and environmentally friendly computational techniques can assess their comparative efficiency against the corrosion of the metal surface. Additionally, it is essential to evaluate the use of DFT and MD simulations (also, MC) methods to gain insight into the interaction of active constituents on the metallic surface. In a short note, extraction and evaluation about each phytochemical / constituent, use of specific drying techniques needed more input and along with it LC-MS, HPLC-MS or GC-MS and computational techniques (DFT, MD, and MC) must be address

and use for exploring the true potential of green corrosion inhibitors.

6 Conclusion

From the intense review and discussion, it can be concluded that the utilization of plant extracts (containing active bio-phytoconstituents) as corrosion inhibitors for metal and their alloy for numerous applications is enticing as they are safe, readily available, non-hazardous, and even bio-sustainable with the natural environment and can substitute existing toxic inhibitors that cause a severe hazard to public health and the environment. Phytochemicals obtained from such extracts, mostly heterocyclic compounds, with heteroatoms such as O, S, N, and P get effectively adsorbed on the metal surface and forms a protective film (defensive layer) that acts as a physical barrier to restrict the diffusion of ions or molecules on the metal surface and consequently retard the rate of corrosion reactions. The protective films formed on the metallic surface by these inhibitors give rise to resistance polarization and concentration polarization affecting both anodic and cathodic reactions. The efficiency of these extracts as corrosion inhibitors is commonly evaluated through electrochemical tests, which include techniques such as potentiodynamic polarization, electrochemical impedance spectroscopy, weight loss measurement and surface analysis techniques such as UV, SEM, AFM. It is impressive to see several reports where a maximum of 95% inhibition efficiency is achieved at minimal concentration. Most of the plant extracts behaved as mixed- and interface-type through in some reports through cathodic predominance was observed in few reports. Adsorption of most of the plant extracts on metallic surface obeyed the Langmuir adsorption isotherm though in few reports Temkin and Freundlich adsorption are also fitted. Molecular dynamic (MD) and DFT-based computational studies are highly employed to describe the interaction between phytochemicals and metallic surfaces. DFT study revealed that phytochemicals interact with the metallic surface using charge sharing (donor-acceptor) mechanism.

Although a significant amount of research has been conducted, this still remains a fairly unmapped area of research with tremendous potential for further development, particularly the methods used to attain the green corrosion inhibitors and formulating designs for corrosion inhibitors. The seismic transition would probably replace the commonly used traditional toxic chemicals to mitigate corrosion on an industrial scale. On the one hand, it will create chemicals that are environmentally friendly and beneficial to human beings and will also avoid severe loss occurring globally due to corrosion. An intensive review of the literature confirms

that the revolution of green corrosion inhibitors has already begun.

Declaration

Conflict of interest The authors declare that they have no known competing financial interests or personal relationships that could have appeared to influence the work reported in this paper.

References

- Bashir S, Sharma V, Lgaz H et al (2018) The inhibition action of analgin on the corrosion of mild steel in acidic medium: a combined theoretical and experimental approach. *J Mol Liq* 263:454–462. <https://doi.org/10.1016/j.molliq.2018.04.143>
- Fares MM, Maayta AK, Al-Qudah MM (2012) Pectin as promising green corrosion inhibitor of aluminum in hydrochloric acid solution. *Corros Sci* 60:112–117. <https://doi.org/10.1016/j.corsci.2012.04.002>
- Grassino AN, Halambek J, Djaković S et al (2016) Utilization of tomato peel waste from canning factory as a potential source for pectin production and application as tin corrosion inhibitor. *Food Hydrocoll* 52:265–274. <https://doi.org/10.1016/j.foodhyd.2015.06.020>
- Gudic S, Vrsalovic L, Kliškic M et al (2016) Corrosion inhibition of aa 5052 aluminium alloy in nacl solution by different types of honey. *Int J Electrochem Sci* 11:998–1011
- Finšgar M, Jackson J (2014) Application of corrosion inhibitors for steels in acidic media for the oil and gas industry: a review. *Corros Sci* 86:17–41. <https://doi.org/10.1016/j.corsci.2014.04.044>
- Bashir S, Lgaz H, Chung IM, Kumar A (2020) Effective green corrosion inhibition of aluminium using analgin in acidic medium: an experimental and theoretical study. *Chem Eng Commun*. <https://doi.org/10.1080/00986445.2020.1752680>
- Bashir S, Singh G, Kumar A (2017) Shatavari (*Asparagus Racemosus*) as green corrosion inhibitor of aluminium in acidic medium. *J Mater Environ Sci* 8:4284–4291
- Bashir S, Singh G, Kumar A (2018) An investigation on mitigation of corrosion of aluminium by origanum vulgare in acidic medium. *Prot Met Phys Chem Surfaces* 54:148–152. <https://doi.org/10.1134/S2070205118010185>
- Ongun Yüce A, Dođru Mert B, Kardaş G, Yazici B (2014) Electrochemical and quantum chemical studies of 2-amino-4-methylthiazole as corrosion inhibitor for mild steel in HCl solution. *Corros Sci* 83:310–316. <https://doi.org/10.1016/j.corsci.2014.02.029>
- Qiang Y, Zhang S, Xu S et al (2016) Effective protection for copper corrosion by two thiazole derivatives in neutral chloride media: experimental and computational study. *Int J Electrochem Sci* 11:3147–3163. <https://doi.org/10.20964/110403147>
- Wen X, Bai P, Luo B et al (2018) Review of recent progress in the study of corrosion products of steels in a hydrogen sulphide environment. *Corros Sci* 139:124–140. <https://doi.org/10.1016/j.corsci.2018.05.002>
- Zaki A (2006) Types of corrosion: materials and environments. Principles of corrosion engineering and corrosion control. Elsevier, Amsterdam, pp 120–270
- Bhawsar J, Jain PK, Jain P (2015) Experimental and computational studies of Nicotiana tabacum leaves extract as green corrosion inhibitor for mild steel in acidic medium. *Alexandria Eng J* 54:769–775. <https://doi.org/10.1016/j.aej.2015.03.022>
- Cordeiro RFB, Belati AJS, Perrone D, D'Elia E (2018) Coffee husk as corrosion inhibitor for mild steel in HCl media. *Int J Electrochem Sci* 13:12188–12207. <https://doi.org/10.20964/2018.12.29>
- Boumhara K, Harhar H, Tabyaoui M et al (2019) Corrosion inhibition of mild steel in 0.5 M H₂SO₄ Solution by *Artemisia herba-alba* Oil. *J Bio Tribo-Corros*. <https://doi.org/10.1007/s40735-018-0202-8>
- Ejikeme PM, Umana SG, Menkiti MC, Onukwuli OD (2015) Inhibition of mild steel and aluminium corrosion in 1M H₂SO₄ by leaves extract of african breadfruit. *Int J Mater Chem* 5:14–23. <https://doi.org/10.5923/j.ijmc.20150501.03>
- Ramdani M, Elmsellem H, Elkhiahi N et al (2015) *Caulerpa prolifera* green algae using as eco-friendly corrosion inhibitor for mild steel in 1 M HCl media. *Der Pharma Chem* 7:67–76
- Muthukumar N, Ilangovan A, Maruthamuthu S et al (2009) 1-Aminoanthraquinone derivatives as a novel corrosion inhibitor for carbon steel API 5L–X60 in white petrol-water mixtures. *Mater Chem Phys* 115:444–452. <https://doi.org/10.1016/j.matchemphys.2008.12.027>
- Alrefae SH, Rhee KY, Verma C et al (2021) Challenges and advantages of using plant extract as inhibitors in modern corrosion inhibition systems: recent advancements. *J Mol Liq* 321:114666. <https://doi.org/10.1016/j.molliq.2020.114666>
- Anitha R, Chitra S, Hemapriya V et al (2019) Implications of eco-addition inhibitor to mitigate corrosion in reinforced steel embedded in concrete. *Constr Build Mater* 213:246–256. <https://doi.org/10.1016/j.conbuildmat.2019.04.046>
- Marzorati S, Verotta L, Trasatti SP (2019) Green corrosion inhibitors from natural sources and biomass wastes. *Molecules*. <https://doi.org/10.3390/molecules24010048>
- Abeng FE, Idim VD (2018) Green corrosion inhibitor for mild steel in 2 M HCl solution : flavonoid extract of erigeron floribundus. *World Sci News* 98:89–99
- El Ouali Y, Bouyanzer A, Majidi L et al (2015) Evaluation of Pelargonium extract and oil as eco-friendly corrosion inhibitor for steel in acidic chloride solutions and pharmacological properties. *Res Chem Intermed* 41:7125–7149. <https://doi.org/10.1007/s11164-014-1802-7>
- El Makrini B, Lgaz H, Larouj M et al (2016) The inhibition performance of sulfamerazine for corrosion of mild steel in HCl. *Der Pharma Chem* 8:256–268
- Eddy NO, Odoemelam SA, Ama IN (2010) Ethanol extract of *Ocimum gratissimum* as a green corrosion inhibitor for the corrosion of mild steel in H₂SO₄. *Green Chem Lett Rev* 3:165–172. <https://doi.org/10.1080/17518251003636428>
- El Hamdani N, Fdil R, Tourabi M et al (2015) Alkaloids extract of *Retama monosperma* (L.) Boiss. seeds used as novel eco-friendly inhibitor for carbon steel corrosion in 1 M HCl solution: electrochemical and surface studies. *Appl Surf Sci* 357:1294–1305. <https://doi.org/10.1016/j.apsusc.2015.09.159>
- Djeddi N, Benahmed M, Akkal S et al (2015) Study on methylene dichloride and butanolic extracts of *Reutera lutea* (Desf.) Maire (Apiaceae) as effective corrosion inhibitions for carbon steel in HCl solution. *Res Chem Intermed* 41:4595–4616. <https://doi.org/10.1007/s11164-014-1555-3>
- Divya P, Saratha R, Priya SV (2016) Chemical science review and letters impediment effect of *Galinsoga parviflora* (quick weed) on mild steel corrosion in 1 M HCl. *Chem Sci Rev Lett* 5:115–126
- Deyab MA (2016) Inhibition activity of Seaweed extract for mild carbon steel corrosion in saline formation water. *Desalination* 384:60–67. <https://doi.org/10.1016/j.desal.2016.02.001>
- Deyab MA (2015) Egyptian licorice extract as a green corrosion inhibitor for copper in hydrochloric acid solution. *J Ind Eng Chem* 22:384–389. <https://doi.org/10.1016/j.jiec.2014.07.036>

31. Kálmán E, Felhosi I, Kármán FH et al (2008) Environmentally friendly corrosion inhibitors. *Mater Sci Technol A Compr Treat* 1–2:471–537. <https://doi.org/10.1002/9783527619306.ch9>
32. Gupta NK, Quraishi MA, Singh P et al (2017) Analytical & curcumine longa: green and sustainable corrosion. *Anal Bioanal Electrochem* 9:245–265
33. Bammou L, Belkhaouda M, Salghi R et al (2014) Corrosion inhibition of steel in sulfuric acid solution by the Chenopodium Ambrosioides extracts. *J Assoc Arab Univ Basic Appl Sci* 16:83–90. <https://doi.org/10.1016/j.jaubas.2013.11.001>
34. Ugi BU, Magu TO, Bu U et al (2018) Phytochemical constituents of Taraxacum officinale leaves as eco-friendly and nontoxic organic inhibitors for stainless steel corrosion in 0.2 M HCl acid medium. *Int J Chem Sci* 2:35–43
35. Fouda AS, Megahed HE, Fouad N, Elbahrawi NM (2016) Corrosion inhibition of carbon steel in 1 M hydrochloric acid solution by aqueous extract of Thevetia peruviana. *J Bio- Tribo-Corros* 2:1–13. <https://doi.org/10.1007/s40735-016-0046-z>
36. Fouda AS, Shalabi K, Idress AA (2014) Thymus vulgaris extract as nontoxic corrosion inhibitor for copper and α -brass in 1 M HNO₃ solutions. *Int J Electrochem Sci* 9:5126–5154
37. Unnithan CR, Muuz M, Woldu A, et al. (2014) Chemical Analysis of the Essential Oil of Erigeron Canadensis L. *UJPBS* 2:8–10
38. Chigondo M, Chigondo F (2016) Recent natural corrosion inhibitors for mild steel: an overview. *J Chem.* <https://doi.org/10.1155/2016/6208937>
39. Chen G, Hou XQ, Gao QL et al (2015) Research on Diospyros Kaki L.f leaf extracts as green and eco-friendly corrosion and oil field microorganism inhibitors. *Res Chem Intermed* 41:83–92. <https://doi.org/10.1007/s11164-013-1170-8>
40. Faiz M, Zahari A, Awang K, Hussin H (2020) Corrosion inhibition on mild steel in 1 M HCl solution by: cryptocarya nigra extracts and three of its constituents (alkaloids). *RSC Adv* 10:6547–6562. <https://doi.org/10.1039/c9ra05654h>
41. Bui HTT, Dang TD, Le HTT, Hoang TTB (2019) Comparative study on corrosion inhibition of Vietnam orange peel essential oil with urotropine and insight of corrosion inhibition mechanism for mild steel in hydrochloric solution. *J Electrochem Sci Technol* 10:69–81. <https://doi.org/10.5229/JECST.2019.10.1.69>
42. Deyab MA (2016) Corrosion inhibition of aluminum in biodiesel by ethanol extracts of Rosemary leaves. *J Taiwan Inst Chem Eng* 58:536–541. <https://doi.org/10.1016/j.jtice.2015.06.021>
43. Yetri Y, Gunawarman E, Jamarun N (2018) Theobroma cacao peel extract as the eco-friendly corrosion inhibitor for mild steel. *Corros Inhib Princ Recent Appl.* <https://doi.org/10.5772/intechopen.73263>
44. Honarvar Nazari M, Shihab MS, Havens EA, Shi X (2020) Mechanism of corrosion protection in chloride solution by an apple-based green inhibitor: experimental and theoretical studies. *J Infrastruct Preserv Resil* 1:1–19. <https://doi.org/10.1186/s43065-020-00007-w>
45. Thanh LT, Vu NSH, Binh PMQ et al (2020) Combined experimental and computational studies on corrosion inhibition of Houlttynia cordata leaf extract for steel in HCl medium. *J Mol Liq* 315:113787. <https://doi.org/10.1016/j.molliq.2020.113787>
46. Ghazouani T, Ben Hmamou D, Meddeb E et al (2015) Antioxidant activity and effect of quince pulp extract on the corrosion of C-steel in 1M HCl. *Res Chem Intermed* 41:7463–7480. <https://doi.org/10.1007/s11164-014-1837-9>
47. Miralrio A, Vázquez AE (2020) Plant extracts as green corrosion inhibitors for different metal surfaces and corrosive media: a review. *Processes.* <https://doi.org/10.3390/PR8080942>
48. Obot IB, Obi-Egbedi NO, Umoren SA (2009) Antifungal drugs as corrosion inhibitors for aluminium in 0.1 M HCl. *Corros Sci* 51:1868–1875. <https://doi.org/10.1016/j.corsci.2009.05.017>
49. Perumal S, Muthumanickam S, Elangovan A et al (2017) Bauhinia tomentosa leaves extract as green corrosion inhibitor for mild steel in 1M HCl medium. *J Bio- Tribo-Corros.* <https://doi.org/10.1007/s40735-017-0072-5>
50. Paul OA (2014) Inhibitory action of Albizia zygia gum on mild steel corrosion in acid medium. *Afr J Pure Appl Chem* 8:37–46. <https://doi.org/10.5897/ajpac2014.0549>
51. Ibrahim T, Gomes E, Obot IB et al (2016) Corrosion inhibition of mild steel by Calotropis procera leaves extract in a CO₂ saturated sodium chloride solution. *J Adhes Sci Technol* 30:2523–2543. <https://doi.org/10.1080/01694243.2016.1185229>
52. Hart K, James AO (2014) The inhibitive effect of aloe vera barbadensis gel on copper in hydrochloric acid medium. *J Emerg Trends Eng Appl Sci* 5:24–29
53. Haruna K, Obot IB, Ankah NK et al (2018) Gelatin: a green corrosion inhibitor for carbon steel in oil well acidizing environment. *J Mol Liq* 264:515–525. <https://doi.org/10.1016/j.molliq.2018.05.058>
54. Hassan KH, Khadom AA, Kurshed NH (2016) Citrus aurantium leaves extracts as a sustainable corrosion inhibitor of mild steel in sulfuric acid. *S Afr J Chem Eng* 22:1–5. <https://doi.org/10.1016/j.sajce.2016.07.002>
55. Khadraoui A, Khelifa A, Hachama K, Mehdaoui R (2016) Thymus algeriensis extract as a new eco-friendly corrosion inhibitor for 2024 aluminium alloy in 1 M HCl medium. *J Mol Liq* 214:293–297. <https://doi.org/10.1016/j.molliq.2015.12.064>
56. Kayed AM, Elghaly E-SM, El-hela AA (2016) New epoxy megastigmane glucoside from Dactyloctenium aegyptium LP Beauv Wild. *J Sci Innov Res* 4:237–244
57. Al KF, Pateiro M, Dominguez R et al (2019) Innovative green technologies of intensification for valorization of seafood and their by-products. *Mar Drugs.* <https://doi.org/10.3390/md17120689>
58. Sarmento CMP, Ferreira SRS, Hense H (2006) Supercritical fluid extraction (SFE) of rice bran oil to obtain fractions enriched with tocopherols and tocotrienols. *Brazilian J Chem Eng* 23:243–249. <https://doi.org/10.1590/S0104-66322006000200012>
59. Njoku DI, Ukaga I, Ikenna OB et al (2016) Natural products for materials protection: corrosion protection of aluminium in hydrochloric acid by Kola nitida extract. *J Mol Liq* 219:417–424. <https://doi.org/10.1016/j.molliq.2016.03.049>
60. Ndukwe AI, Anyakwo CN (2017) Modelling of corrosion inhibition of mild steel in hydrochloric acid by crushed leaves of Sida Acuta (Malvaceae). *Int J Eng Sci* 06:22–33. <https://doi.org/10.9790/1813-0601032233>
61. Nazeer AA, Shalabi K, Fouda AS (2015) Corrosion inhibition of carbon steel by Roselle extract in hydrochloric acid solution: electrochemical and surface study. *Res Chem Intermed* 41:4833–4850. <https://doi.org/10.1007/s11164-014-1570-4>
62. Turner C, Waldebäck M (2013) Principles of pressurized fluid extraction and environmental, food and agricultural applications. Woodhead Publishing Limited, Cambridge
63. Swamy MK, Akhtar MS (2019) Natural bio-active compounds: chemistry, pharmacology and health care practices. *Nat Bio-Active Compd Chem Pharmacol Heal Care Pract* 2:1–492. <https://doi.org/10.1007/978-981-13-7205-6>
64. Dhaundiyal P, Bashir S, Sharma V, Kumar A (2019) An investigation on mitigation of corrosion of mildsteel by origanum vulgare in acidic medium. *J Chem Inf Model* 33:159–168. <https://doi.org/10.1017/CBO9781107415324.004>
65. Sharma V, Kumar S, Bashir S, Ghelichkha Z, Obot IBKA (2018) Use of Sapindus (reetha) as corrosion inhibitor of aluminium in acidic medium. *Mater Res Express* 5:076510
66. Khanari K, Finšgar M, Knez Hrncič M et al (2017) Green corrosion inhibitors for aluminium and its alloys: a review. *RSC Adv* 7:27299–27330. <https://doi.org/10.1039/c7ra03944a>

67. Gapsari F, Soenoko R, Suprpto A, Suprpto W (2015) Bee wax propolis extract as eco-friendly corrosion inhibitors for 304SS in sulfuric acid. *Int J Corros*. <https://doi.org/10.1155/2015/567202>
68. Fouda E-A, El-Hossiany A, Ramadan H (2017) Calotropis Pro-cera plant extract as green corrosion inhibitor for 304 stainless steel in hydrochloric acid solution. *Zast Mater* 58:541–555. <https://doi.org/10.5937/zasmat1704541f>
69. Fouda AS, Rashwan SM, Abo-Mosallam HA (2014) Fennel seed extract as green corrosion inhibitor for 304 stainless steel in hydrochloric acid solutions. *Desalin Water Treat* 52:5175–5186. <https://doi.org/10.1080/19443994.2013.806223>
70. Ehsani A, Mahjani MG, Hosseini M et al (2017) Evaluation of *Thymus vulgaris* plant extract as an eco-friendly corrosion inhibitor for stainless steel 304 in acidic solution by means of electrochemical impedance spectroscopy, electrochemical noise analysis and density functional theory. *J Colloid Interface Sci* 490:444–451. <https://doi.org/10.1016/j.jcis.2016.11.048>
71. Singh A, Ahamad I, Singh VK, Quraishi MA (2011) Inhibition effect of environmentally benign Karanj (*Pongamia pinnata*) seed extract on corrosion of mild steel in hydrochloric acid solution. *J Solid State Electrochem* 15:1087–1097. <https://doi.org/10.1007/s10008-010-1172-z>
72. Orubite KO, Oforka NC (2004) Inhibition of the corrosion of mild steel in hydrochloric acid solutions by the extracts of leaves of *Nypa fruticans* Wurmb. *Mater Lett* 58:1768–1772. <https://doi.org/10.1016/j.matlet.2003.11.030>
73. Lebrini M, Robert F, Lecante A, Roos C (2011) Corrosion inhibition of C38 steel in 1M hydrochloric acid medium by alkaloids extract from *Oxandra asbeckii* plant. *Corros Sci* 53:687–695. <https://doi.org/10.1016/j.corsci.2010.10.006>
74. Oguzie EE (2005) Inhibition of acid corrosion of mild steel by *Telfaria occidentalis* extract. *Pigment Resin Technol* 34:321–326. <https://doi.org/10.1108/03699420510630336>
75. Chevalier M, Robert F, Amusant N et al (2014) Enhanced corrosion resistance of mild steel in 1 M hydrochloric acid solution by alkaloids extract from *Aniba rosaeodora* plant: electrochemical, phytochemical and XPS studies. *Electrochim Acta* 131:96–105. <https://doi.org/10.1016/j.electacta.2013.12.023>
76. El Bribri A, Tabyaoui M, Tabyaoui B et al (2013) The use of *Euphorbia falcata* extract as eco-friendly corrosion inhibitor of carbon steel in hydrochloric acid solution. *Mater Chem Phys* 141:240–247. <https://doi.org/10.1016/j.matchemphys.2013.05.006>
77. Ji G, Shukla SK, Dwivedi P et al (2012) Green *Capsicum annum* fruit extract for inhibition of mild steel corrosion in hydrochloric acid solution. *Int J Electrochem Sci* 7:12146–12158
78. Verma DK, Khan F (2016) Corrosion inhibition of mild steel in hydrochloric acid using extract of glycine max leaves. *Res Chem Intermed* 42:3489–3506. <https://doi.org/10.1007/s11164-015-2227-7>
79. Arockiasamy P, Sheela XQR, Thenmozhi G et al (2014) Evaluation of corrosion inhibition of mild steel in 1 M hydrochloric acid solution by *Mollugo cerviana*. *Int J Corros*. <https://doi.org/10.1155/2014/679192>
80. Abdallah M, Altass HM, Al-Gorair AS et al (2021) Natural nutmeg oil as a green corrosion inhibitor for carbon steel in 1.0 M HCl solution: chemical, electrochemical, and computational methods. *J Mol Liq* 323:115036. <https://doi.org/10.1016/j.molliq.2020.115036>
81. Alibakhshi E, Ramezanzadeh M, Bahlakeh G et al (2018) *Glycyrrhiza glabra* leaves extract as a green corrosion inhibitor for mild steel in 1 M hydrochloric acid solution: experimental, molecular dynamics, Monte Carlo and quantum mechanics study. *J Mol Liq* 255:185–198. <https://doi.org/10.1016/j.molliq.2018.01.144>
82. Cang H, Fei Z, Shao J et al (2013) Corrosion inhibition of mild steel by Aloes extract in HCL solution medium. *Int J Electrochem Sci* 8:720–734
83. Ating EI, Umoren SA, Udousoro II et al (2010) Leaves extract of ananas sativum as green corrosion inhibitor for aluminium in hydrochloric acid solutions. *Green Chem Lett Rev* 3:61–68. <https://doi.org/10.1080/17518250903505253>
84. Singh A, Singh VK, Quraishi MA (2010) Aqueous extract of kalmegh (*andrographis paniculata*) leaves as green inhibitor for mild steel in hydrochloric acid solution. *Int J Corros*. <https://doi.org/10.1155/2010/275983>
85. Satapathy AK, Gunasekaran G, Sahoo SC et al (2009) Corrosion inhibition by *Justicia gendarussa* plant extract in hydrochloric acid solution. *Corros Sci* 51:2848–2856. <https://doi.org/10.1016/j.corsci.2009.08.016>
86. Karthik R, Muthukrishnan P, Chen SM et al (2014) Anti-corrosion inhibition of mild steel in 1M hydrochloric acid solution by using *Tiliacora accuminata* leaves extract. *Int J Electrochem Sci* 10:3707–3725
87. Singh A, Ahamad I, Yadav DK et al (2012) The effect of environmentally benign fruit extract of *Shahjan* (*Moringa oleifera*) on the corrosion of mild steel in hydrochloric acid solution. *Chem Eng Commun* 199:63–77. <https://doi.org/10.1080/00986445.2011.570390>
88. Quraishi MA, Yadav DK, Ahamad I (2009) Green approach to corrosion inhibition by black pepper extract in hydrochloric acid solution. *Open Corros J* 2:56–60. <https://doi.org/10.2174/1876503300902010056>
89. Shyamala M, Kasthuri PK (2012) The inhibitory action of the extracts of *adathoda vasica*, *eclipta alba*, and *centella asiatica* on the corrosion of mild steel in hydrochloric acid medium: a comparative study. *Int J Corros*. <https://doi.org/10.1155/2012/852827>
90. Lebrini M, Robert F, Roos C (2011) Alkaloids extract from *Pali-courea guianensis* plant as corrosion inhibitor for C38 steel in 1 M hydrochloric acid medium. *Int J Electrochem Sci* 6:847–859
91. Quartarone G, Ronchin L, Vavasori A et al (2012) Inhibitive action of gramine towards corrosion of mild steel in deaerated 1.0M hydrochloric acid solutions. *Corros Sci* 64:82–89. <https://doi.org/10.1016/j.corsci.2012.07.008>
92. Krishnegowda PM, Venkatesha VT, Krishnegowda PKM, Shivayogiraju SB (2013) *Acalypha torta* leaf extract as green corrosion inhibitor for mild steel in hydrochloric acid solution. *Ind Eng Chem Res* 52:722–728. <https://doi.org/10.1021/ie3018862>
93. Anbarasi K, Vasudha VG (2014) Mild steel corrosion inhibition by *cucurbitamaxima* plant extract in hydrochloric acid solution. *J Environ Nanotechnol* 3:16–22. <https://doi.org/10.13074/jent.2014.01.132047>
94. Singh A, Singh VK, Quraishi MA (2010) Inhibition effect of environmentally benign *Kuchla* (*Strychnos Nuxvomica*) seed extract on corrosion of mild steel in hydrochloric acid solution. *Rasayan J Chem* 3:811–824
95. Lebrini M, Robert F, Blandinières PA, Roos C (2011) Corrosion inhibition by *Isertia coccinea* plant extract in hydrochloric acid solution. *Int J Electrochem Sci* 6:2443–2460
96. Ibrahim TH, Zour MA (2011) Corrosion inhibition of mild steel using fig leaves extract in hydrochloric acid solution. *Int J Electrochem Sci* 6:6442–6455
97. Chauhan LR, Gunasekaran G (2007) Corrosion inhibition of mild steel by plant extract in dilute HCl medium. *Corros Sci* 49:1143–1161. <https://doi.org/10.1016/j.corsci.2006.08.012>
98. Anupama KK, Ramya K, Shainy KM, Joseph A (2015) Adsorption and electrochemical studies of *Pimenta dioica* leaf extracts as corrosion inhibitor for mild steel in hydrochloric acid. *Mater*

- Chem Phys 167:28–41. <https://doi.org/10.1016/j.matchemphys.2015.09.013>
99. Anupama KK, Ramya K, Joseph A (2017) Electrochemical measurements and theoretical calculations on the inhibitive interaction of *Plectranthus amboinicus* leaf extract with mild steel in hydrochloric acid. *Measurement* 95:297–305. <https://doi.org/10.1016/j.measurement.2016.10.030>
 100. Benali O, Benmehdi H, Hasnaoui O et al (2013) Green corrosion inhibitor: inhibitive action of tannin extract of *Chamaerops humilis* plant for the corrosion of mild steel in 0.5M H₂SO₄. *J Mater Environ Sci* 4:127–138
 101. Benali O, Selles C, Salghi R (2014) Inhibition of acid corrosion of mild steel by *Anacyclus pyrethrum* L. extracts. *Res Chem Intermed* 40:259–268. <https://doi.org/10.1007/s11164-012-0960-8>
 102. Bhuvaneshwari TK, Vasantha VS, Jeyaprabha C (2018) *Pongamia pinnata* as a green corrosion inhibitor for mild steel in 1N sulfuric acid medium. *SILICON* 10:1793–1807. <https://doi.org/10.1007/s12633-017-9673-3>
 103. Bothi Raja P, Sethuraman MG (2009) *Strychnos nux-vomica* an eco-friendly corrosion inhibitor for mild steel in 1 M sulfuric acid medium. *Mater Corros* 60:22–28. <https://doi.org/10.1002/maco.200805027>
 104. Bothi Raja P, Sethuraman MG (2008) Inhibitive effect of black pepper extract on the sulphuric acid corrosion of mild steel. *Mater Lett* 62:2977–2979. <https://doi.org/10.1016/j.matlet.2008.01.087>
 105. Gobara M, Zaghoul B, Baraka A et al (2017) Green corrosion inhibition of mild steel to aqueous sulfuric acid by the extract of *Corchorus olitorius* stems. *Mater Res Express*. <https://doi.org/10.1088/2053-1591/aa664a>
 106. Ji G, Shukla SK, Dwivedi P et al (2011) Inhibitive effect of argemone mexicana plant extract on acid corrosion of mild steel. *Ind Eng Chem Res* 50:11954–11959. <https://doi.org/10.1021/ie201450d>
 107. Ji G, Shukla SK, Ebenso EE, Prakash R (2013) Argemone mexicana leaf extract for inhibition of mild steel corrosion in sulfuric acid solutions. *Int J Electrochem Sci* 8:10878–10889
 108. Mourya P, Banerjee S, Singh MM (2014) Corrosion inhibition of mild steel in acidic solution by *Tagetes erecta* (Marigold flower) extract as a green inhibitor. *Corros Sci* 85:352–363. <https://doi.org/10.1016/j.corsci.2014.04.036>
 109. Muthukrishnan P, Jeyaprabha B, Prakash P (2017) Adsorption and corrosion inhibiting behavior of *Lannea coromandelica* leaf extract on mild steel corrosion. *Arab J Chem* 10:S2343–S2354. <https://doi.org/10.1016/j.arabjc.2013.08.011>
 110. Okafor PC, Osabor VI, Ebenso EE (2007) Eco-friendly corrosion inhibitors: Inhibitive action of ethanol extracts of *Garcinia kola* for the corrosion of mild steel in H₂SO₄ solutions. *Pigment Resin Technol* 36:299–305. <https://doi.org/10.1108/03699420710820414>
 111. Patel NL, Jauhariand S, Mehta GN et al (2013) Mild steel corrosion inhibition by various plant extracts in 0.5 M sulphuric acid. *Int J Electrochem Sci* 8:2635–2655
 112. Pitchaipillai M, Raj K, Balasubramanian J, Periakaruppan P (2014) Benevolent behavior of *Kleinia grandiflora* leaf extract as a green corrosion inhibitor for mild steel in sulfuric acid solution. *Int J Miner Metall Mater* 21:1083–1095. <https://doi.org/10.1007/s12613-014-1013-7>
 113. Prabakaran M, Kim SH, Mugila N et al (2017) *Aster koraiensis* as nontoxic corrosion inhibitor for mild steel in sulfuric acid. *J Ind Eng Chem* 52:235
 114. Quraishi MA, Singh A, Singh VK et al (2010) Green approach to corrosion inhibition of mild steel in hydrochloric acid and sulphuric acid solutions by the extract of *Murraya koenigii* leaves. *Mater Chem Phys* 122:114–122. <https://doi.org/10.1016/j.matchemphys.2010.02.066>
 115. Sethuraman MG, Raja PB (2005) Corrosion inhibition of mild steel by *Datura metel* in acidic medium. *Pigment Resin Technol* 34:327–331. <https://doi.org/10.1108/03699420510630345>
 116. Singh A, Quraishi MA (2015) The extract of Jamun (*Syzygium cumini*) seed as green corrosion inhibitor for acid media. *Res Chem Intermed* 41:2901–2914. <https://doi.org/10.1007/s11164-013-1398-3>
 117. Umoren SA, Obot IB, Obi-Egbedi NO (2009) *Raphia hookeri* gum as a potential eco-friendly inhibitor for mild steel in sulfuric acid. *J Mater Sci* 44:274–279. <https://doi.org/10.1007/s10853-008-3045-8>
 118. Al-Nowaiser FM, Abdallah M, El-Mossalamy EH (2011) Rosemary oil as a corrosion inhibitor for carbon steel in 0.5 M sulfuric acid solution. *Chem Technol Fuels Oils* 47:66–74. <https://doi.org/10.1007/s10553-011-0258-3>
 119. Abdallah M, Altass HM, AL-Jahdaly BA, Salem MM (2018) Some natural aqueous extracts of plants as green inhibitor for carbon steel corrosion in 0.5 M sulfuric acid. *Green Chem Lett Rev* 11:189–196. <https://doi.org/10.1080/17518253.2018.1458161>
 120. Singh A, Soni N, Deyuan Y, Kumar A (2019) A combined electrochemical and theoretical analysis of environmentally benign polymer for corrosion protection of N80 steel in sweet corrosive environment. *Results Phys* 13:102116. <https://doi.org/10.1016/j.rinp.2019.02.052>
 121. Akin M, Nalbantoglu S, Cuhadar O et al (2015) *Juglans regia* L. extract as green inhibitor for stainless steel and aluminium in acidic media. *Res Chem Intermed* 41:899–912. <https://doi.org/10.1007/s11164-013-1241-x>
 122. Behpour M, Ghoreishi SM, Khayat Kashani M, Soltan N (2009) Inhibition of 304 stainless steel corrosion in acidic solution by *Ferula gumosa* (galbanum) extract. *Mater Corros* 60:895–898. <https://doi.org/10.1002/maco.200905182>
 123. Bentrach H, Rahali Y, Chala A (2014) Gum Arabic as an eco-friendly inhibitor for API 5L X42 pipeline steel in HCl medium. *Corros Sci* 82:426–431. <https://doi.org/10.1016/j.corsci.2013.12.018>
 124. Boudalia M, Guenbour A, Bellaouchou A et al (2013) Corrosion inhibition of organic oil extract of leaves of *lanvandula stoekas* on stainless steel in concentrated phosphoric acid solution. *Int J Electrochem Sci* 8:7414–7424
 125. Fouda AEAS, Rashwan SM, Abo-Mosallam HA (2014) Aqueous extract of coriander seeds as green corrosion inhibitor for 304 stainless steel in Hydrochloric Acid solutions. *J Korean Chem Soc* 58:25–32. <https://doi.org/10.5012/jkcs.2014.58.1.25>
 126. Garai S, Garai S, Jaisankar P et al (2012) A comprehensive study on crude methanolic extract of *Artemisia pallens* (Asteraceae) and its active component as effective corrosion inhibitors of mild steel in acid solution. *Corros Sci* 60:193–204. <https://doi.org/10.1016/j.corsci.2012.03.036>
 127. Jokar M, Farahani TS, Ramezanzadeh B (2016) Electrochemical and surface characterizations of *morus alba pendula* leaves extract (MAPLE) as a green corrosion inhibitor for steel in 1M HCl. *J Taiwan Inst Chem Eng* 63:436–452. <https://doi.org/10.1016/j.jtice.2016.02.027>
 128. Kadapparambil S, Yadav K, Ramachandran M, Victoria Selvam N (2017) Electrochemical investigation of the corrosion inhibition mechanism of *Tectona grandis* leaf extract for SS304 stainless steel in hydrochloric acid. *Corros Rev* 35:111–121. <https://doi.org/10.1515/corrrev-2016-0074>


129. Li X, Deng S, Fu H (2012) Inhibition of the corrosion of steel in HCl, H₂SO₄ solutions by bamboo leaf extract. *Corros Sci* 62:163–175. <https://doi.org/10.1016/j.corsci.2012.05.008>
130. Loto CA, Etete PL, Popoola API (2011) Inhibition effect of kola tree and tobacco extracts on the corrosion of austenitic stainless steel in acid chloride environment. *Int J Electrochem Sci* 6:4876–4890
131. Mehdipour M, Ramezanzadeh B, Arman SY (2015) Electrochemical noise investigation of Aloe plant extract as green inhibitor on the corrosion of stainless steel in 1M H₂SO₄. *J Ind Eng Chem* 21:318–327. <https://doi.org/10.1016/j.jiec.2014.02.041>
132. Obiukwu OO, Opara IO, Oyinnu BC (2013) Corrosion inhibition of stainless steel using plant extract *Vernonia amygdalina* and *Azadirachta indica*. *Pacific J Sci Technol* 14:31–35
133. Obiukwu O, Opara I, Asoluka C (2016) The inhibitive effect of *Gnetum africanum*, *Gongronema latifolium* and *Chromolena odoratum* extracts on corrosion of stainless steel in 1 M HCl and H₂SO₄ solutions. *Int Lett Chem Phys Astron* 66:25–37
134. Qiang Y, Zhang S, Tan B, Chen S (2018) Evaluation of Ginkgo leaf extract as an eco-friendly corrosion inhibitor of X70 steel in HCl solution. *Corros Sci* 133:6–16. <https://doi.org/10.1016/j.corsci.2018.01.008>
135. Shabani-Nooshabadi M, Ghandchi MS (2015) Introducing the *Santolina chamaecyparissus* extract as a suitable green inhibitor for 304 stainless steel corrosion in strong acidic medium. *Metall Mater Trans A Phys Metall Mater Sci* 46:5139–5148. <https://doi.org/10.1007/s11661-015-3101-3>
136. Soltani N, Tavakkoli N, Khayat Kashani M et al (2012) Green approach to corrosion inhibition of 304 stainless steel in hydrochloric acid solution by the extract of *Salvia officinalis* leaves. *Corros Sci* 62:122–135. <https://doi.org/10.1016/j.corsci.2012.05.003>
137. Singh A, Pramanik T, Kumar A, Gupta M (2013) Phenobarbital: a new and effective corrosion inhibitor for mild steel in 1 M HCl solution. *Asian J Chem* 25:9808–9812. <https://doi.org/10.14233/ajchem.2013.15414>
138. Abakedi O, Moses I (2016) Aluminium corrosion inhibition by *maesobatria barteri* root extract in hydrochloric acid solution. *Am Chem Sci J* 10:1–10. <https://doi.org/10.9734/acsj/2016/21812>
139. Abiola OK, Oforka NC, Ebenso EE, Nwinuka NM (2007) Eco-friendly corrosion inhibitors: the inhibitive action of *Delonix Regia* extract for the corrosion of aluminium in acidic media. *Anti-Corros Methods Mater* 54:219–224. <https://doi.org/10.1108/00035590710762357>
140. Abiola OK, Otaigbe JOE (2009) The effects of *Phyllanthus amarus* extract on corrosion and kinetics of corrosion process of aluminum in alkaline solution. *Corros Sci* 51:2790–2793. <https://doi.org/10.1016/j.corsci.2009.07.006>
141. Abiola OK, Otaigbe JOE, Kio OJ (2009) *Gossipium hirsutum* L. extracts as green corrosion inhibitor for aluminum in NaOH solution. *Corros Sci* 51:1879–1881. <https://doi.org/10.1016/j.corsci.2009.04.016>
142. Ambrish S (2012) *Azwaïn* (*Trachyspermum copticum*) seed extract as an efficient corrosion inhibitor for Aluminium in NaOH solution. *Res J Recent Sci* 1:57–61
143. Arora P, Kumar S, Sharma MK, Mathur SP (2007) Corrosion inhibition of aluminium by *Capparis decidua* in acidic media. *J Chem* 4:450–456. <https://doi.org/10.1155/2007/487820>
144. Ayeni FA, Alawode S, Joseph D et al (2014) Investigation of *Sida acuta* (wire weed) plant extract as corrosion inhibitor for aluminium-copper-magnesium alloy in acidic medium. *J Miner Mater Charact Eng* 02:286–291. <https://doi.org/10.4236/jmmce.2014.24033>
145. Chauhan R, Garg U, Tak RK (2011) Corrosion inhibition of aluminium in acid media by *Citrullus colocynthis* extract. *J Chem* 8:85–90. <https://doi.org/10.1155/2011/340639>
146. Deng S, Li X (2012) Inhibition by *Jasminum nudiflorum* Lindl. leaves extract of the corrosion of aluminium in HCl solution. *Corros Sci* 64:253–262. <https://doi.org/10.1016/j.corsci.2012.07.017>
147. El-Etre AY (2003) Inhibition of aluminum corrosion using *Opuntia* extract. *Corros Sci* 45:2485–2495. [https://doi.org/10.1016/S0010-938X\(03\)00066-0](https://doi.org/10.1016/S0010-938X(03)00066-0)
148. Li X, Deng S (2012) Inhibition effect of *Dendrocalamus brandisii* leaves extract on aluminum in HCl, H₃PO₄ solutions. *Corros Sci* 65:299–308. <https://doi.org/10.1016/j.corsci.2012.08.033>
149. Mejeha IM, Nwandu MC, Okeoma KB et al (2012) Experimental and theoretical assessment of the inhibiting action of *Aspilia africana* extract on corrosion aluminium alloy AA3003 in hydrochloric acid. *J Mater Sci* 47:2559–2572. <https://doi.org/10.1007/s10853-011-6079-2>
150. Nathiya RS, Raj V (2017) Evaluation of *Dryopteris cochleata* leaf extracts as green inhibitor for corrosion of aluminium in 1 M H₂SO₄. *Egypt J Pet* 26:313–323. <https://doi.org/10.1016/j.ejpe.2016.05.002>
151. Nnanna LA, Obasi VU, Nwadiuko OC et al (2012) Inhibition by *Newbouldia leavis* leaf extract of the corrosion of aluminium in HCl and H₂SO₄ solutions. *Arch Appl Sci Res* 4:207–217
152. Nnanna LA, Nwadiuko OC, Ekekwe ND et al (2012) Adsorption and inhibitive properties of leaf extract of *Newbouldia leavis* as a green inhibitor for aluminium alloy in H₂SO₄. *Am J Mater Sci* 1:143–148. <https://doi.org/10.5923/j.materials.20110102.24>
153. Aladesuyi O, Ajanaku CO, Adedapo EA, Akinsiku AA, Sodiya FE (2015) Adsorption properties of *Azadirachta indica* extract on corrosion of aluminium in 185 M Hydrochloric acid. *J Int Assoc Adv Technol Sci* 2:23
154. Obi-Egbedi NO, Obot IB, Umoren SA (2012) *Spondias mombin* L. as a green corrosion inhibitor for aluminium in sulphuric acid: correlation between inhibitive effect and electronic properties of extracts major constituents using density functional theory. *Arab J Chem* 5:361–373. <https://doi.org/10.1016/j.arabjc.2010.09.002>
155. Oguzie EE (2007) Corrosion inhibition of aluminium in acidic and alkaline media by *Sansevieria trifasciata* extract. *Corros Sci* 49:1527–1539. <https://doi.org/10.1016/j.corsci.2006.08.009>
156. Singh A, Kumar A, Pramanik T (2013) A theoretical approach to the study of some plant extracts as green corrosion inhibitor for mild steel in HCl solution. *Orient J Chem* 29:1–7
157. Abd-El-Nabey BA, Abdel-Gaber AH, Ali MES et al (2013) Inhibitive action of cannabis plant extract on the corrosion of copper in 0.5 M H₂SO₄. *Int J Electrochem Sci* 8:7124–7137
158. Fouda AS, Abdallah YM, Elawady GY, Ahmed RM (2014) *Zygophyllum coccineum* L. Extract as green corrosion inhibitor for copper in 1 M HNO₃ Solutions. *Int J Adv Res* 2:517–531
159. Fouda AS, Elmorsi MA, Abou-Elmagd BS (2017) Adsorption and inhibitive properties of methanol extract of *Euphorbia heterophylla* for the corrosion of copper in 0.5 M nitric acid solutions. *Polish J Chem Technol* 19:95–103. <https://doi.org/10.1515/pjct-2017-0014>
160. Fouda AS, Shalabi K, Idress AA (2015) *Ceratonia siliqua* extract as a green corrosion inhibitor for copper and brass in nitric acid solutions. *Green Chem Lett Rev* 8:17–29. <https://doi.org/10.1080/17518253.2015.1073797>
161. Hart K, James A (2014) Corrosion inhibition of copper in hydrochloric and tetraoxosulphate (VI) acid solutions using *Aloe Vera* barbadensis gel. *Br J Appl Sci Technol* 4:4052–4065. <https://doi.org/10.9734/bjast/2014/9658>
162. Krishnaveni K, Ravichandran J (2014) Influence of aqueous extract of leaves of *Morinda tinctoria* on copper corrosion in

- HCl medium. *J Electroanal Chem* 735:24–31. <https://doi.org/10.1016/j.jelechem.2014.09.032>
163. Nawafleh E, Irshadat M, Bataineh T et al (2012) The effects of inula visciosa extract on corrosion of copper in NaOH solution. *Res J Chem Sci* 2:37–41
 164. Osarolube E, James A (2014) Corrosion inhibition of copper using African black velvet tamarind (*Dialium indium*) extract in sulphuric acid environment. *J Sci Res Rep* 3:2450–2458. <https://doi.org/10.9734/jsrr/2014/9434>
 165. Raghavendra N, Bhat JI (2018) Chemical components of mature areca nut husk extract as a potential corrosion inhibitor for mild steel and copper in both acid and alkali media. *Chem Eng Commun* 205:145–160. <https://doi.org/10.1080/00986445.2017.1370709>
 166. Sangeetha TV, Fredimoses M (2011) Inhibition of mild copper metal corrosion in HNO₃ Medium by acid extract of *Azadirachta Indica* seed. *J Chem* 8:1–7. <https://doi.org/10.1155/2011/135952>
 167. El-Dossoki FI, El-Nadr HA, El-Hussein A (2018) *Moringa oleifera* plant extract as a copper corrosion inhibitor in binary acid mixture (HNO₃ + H₃PO₄). *Zast Mater* 59:422–435. <https://doi.org/10.5937/zasmat1803422f>
 168. Honarvar F, Salehi F, Safavi V et al (2013) Ultrasonic monitoring of erosion/corrosion thinning rates in industrial piping systems. *Ultrasonics* 53:1251–1258. <https://doi.org/10.1016/j.ultras.2013.03.007>
 169. Khalili P, Cawley P (2018) The choice of ultrasonic inspection method for the detection of corrosion at inaccessible locations. Elsevier, Amsterdam
 170. Zhang H, Tian GY, Simm A, Alamin M (2013) Electromagnetic methods for corrosion under paint coating measurement. Eighth Int Symp Precis Eng Meas Instrum 8759:875919. <https://doi.org/10.1117/12.2014567>
 171. Hu B, Yu R, Liu J (2016) Experimental study on the corrosion testing of a buried metal pipeline by transient electromagnetic method. *Anti-Corros Methods Mater* 63:262–268. <https://doi.org/10.1108/ACMM-10-2014-1444>
 172. Bubenik T (2014) Electromagnetic methods for detecting corrosion in underground pipelines: magnetic flux leakage (MFL). Woodhead Publishing Limited, Cambridge
 173. Hansen JP (2007) Using Eddy current for corrosion inspection. *Insp Trends* 10:29–31
 174. Zergoug M, Lebaillia S, Kamel G (2004) Characterization of the corrosion by eddy current. EUROCORR 2004 - Prevision a long terme et modelisation de la corrosion, Nice (France), 12–16 Sep, p 1–7.
 175. de Alcantara NP, da Silva FM, Guimarães MT, Pereira MD (2015) Corrosion assessment of steel bars used in reinforced concrete structures by means of eddy current testing. *Sensors (Switzerland)*. <https://doi.org/10.3390/s16010015>
 176. Ghoni R, Dollah M, Sulaiman A, Mamat Ibrahim F (2014) Defect characterization based on Eddy current technique: technical review. *Adv Mech Eng*. <https://doi.org/10.1155/2014/182496>
 177. He Y, Tian G, Zhang H et al (2012) Steel corrosion characterization using pulsed eddy current systems. *IEEE Sens J* 12:2113–2120. <https://doi.org/10.1109/JSEN.2012.2184280>
 178. Edalati K, Rastkhah N, Kermani A et al (2006) The use of radiography for thickness measurement and corrosion monitoring in pipes. *Int J Press Vessel Pip* 83:736–741. <https://doi.org/10.1016/j.ijpvp.2006.07.010>
 179. Ewert U, Tschalkner M, Hohendorf S et al (2016) Corrosion monitoring with tangential radiography and limited view computed tomography. *AIP Conf Proc*. <https://doi.org/10.1063/1.4940574>
 180. Mohana KN, Shivakumar SS, Badiea AM (2011) Inhibition of mild steel corrosion in 0.25 M sulphuric acid solution by imatinib mesylate. *J Korean Chem Soc* 55:364–372. <https://doi.org/10.5012/jkcs.2011.55.3.364>
 181. Bashir S, Lgaz H, Chung IHM, Kumar A (2019) Potential of Venlafaxine in the inhibition of mild steel corrosion in HCl: insights from experimental and computational studies. *Chem Pap* 73:2255–2264. <https://doi.org/10.1007/s11696-019-00775-0>
 182. Abdallah M (2004) Antibacterial drugs as corrosion inhibitors for corrosion of aluminium in hydrochloric solution. *Corros Sci* 46:1981–1996. <https://doi.org/10.1016/j.corsci.2003.09.031>
 183. Eddy NO, Odoemelam SA, Ekwumemgbo P (2008) Inhibition of the corrosion of mild steel in H₂SO₄ by penicillin G. *Sci Res Essays* 4:033–038
 184. Adejoro IA, Ojo FK, Obafemi SK (2015) Corrosion inhibition potentials of ampicillin for mild steel in hydrochloric acid solution. *J Taibah Univ Sci* 9:196–202. <https://doi.org/10.1016/j.jtusci.2014.10.002>
 185. Abdel Hameed RS, AlShafey HI, Abu-Nawwas AH (2014) 2-(2,6-dichloranilino) phenyl acetic acid drugs as eco-friendly corrosion inhibitors for mild steel in 1M HCl. *Int J Electrochem Sci* 9:6006–6019
 186. Eddy NO, Odoemelam SA, Mbaba AJ (2008) Inhibition of the corrosion of mild steel in HCl by sparfloxacin. *Pure Appl Chem* 2:132–138
 187. Papavinasam S (2008) Electrochemical polarization techniques for corrosion monitoring. *Tech Corros Monit*. <https://doi.org/10.1533/9781845694050.1.49>
 188. Bashir S, Sharma V, Singh G et al (2019) Electrochemical behavior and computational analysis of phenylephrine for corrosion inhibition of aluminum in acidic medium. *Metall Mater Trans A* 50:468–479. <https://doi.org/10.1007/s11661-018-4957-9>
 189. Haruna T, Morikawa Y, Fujimoto S, Shibata T (2003) Electrochemical noise analysis for estimation of corrosion rate of carbon steel in bicarbonate solution. *Corros Sci* 45:2093–2104. [https://doi.org/10.1016/S0010-938X\(03\)00031-3](https://doi.org/10.1016/S0010-938X(03)00031-3)
 190. Munir S, Walsh WR (2016) The quantification of corrosion damage for pre-stressed conditions: a model using stainless steel. *J Bio- Tribo-Corros* 2:1–10. <https://doi.org/10.1007/s40735-016-0033-4>
 191. Elachouri M, Hajji MS, Salem M et al (1996) Some nonionic surfactants as inhibitors of the corrosion of iron in acid chloride solutions. *Corrosion* 52:103–108. <https://doi.org/10.5006/1.3292100>
 192. El Achouri M, Kertit S, Gouttaya HM et al (2001) Corrosion inhibition of iron in 1 M HCl by some gemini surfactants in the series of alkanediyl- α , ω -bis-(dimethyl tetradecyl ammonium bromide). *Prog Org Coatings* 43:267–273. [https://doi.org/10.1016/S0300-9440\(01\)00208-9](https://doi.org/10.1016/S0300-9440(01)00208-9)
 193. Asefi D, Mahmoodi NM, Arami M (2010) Effect of nonionic co-surfactants on corrosion inhibition effect of cationic gemini surfactant. *Colloids Surf A Physicochem Eng Asp* 355:183–186. <https://doi.org/10.1016/j.colsurfa.2009.12.019>
 194. Bashir S, Thakur A, Lgaz H et al (2020) Corrosion inhibition efficiency of bronopol on aluminium in 0.5 M HCl solution Insights from experimental and quantum chemical studies. *Surf Interfaces* 20:100542. <https://doi.org/10.1016/j.surfin.2020.100542>
 195. Oparaodu KO, Okpokwasili GC (2014) Comparison of percentage weight loss and corrosion rate trends in different metal coupons from two soil environments. *Int J Environ Bioremediation Biodegrad* 2:243–249. <https://doi.org/10.12691/ijebb-2-5-5>
 196. Xu Y, Liu L, Zhou Q et al (2020) An overview of major experimental methods and apparatus for measuring and investigating erosion-corrosion of ferrous-based steels. *Metals (Basel)* 10:1–32. <https://doi.org/10.3390/met10020180>
 197. Mobin M, Zehra S, Parveen M (2016) L-Cysteine as corrosion inhibitor for mild steel in 1 M HCl and synergistic effect of

- anionic, cationic and non-ionic surfactants. *J Mol Liq* 216:598–607. <https://doi.org/10.1016/j.molliq.2016.01.087>
198. Tawfik SM, Sayed A, Aiad I (2012) Corrosion inhibition by some cationic surfactants in oil fields. *J Surfactants Deterg* 15:577–585. <https://doi.org/10.1007/s11743-012-1339-y>
199. Bashir S, Thakur A, Lgaz H et al (2019) Computational and experimental studies on Phenylephrine as anti-corrosion substance of mild steel in acidic medium. *J Mol Liq* 293:111539. <https://doi.org/10.1016/j.molliq.2019.111539>
200. Bashir S, Thakur A, Lgaz H et al (2020) Corrosion inhibition performance of acarbose on mild steel corrosion in acidic medium: an experimental and computational Study. *Arab J Sci Eng*. <https://doi.org/10.1007/s13369-020-04514-6>
201. Liu H, Meng G, Li W et al (2019) Microbiologically influenced corrosion of carbon steel beneath a deposit in CO₂-saturated formation water containing *Desulfotomaculum nigrificans*. *Front Microbiol* 10:1–13. <https://doi.org/10.3389/fmicb.2019.01298>
202. Parveen G, Bashir S, Thakur A et al (2020) Experimental and computational studies of imidazolium based ionic liquid 1-methyl-3-propylimidazolium iodide on mild steel corrosion in acidic solution experimental and computational studies of imidazolium based ionic liquid 1-methyl-3-propylimidazolium. *Mater Res Express* 7:016510. <https://doi.org/10.1088/2053-1591/ab5c6a>
203. Bernal V, Giraldo L, Moreno-Piraján JC (2020) Insight into adsorbate–adsorbent interactions between aromatic pharmaceutical compounds and activated carbon: equilibrium isotherms and thermodynamic analysis. *Adsorption* 26:153–163. <https://doi.org/10.1007/s10450-019-00057-x>
204. Mohd NK, Ghazali MJ, Kian YS et al (2017) Corrosion inhibition of mild steel in hydrochloric acid solution using fatty acid derivatives. *J Oil Palm Res* 29:97–109. <https://doi.org/10.21894/jopr.2017.2901.11>
205. Sharma SK, Peter A, Obot IB (2015) Potential of *Azadirachta indica* as a green corrosion inhibitor against mild steel, aluminum, and tin: a review. *J Anal Sci Technol*. <https://doi.org/10.1186/s40543-015-0067-0>
206. Fiori-Bimbi MV, Alvarez PE, Vaca H, Gervasi CA (2015) Corrosion inhibition of mild steel in HCL solution by pectin. *Corros Sci* 92:192–199. <https://doi.org/10.1016/j.corsci.2014.12.002>

Publisher's Note Springer Nature remains neutral with regard to jurisdictional claims in published maps and institutional affiliations.

Authors and Affiliations

Abhinay Thakur¹ · Ashish Kumar¹ 

✉ Ashish Kumar
drashishchemlpu@gmail.com

Sciences, Lovely Professional University, Phagwara,
Punjab 144411, India

¹ Department of Chemistry, Faculty of Technology and Science, School of Chemical Engineering and Physical